A dissection and angiographic study of anatomical variations in the anterior communicating artery complex in a South African sample

Mbalentle Madolo

MSc Med Applied Anatomy

Supervisor: [1]Dr Kentse Mpolokeng

Co-supervisors: [1]A/Prof. Geney Gunston and [2]Dr Stuart More

[1]Division of Clinical Anatomy and Biological Anthropology

Department of Human Biology

University of Cape Town

[2]Division of Nuclear Medicine

Department of Radiation Medicine
Groote Schuur Hospital.

Plagiarism Declaration

1. I know that plagiarism is wrong. Plagiarism is to use another's work and pretend that it is one's own.

2. I have used the required convention for citation and referencing. Each contribution to and quotation in this assignment from the work(s) of other people has been attributed and has been cited and referenced.

3. This assignment is my own work.

4. I have not allowed and will not allow anyone to copy my work with the intention of passing it off as his or her own work.

5. I acknowledge that copying someone else's assignment or essay, or part of it, is wrong, and declare that this is my own work.

6. I have submitted this thesis through Turnitin and submitted the Turnitin report to my supervisors. The supervisors approved the report.

Name: MBALENTLE YOLANDA MADOLO

Student number: MDLMBA005

Signature: Signed by candidate

Date: 12/02/2024

Harvard referencing style was used for this document.

Table of Contents

Acknowledgements

I would like to express my sincerest gratitude to the following:

- The body donors, their families and the patients who visited Groote Schuur Hospital for their immeasurable contributions to science, without which, this study would not have been possible.
- My supervisors Dr Kentse Mpolokeng, Associate Professor Geney Gunston and Dr Stuart More for their assistance, expertise, constant encouragement, and support. Thank you for being of my mentors and providing me with constant reassurance.
- The technical staff at in the Department of Human Biology, for all your assistance in arranging the bodies for my research project and assisting during the data collection process.
- Mr Trevor Mafu for his assistance with statistical analyses.
- Associate Professor Sulaiman Moosa, Head of the Department of Radiology at the Groote Schuur Hospital for granting me an opportunity to access the patient records through the PACS system.
- Ms Jessica Garlick, for her contributions during the data collection process and for her constant support.
- My colleague and friend, Ms Reagobaka Lichaba for her contributions as my interpersonal error observer and support system. Thank you for the person that you are.
- Mr Sandile Ntuli, for your constant advice and encouragement. Thank you for rooting for me.
- My mother, Gcobisa Madolo, for her constant love, support, understanding and prayers.
- My grandfather, Lenny Makhwenkwe Madolo - my greatest inspiration. Thank you for believing in me even when I do not believe in myself.
- My grandmother, Iris Nozibele Madolo- my role model. Thank you for your unconditional love and support.
- To both my grandparents, you are the reason I am where I am today. Thank you for all that you have done for me. I love and appreciate you fiercely. ***Ndiyabulela bazali bam.***
- My aunts, Ms Chwayita Madolo (Getrude), Mrs Xatyiswa Mtshayi (Khuti), Mrs Thobeka Maja and Mrs Bulelwa Madolo for always reminding me that I can reach the stars.
- My uncles Mr Vuyo Madolo for always being in my corner and Mr Lwandile Madolo for always reminding me that I'm destined for greatness.
- My little best friends, Mr Likho Madolo, Ms Aphiwe Madolo, Ms Awomi Madolo, Ms Oluthando Madolo, Ms Avethandwa Mtshayi and Ms Inganathi Mtshayi for being my constant source of happiness.
- My friends that have kept me sane during this journey. You all have my heart. May God bless you all.
- UCT Masters financial aid for the financial assistance towards this research.

Finally, to God. Thank you.

List of Abbreviations

3D-TOF	**Three-dimensional time-of-flight**
A	Artery
ACA	Anterior cerebral artery
ACAC	Anterior communicating artery complex
AChA	Anterior choroidal artery
ACoA	Anterior communicating artery
ACoA	Anterior communicating artery
BA	Basilar artery
CAC	Circulus arteriosus cerebri
CCA	Common carotid artery
CRGC	Cadaver Research Governance Committee
CRL	Cranial to rump length
CT	Computed tomography
DD	Distal diameter
ECA	External carotid artery
HA	Hypoglossal artery
HREC	Human research ethics committee
I	First pharyngeal arch artery
ICA	Internal carotid artery
ICC	Intraclass correlation coefficient
II	Second pharyngeal arch artery
III	Third pharyngeal arch artery
IV	Fourth pharyngeal arch artery
MCA	Middle cerebral artery
MD	Middle diameter
MPR	Multiplanar reformation
MRA	Magnetic resonance angiogram
MRI	Magnetic resonance image
OA	Optic artery
PACS	Picture archiving and communication digital imaging system
PCA	Posterior cerebral artery
PChA	Posterior choroidal artery
PcoA	Posterior communicating arteries
PCOMM	Posterior communicating artery
PD	Proximal diameter
PET	Positron emission tomography
POPIA	Protection of personal information act
ProA	Proatlantal artery
ProA	Proatlantal artey
REDcap	Research electronic data capture
RF	Radiofrequency pulse
SAH	Subarachnoid haemorrhages
SPSS	Statistical package for the social sciences
TA	Trigeminal artery
TOF	Time-of-flight
V	Fifth pharyngeal arch artery

VA	Vertebral artery
VI	Sixth pharyngeal arch artery

List of Figures

List of Tables

Abstract

The anterior communicating artery complex (ACAC) consists of the A1 and A2 segments of the anterior cerebral artery (ACA) and the anterior communicating artery (ACoA). The ACAC is said to be the most frequent site of aneurysms and anterior cerebral circulation variations. Clear correlation between cerebral arterial circulation variations and aneurysm development has been reported. Cerebrovascular diseases play a significant role in the causes of morbidity in South Africa. South African data in this area of research is currently lacking and thus more knowledge is needed. This study aims to report the prevalence of variations in the ACAC and their link to the prevalence of cerebral aneurysms. For the dissection portion of this study, a total of 68 (35 female and 33 male) adult formalin fixed brains were included. These brains were from the bodies that were previously dissected in the Department of Human Biology, University of Cape Town by the medical undergraduate and honours post-graduate students. For the angiographic portion of this study, a total of 208 (151 female and 57 male) adult MRA scans were included. All the MRA images used were obtained from the picture archiving and communication digital imaging system (PACS) of the Department of Radiology, Groote Schuur Hospital. The occurrence of variations across the dissection and angiographic samples of the study was significant, 67,6% and 43,5% of the brains respectively, presented with ACAC variations. Additionally, variations in the ACoA were the most frequent at 57,4% and 36,7% in the dissection sample and the angiographic study, respectively. Of the 21 types of ACAC variations, hypoplasia, duplication, and fenestration hypoplasia were the most common types of A1 variations reported. A newly described 'anastomosed' was the most common A2 segment variation in the dissection sample. Whereas in the angiographic component, triple ACA was the most common A2 variation. For the ACoA, X-shaped and hypoplasia were among the most common ACoA variations found across both components of this study. The morphometric parameters of the ACAC measured in this study were within similar ranges that were reported in previous international and national studies. In the angiographic component, 23,9% of the MRA images presented with a history of ACAC aneurysms. No association was found between the prevalence of ACAC variations and the history of ACAC aneurysms. This finding is not in agreement with previous literature. Further studies are recommended, with a larger sample size, to investigate this relationship and the potential reasons why these findings differ from previous studies. Understanding ACAC anatomy, variations, and their potential link to the prevalence of ACAC aneurysms is vital to clinicians and neurosurgeons for the diagnosis of cerebral conditions and could advance the efficacy of interventional procedures.

Chapter 1: Introduction

Cerebrovascular diseases are described as conditions that impact the blood vessels and blood supply to the brain, resulting in brain injury. Furthermore, these conditions encompass situations in which a segment of the brain experiences temporary or permanent impairment due to bleeding or ischaemia, commonly known as a stroke (Good, 1990; Margeta and Perry 2020). In South Africa, cerebrovascular diseases were ranked fourth amongst the top ten leading natural causes of death in both 2016 and 2017 (Stats SA, 2018). However, as of 2018, there was a notable shift as cerebrovascular diseases increased in rank to the third among the top ten leading natural causes of mortality in South Africa (Stats SA, 2018). Furthermore, these diseases were reported to have accounted for 5.1% of deaths across all causes of mortality in South Africa in the year 2018 (Stats SA, 2018).

Among the various types of cerebrovascular diseases are cerebral aneurysms which are described as weak focalised regions of cerebral arteries that are dilated and filled with blood (Kayembe *et al*., 1984). As seen in figure 1.1, cerebral aneurysms may be classified into two main types, namely, ruptured and unruptured aneurysms (National Institute of Neurological Disorders and Stroke, 2023). Ruptured aneurysms occur when aneurysms burst and result in subarachnoid haemorrhages (SAH) which are accompanied by extremely severe headaches alongside other symptoms (Brisman, Song and Newell, 2006). Additionally, leaking aneurysms or sentinel bleeds, a subset of ruptured aneurysms, occur when there is a small leakage of blood from the aneurysm into the brain tissue surrounding the aneurysms or into the area surrounding the brain preceding aneurysm rupture (Backes *et al.*, 2014). Sentinel or warning headaches usually occur when this small leakage of blood from the aneurysms occur (Jersey, 2022). Furthermore, pseudoaneurysms are classified within the category of leaking aneurysms, but they differ in that they do not involve all layers of the vessel wall, and usually follow injury or tearing of the vessel wall due to complications arising from medical procedures (Rivera and Dattilo, 2022). Unruptured cerebral aneurysms in the United States are reported to affect approximately 1 in 50 people and about 30 000 people suffer from ruptured aneurysms annually (Brisman, Song and Newell, 2006; Burlakoti *et al.*, 2020). Rupture of cerebral aneurysms not only causes subarachnoid haemorrhages (SAH) but leads to high mortality and morbidity (D'Souza, 2015). The incidence of SAH lies between 10 and 36 per 100 000 people per year (Burlakoti *et al.*, 2020) depending on geographical location. Worldwide, approximately 500,000 individuals will experience SAH each year, with the majority of individuals being in low and middle income countries (Hughes *et al.*, 2018).

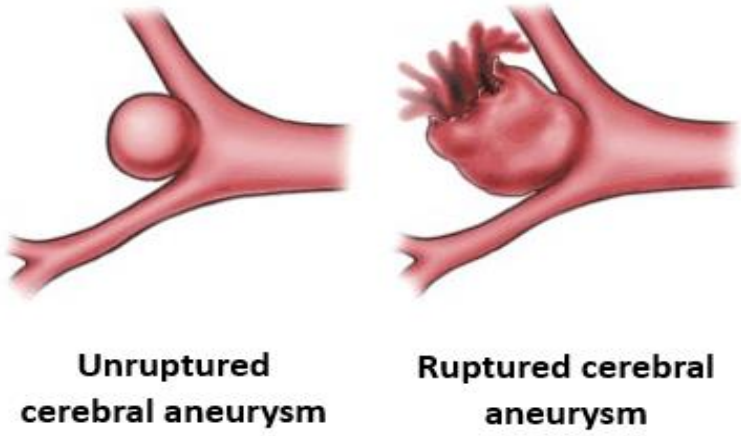

Figure 1.1: A generic illustration showing two main types of cerebral aneurysms (Adapted from Jung, 2018).

The exact cause of intracranial aneurysms is said to be unknown. However, congenital variations of the arterial wall of cerebral arteries are said to be one of the plausible causes of cerebral aneurysms (Kayembe *et al.,* 1984). Earlier reports by Kayembe *et al.,* 1984 and Sforza *et al.,* 2009 have indicated that there is a clear correlation between variations in cerebral arterial circulation and aneurysm development through the effects

of haemodynamic stress caused by the variations. The circulus arteriosus cerebri (CAC), a circular anastomosis of arteries at the base of the brain, is responsible for supplying blood to the brain and surrounding structures (Karatas *et al.*, 2015). The CAC may be divided into the anterior and posterior circulation. It is the anterior cerebral circulation that is reported to have the most anatomical variations (Makowicz, Poniatowska and Lusawa, 2013). Thus, the anatomical variation in the anterior cerebral circulation may increase the risk of intracranial aneurysms development (Gunnal and Wabale, 2013; Tahir *et al.*, 2019).

As further explained in chapter 2, the anterior communicating artery complex (ACAC) is a region within the anterior circulation of the CAC, consisting of the A1 segment and A2 segment of the anterior cerebral artery (ACA) and the anterior communicating artery (ACoA) (Krzyżewski *et al.*, 2015). This complex is said to be the most frequent site of cerebral aneurysms (Krzyżewski *et al.*, 2015; Tahir *et al.*, 2019; Shatri *et al.*, 2021). Gunnal *et al*. (2013) and Tahir *et al*. (2019) have also highlighted that A1 segment variations are the most frequent anomalies that accompany ACoA aneurysms. Hence, in addition to the high frequency of variation in the ACAC, there seems to be a link between the prevalence of intracranial aneurysms and anterior cerebral circulation variations.

The United States of America, Asia and Australia seem to produce most of the published literature, reporting on the anterior cerebral circulation and vascular variation. The epidemiology of intracranial aneurysms also remains poorly understood as these cerebral aneurysms remain underdiagnosed and inadequately treated locally (Tetinou *et al.*, 2021). Albeit, Africa has very limited research in this area, evidence from various regions including Morocco, South Africa, Nigeria, Egypt, Mali, Ghana, and Kenya suggests a higher prevalence of cerebral aneurysms in females. Across the study cohorts, the recorded prevalence in females was 54% (Tetinou *et al.*, 2021). Additionally, it has been reported that while cerebral aneurysms can occur at any age, they are more likely to occur after the age of 30 (Fréneau *et al.*, 2022). Furthermore, the women-to-men prevalence ratio of cerebral aneurysms have been reported to increase with age (Ghods *et al.*, 2012; Blignaut *et al*., 2014; Fréneau *et al.*, 2022). At the mean age of 40 years, the female predominance ratio has been reported to be between 1.1 to 1.57 (Ghods *et al*., 2012; Fréneau *et al.*, 2022). However, after the mean age of 50 years the female predominance is reported to be in between 2.2 to 4.16 (Fréneau *et al.*, 2022). This is in agreement with findings from studies that have been carried out in other countries such as in South America, Central America, Finland, and Japan, where it has been reported that women are twice as likely to have unruptured cerebral aneurysms than males (Fréneau *et al.*, 2022). According to a 2014 study conducted in South Africa, it was observed that among all recorded intracranial aneurysms in the study, the most prevalent cases were anterior communicating aneurysms (Blignaut et al., 2014; Luckrajh *et al.*, 2022a). The existing gap in literature, combined with the substantial impact of cerebrovascular diseases on morbidity in South Africa, emphasise the imperative need for additional research and understanding in this field.

Due to the limited research in this area in a South African context, understanding the basic anatomy of cerebral arterial supply and by extension the variations and the cerebral aneurysms that occur would be of great importance. Furthermore, gaining and understanding the knowledge behind ACAC variations will be of great use to the field of anatomy, clinicians, and neurosurgeons for the diagnosis of cerebral conditions such as aneurysms and strokes. Additionally, this knowledge will aid in the efficacy of neurosurgical and interventional procedures (Castro *et al.*, 2009; Jou *et al.,* 2010; Gunnal and Wabale, 2013; Iqbal, 2013).

1.1 Aim

The aim of this study was to investigate the morphological and morphometrical aspects of the ACA (A1 segment and A2 segment) and ACoA in a South African population. The origin, course, and the variations of the ACAC were assessed from human dissections and angiograms.

1.2 Objectives

To achieve these aims, the following objectives for a South African sample were studied:

1. To describe the prevalence of standard A1 and A2 ACA segments and their variations. (Both dissection and angiographic samples)
2. To describe the prevalence of the standard ACoA anatomy and its variations. (Both dissection and angiographic samples)
3. To measure the internal diameters of the A1, A2 segments of the ACA and that of the ACoA. (Angiographic sample)
4. To describe the prevalence of anterior cerebral circulation aneurysms. (Angiographic sample)
5. To explore the association between cerebral aneurysms and the prevalence of anterior cerebral circulation variations. (Angiographic sample)
6. To explore the association between anterior communicating circulation variations and demographic data in terms of age and sex. (Both dissection and angiographic samples)

Chapter 2. Literature Review

2.1 Blood supply to the brain

The human brain is dependent on sufficient arterial supply for maximal performance as the circulating blood provides the brain with oxygen and nutrients that it requires for the cells of the brain to perform optimally (Gupta, 2022). The circulus arteriosus cerebri (CAC), commonly known as the Circle of Willis is described as an arterial ring at the base of the skull in the region of the hypothalamus and cerebral peduncles encircling the pituitary gland (Du Toit, 2015; Gupta, 2022). The CAC gets its name from the physician Thomas Willis who described the ring-like nature of this region in 1664 (Feindel, 1962). It is the two internal carotid arteries (left and right), the basilar artery and the two vertebral arteries (left and right) that supply blood to this arterial network (Chandra *et al.*, 2017). Functionally, the CAC is the major arterial anastomosis in the brain that supplies the organ with oxygenated blood throughout the whole cerebral mass, allowing for the proper flow of blood from the arteries to both the anterior and posterior of the hemispheres (Tarulli *et al*., 2014; Chandra *et al*., 2017; Gupta, 2022).

This arterial anastomosis provides a crucial safety mechanism with regards to the blood flow to the brain (Van Den Bergh and Van Der Eecken, 1968). In essence, should there be prevention or slowing of blood flow due to a form of blockage or narrowing in one of the arteries in this network, it is compensated by a redirection of blood either by backward or forward flow in the CAC due to the change in pressure (Purves *et al*., 2001; Gupta, 2022). By extension, this type of mechanism could assist the blood flow from one side of the brain to the other if arteries on one half of the brain experience a reduced level of blood flow (Gupta, 2022). This is crucial in events such as a stroke, where this mechanism is said to reduce the aftermath or damage to the brain (Tarulli *et al.*, 2014). The CAC carries out this function in a passive manner and not an active one because it is the inherent circular shape of the ring and the effects of pressure in the area that allows for the bidirectional flow of blood in the circle (Shatri *et al.*, 2021). The carotid arteries run along the sides of the neck to eventually deposit into the CAC as cerebral arteries (Chandra *et al.*, 2017). In figure 2.1, an example of the anatomy of the CAC is seen.

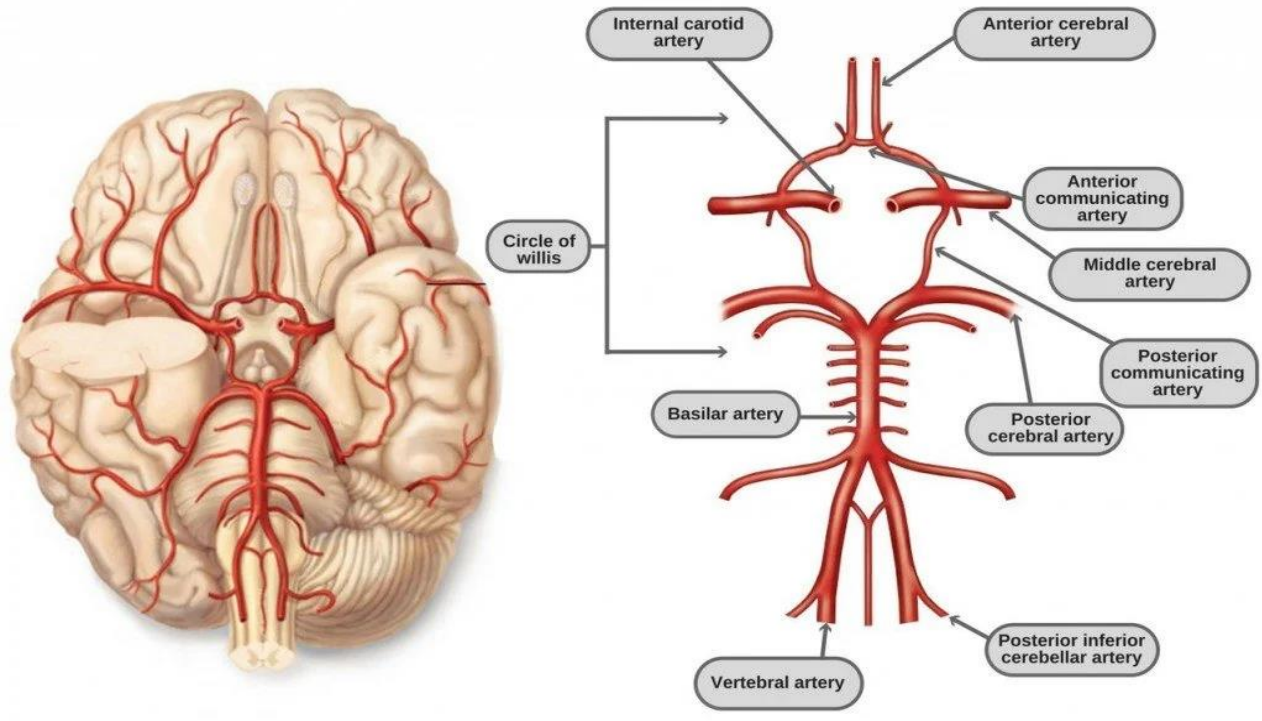

Figure 2.1: Basic anatomy of the circulus arteriosus cerebri (Purves *et al.*, 2001).

The left and right internal carotid arteries (ICA) and the left and right vertebral arteries are considered to be the two sources of blood supply to the brain (Purves *et al*., 2001; Avci et al., 2003). As seen in figure 2.2, it is at the level of the carotid sinus that branches of the common carotid arteries bifurcate to form the external carotid arteries (ECA) and ICA (Purves *et al.*, 2001).

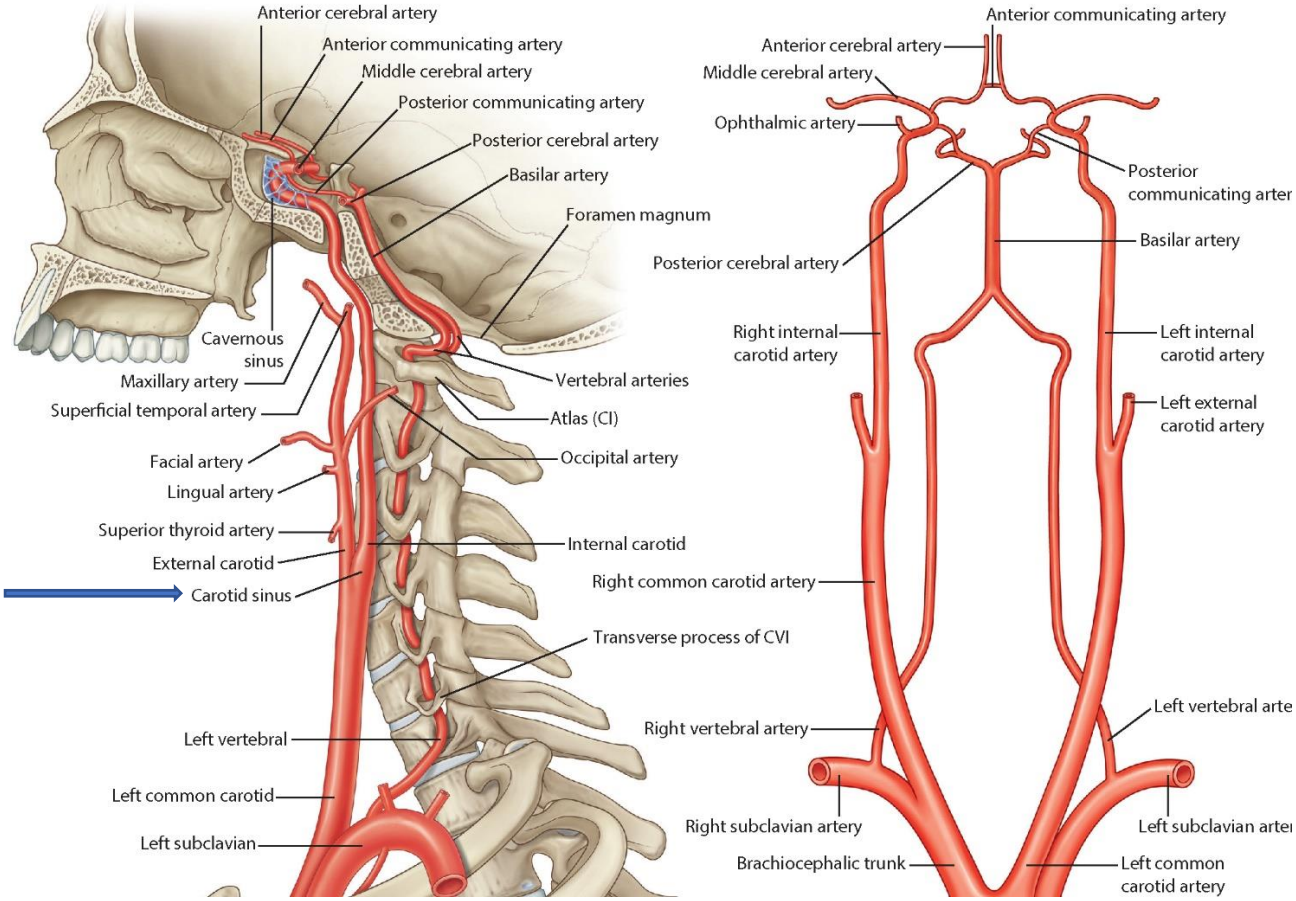

Figure 2.2: Diagram showing arterial supply of the brain (Standring, 2020).

*Blue arrow= carotid sinus

The ICA then crosses through the skull base through the carotid canal and travels superiorly before turning anteriorly and medially towards the foramen lacerum (Kayembe *et al*., 1984). They travel over the cartilage covering the foramen and travel further to reach the cavernous sinus where they emerge through the cavernous sinus to eventually reach the distal dural ring (Purves *et al.*, 2001). At this point, they will travel parallel and horizontal in an inferior and lateral position to the optic nerves to end where the posterior communicating arteries (PCoA) begin. The ICA supplies intracranial structures, including the eyes through the ophthalmic arteries (Purves *et al.*, 2001). The pre-terminal branch of the ICA is called the anterior choroidal artery (AChA) and it supplies various subcortical structures (Javed and M Das, 2022). The ACA supplies the medial portions of the frontal and parietal lobes and anterior portions of basal ganglia (Purves *et al.*, 2001). The ACA courses superior to the optic nerve forward and medially across the anterior perforated substance to the beginning of the lateral sulcus (Hacking and Safitiri, 2019). The ACA will then connect to the other ACA on the opposite side through the anterior communicating artery (ACoA). The anterior cerebral arteries will also connect to the posterior circulation through the posterior communicating arteries, smaller branches of the ICA that run backward to join with the posterior cerebral arteries (PCA) (Abuelnor, 2017; Hacking and Safitiri, 2019). As the ACA arches anteromedially and passes the anterior genu of the corpus callosum, it divides into two major branches namely, the pericallosal artery and the callosomarginal artery supplying the medial aspects of the cerebral hemispheres back to the parietal lobe (Avci *et al.*, 2003). It is the branches of the ICA that form

two vital cerebral arteries, being the anterior cerebral arteries (ACA) and middle cerebral arteries (MCA), which form the anterior circulation of the brain.

On the ventral surface of the brainstem, at the level of the pons, the midline basilar artery is formed by the joining of the left and right vertebral arteries (Purves *et al.*, 2001). The right and left posterior cerebral arteries arise from the basilar artery (BA) which lies in the pontine cistern. It follows a shallow groove on the ventral surface of the pons, extending to the upper pontine border (Javed, Reddy and M Das, 2022). Thus, the posterior circulation of the brain will include the posterior cerebral arteries, namely the basilar artery and the two vertebral arteries which collectively supply the posterior cortex, the midbrain and brainstem (Javed, Reddy and M Das, 2022). The basilar artery divides to give off the posterior cerebral arteries that curl around the cerebral peduncle and pass above the tentorium (Jones, 2009). From these arteries, the main vessels will supply the posterior portion of the brain.

The posterior circulation will connect to the anterior cerebral circulation through the posterior communicating arteries which are located at the back of the head at the end of the Circle of Willis (Jones, 2009). The posterior circulation of the brain will supply the back portion of the brain which includes the cerebellum, occipital lobes, and brainstem (Javed, Reddy and M Das, 2022; Luckrajh *et al.*, 2022).

2.2 The segments and branches of the anterior cerebral artery

As seen in figures 2.3 and 2.4, each anterior cerebral artery has five segments:

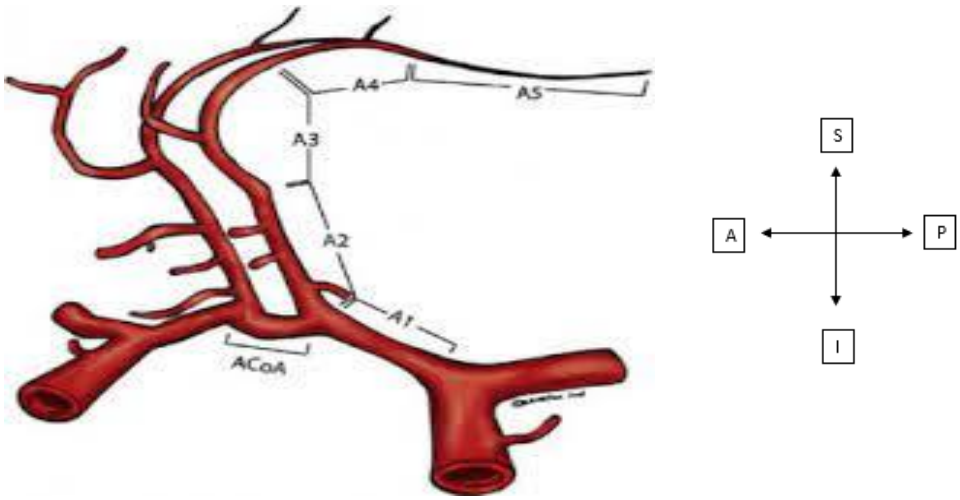

Figure 2.3: Segmental pattern of the anterior cerebral artery (Lehecka *et al.*, 2010).

Key: A1- Pre-communicating segment, A2- Post-communicating segment, A3- Precallosal segment, A4- Supracallosal segment, A5-Postcallosal segment, ACoA- Anterior communicating artery, S- superior, I- inferior, P- posterior, A- anterior

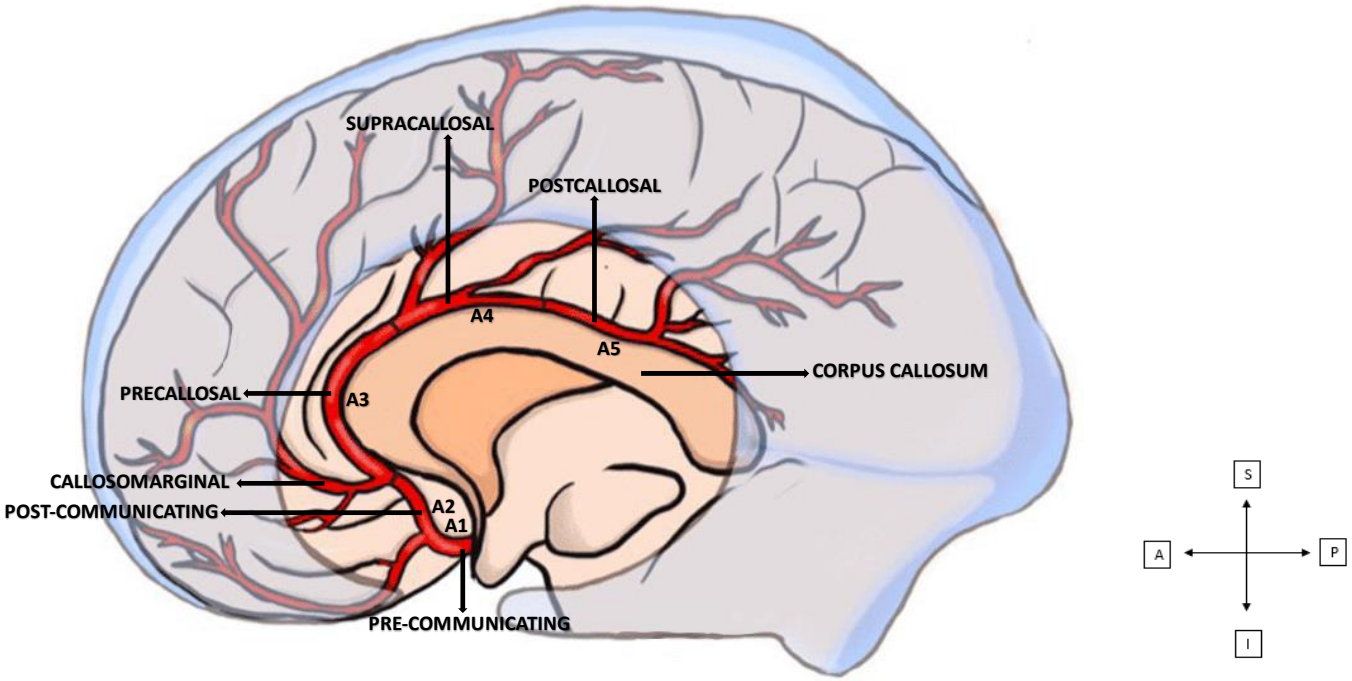

Figure 2.4: Segmental pattern and course of the anterior cerebral artery (Adapted from Bonasia and Robert, 2021).

Key: A1- Pre-communicating segment, A2- Post-communicating segment, A3- Precallosal segment, A4-Suoracallosal segment, A5-Postcallosal segment, S- superior, I- inferior, P- posterior, A- anterior.

After the origin of the ACoA from the distal A2 segment or in some cases from A3 segment, the pericallosal artery is defined. Thus, in the former instance, segment A2, A3 and A4-A5 are called the proximal, middle, and distal segments of the pericallosal artery, respectively (Gaillard, 2008a; López-Sala *et al.*, 2020). The ACA has two chief branching patterns, the first arrangement includes the callosomarginal artery arising from the A2 segment and the A2 segment proceeding on to be the pericallosal artery (Gaillard, 2008a). The callosomarginal artery will give off the terminal branches. In the second configuration the callosomarginal artery is not present thus the terminal branches arise directly from the pericallosal artery (Gaillard, 2008; Luckrajh et al., 2022).

A1: Pre-communicating segment

This segment is also referred to as the horizontal segment. The origin of this segment is from the terminal bifurcation of the ICA. It extends approximately 14mm in length and adjourns at the anterior communicating artery and gives rise to anteromedial central arteries known as the medial lenticulostriate arteries (Hacking and Safitiri, 2019).

A2: Post-communicating segment

This segment is also referred to as the vertical segment. The ACoA is the origin of this segment, thereafter the segment extends anteriorly to the lamina terminalis and alongside the rostrum section of the corpus callosum (Tahir *et al.*, 2019). The genu of the corpus callosum or the callosomarginal artery is the termination point of this segment. The medial striate artery (recurrent artery of Heubner), the orbitofrontal artery and the polar frontal artery are the three main branches that arise from this A2 segment (Avci *et al.*, 2003; Luckrajh *et al.*, 2022).

A3: Precallosal segment

This segment extends around the genu of the corpus callosum or distally to the origin of the callosomarginal artery where it eventually terminates posteriorly above the corpus callosum (Chandra *et al.*, 2017; Tahir *et al.*,

2019). The divisions that arise from this segment are the pericallosal artery and the callosomarginal artery which run in the cingulate sulcus (Avci *et al.*, 2003; Tahir *et al.*, 2019).

The callosomarginal artery and the distal portion of the pericallosal artery give rise to five principal cortical branches (Gaillard, 2008a). These branches include: orbitofrontal, frontopolar, internal frontal, paracentral and parietal arteries (Avci *et al.*, 2003; Gaillard, 2008a). The orbital branches which extend over the orbital region to the frontal lobe supply the olfactory cortex, medial orbital gyrus, and the gyrus rectus. Whereas the cingulate gyrus, corpus collosum (not including the splenium), medial frontal gyrus and the paracentral lobule are supplied by the frontal branches (Gaillard, 2008; Konan et al., 2023). The posterior-medial aspect of the superior parietal lobe which is referred to as the precuneus is supplied by the parietal branches (Konan, Reddy and Mesfin, 2023). Whereas the central cortical branches supply regions such as anterior perforated substance, lamina terminalis, rostrum of the corpus callosum, septum pellucidum, anterior portion of the putamen, caudate nucleus head and the anteromedial portion of the anterior limb of the internal capsule which is bounded by the head of the caudate nucleus (Gaillard, 2008a; Konan, Reddy and Mesfin, 2023).

A4: Supracallosal segment

The A4 segment runs anteriorly to the plane of the coronal suture, above the corpus collosum or in some cases medial to the cingulate gyrus (Avci *et al.*, 2003).

A5: Postcallosal segment

This segment runs posteriorly to the plane of the coronal suture, above the corpus callosum or in some cases medial to the cingulate gyrus (Avci *et al.*, 2003). In most cases, the A4 and A5 segments run along the callosal sulcus but in rare cases run medial to the cingulate gyrus (Gaillard, 2008a) . The ACoA forms the anterior border of the CAC and is generally described as an unpaired, short blood vessel approximately 4mm in length, that serves as the connection between the right and left anterior cerebral arteries (Gaillard, 2008b; López-Sala *et al.*, 2020; Gupta, 2022). There are various branches of this artery that supply several areas of the brain i.e. hypothalamus, optic chiasm, cingulate gyrus, para-olfactory areas, and the lamina terminalis (Iqbal, 2013).

Alongside the ACoA, the A1 and A2 segments of the ACA are collectively known as the ACAC (Luckrajh *et al.*, 2022). The middle cerebral artery is the largest branch and the second terminal branch of internal carotid artery (Chandra *et al.*, 2017; Vilela, 2019). This artery lodges in the lateral sulcus, the deep fold on the lateral surface of the hemisphere running anteriorly and posteriorly on the hemispheric surface that separates the temporal lobe from the parietal and frontal lobe (Javed, Reddy and Lui, 2022).The middle cerebral arteries additionally supply the majority of lateral surfaces of the hemispheres and temporal poles (Purves *et al.*, 2001). The multiplex system of cerebral arterial circulation and the possible variations that may occur in this system are closely related to the embryological development of the cerebral arterial circulation (Tahir *et al.*, 2019).

2.3 Embryological development of cerebral arterial circulation

Vascular system development in humans begins before the heart starts beating and is classified as two main stages, namely vasculogenesis and angiogenesis (Gerecht-Nir *et al.*, 2004). Vasculogenesis is the process by which de novo blood vessels form through the differentiation of precursor angioblasts whereby the hemangioblasts are differentiated into angioblasts (Gerecht-Nir *et al.*, 2004; Vilela, 2019; Bertulli and Robert, 2021). In contrast, angiogenesis is the process by which blood vessel formation occurs from pre-existing blood vessels through sprouting or remodelling (Van Den Bergh and Van Der Eecken, 1968). The vascular system supplying the brain is complex but follows a chronological order as seen in figure 2.5.

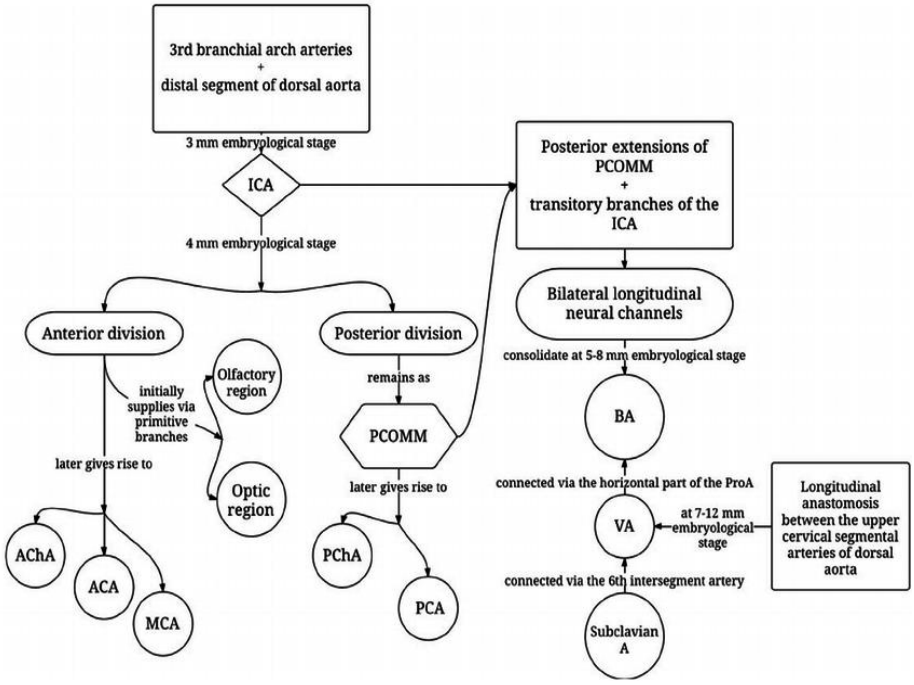

Figure 2.5: An illustration of the chronological order of the cerebral circulatory system development (Menshawi *et al*., 2015).
ICA-Internal carotid artery, PCOMM-Posterior communicating artery, AChA- Anterior choroidal artery, ACA-Anterior cerebral artery, MCA-Middle cerebral artery, ProA- Proatlantal artey PChA- Posterior choroidal artery, PCA- Posterior cerebral artery, BA- Basilar artery, VA- Vertebral artery, A- artery.

The major embryonic arteries are classified as either pharyngeal arch arteries (aortic arch arteries) or arteries of the trunk or limbs (Gerecht-Nir *et al.*, 2004). There are six pharyngeal arch arteries, as seen in figure 2.6, that arise in the embryo. However, not all six of these arteries persist throughout embryonic life (Casale and Giwa, 2022). At a cranial to rump length (CRL) of 1.3 mm, the first pharyngeal arch arteries form, which marks the beginning of the development of the circulatory system supplying the brain (Tahir *et al.*, 2019). Between a 3mm and 4mm CRL, ventral and dorsal divisions are made by the newly formed second branchial arch arteries (Tahir *et al.*, 2019). The dorsal divisions will connect to the cranial dorsal aorta which will later contribute to the formation of the internal carotid artery (Gerecht-Nir *et al*., 2004; Klostranec and Krings, 2022). The ventral portions of the second pharyngeal arch arteries will detach from the dorsal aorta giving rise to the ventral pharyngeal artery where the distal portion of the ventral pharyngeal artery will then be the precursor to the (Vilela, 2019; Bertulli and Robert, 2021). The common carotid artery (CCA) will then be formed from the proximal fusion of the ventral pharyngeal artery and the ICA (Casale and Giwa, 2022). The caroticotympanic artery will be the remnant of the second pharyngeal arch artery at the end of fetal development (Vilela, 2019).

At a CRL of 4mm, the third and fourth pharyngeal arch arteries appear (Klostranec and Krings, 2022). The proximal portion of the ICA is said to be formed from the fusion of the third pharyngeal arch arteries and the distal segments of the paired dorsal aortae (Vilela, 2019). Thereafter, there is a bilateral regression of the dorsal aorta, between the third and fourth pharyngeal arteries (Klostranec and Krings, 2022). The aortic arch on the left and the proximal subclavian artery on the right both are contributed to by the fourth pharyngeal arch artery. It is the 7th intersegmental artery that will contribute to the distal portion of the right subclavian artery (Menshawi *et al.*, 2015; Klostranec and Krings, 2022).

The presence of the fifth pharyngeal arch artery is considered a point of contention as it said to exist for a very short amount of time and has little to no contribution (Gupta, Gulati and Anderson, 2016). After the 4mm CRL, if the fifth pharyngeal arch artery had been present at all it would disappear completely (Casale and Giwa, 2022).

The sixth pharyngeal arch artery appears between 5mm and 7mm CRL (Klostranec and Krings, 2022). This artery becomes continuous with the pulmonary trunk where branches will extend to the lungs as pulmonary arteries. The more dorsal aspect of this will remain attached to the dorsal aorta (Klostranec and Krings, 2022). This attachment is known as the ductus arteriosus. The ductus arteriosus will direct blood from the pulmonary trunk to the embryonic and fetal dorsal aorta (Klostranec and Krings, 2022).

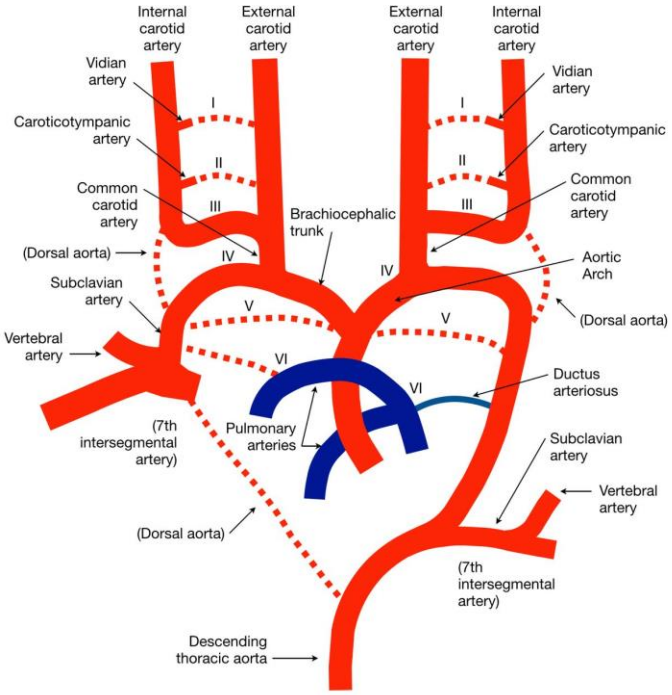

Figure 2.6: Pharyngeal arch arteries and the final adult form of the aortic arch and origins of the great vessels. The transient vessels are represented with dashed lines (Klostranec and Krings, 2022).
I- First pharyngeal arch artery, II- Second pharyngeal arch artery, III- Third pharyngeal arch artery, IV- fourth pharyngeal arch artery, V- Fifth pharyngeal arch artery, VI-Sixth pharyngeal arch artery

The ICA will also have had divided into an anterior and posterior section at the 4mm CRL (Bertulli and Robert, 2021). Through primitive arteries, the optic nerve and olfactory areas will be supplied by the anterior section (Menshawi *et al*., 2015). Eventually, the ACA, MCA, and the anterior choroidal artery (AChA) will be generated by this anterior division (Menshawi *et al.*, 2015; Casale and Giwa, 2022). Whilst the posterior division will give rise to the posterior cerebral artery (PCA) and the posterior choroidal artery (PChA) (Javed and M Das, 2022). The initial stimulus for posterior circulation formation is the growth of the occipital lobe and brainstem, initially with the basilar artery (BA) and at a later stage, the vertebral arteries (VA) (Menshawi *et al.,* 2015). At a 4mm CRL, the future posterior fossa is supplied by two neural arteries (Klostranec and Krings, 2022). These parallel neural arteries receive their blood supply from carotid-vertebrobasilar anastomoses supplied by the trigeminal artery (TA), the otic artery (OA), the hypoglossal artery (HA), and the proatlantal artery (ProA) *(Menshawi et al.*, 2015). During the 5mm-8mm CRL, the basilar artery (BA) is formed through the association of the neural arteries (Vilela, 2019). The three segmental arteries, TA, OA, and HA degenerate when the posterior communicating artery (PCOMM) grows and joins with the distal segment of the BA. In contrast, the ProA will be present up until the full development of the VA (Menshawi *et al.,* 2015).
Eventually, the ACoA is formed when the ACA grows in a medial direction towards the contralateral ACA at the 21-24mm CRL (Castro *et al.*, 2009). When the fetal PCA converts into the PCOMM, the posterior portion of the circle of Willis is formed (Klostranec and Krings, 2022). The full development of the ACA and ACoA will be an indication of the adult circle of Willis (Castro *et al.*, 2009; Menshawi *et al.*, 2015; Bertulli and Robert, 2021).

2.4 Developmental variations in the cerebral circulatory system

Various literature unanimously support that embryological development is the causative factor for anatomical cerebral arterial variations (Gunnal and Wabale, 2013; Menshawi *et al*., 2015; Burlakoti *et al.*, 2020). It is the complex nature of the embryology of intracranial circulation that allows for a variety of anatomical cerebral arterial variations (Menshawi *et al*., 2015). The most common variations include fenestrations, duplication and hypoplasia alongside other variations (Gunnal and Wabale, 2013; Burlakoti *et al.*, 2020). In the CAC, anterior cerebral circulation variations vary and are reported to be most frequent in the ACAC (Figure 2.7).

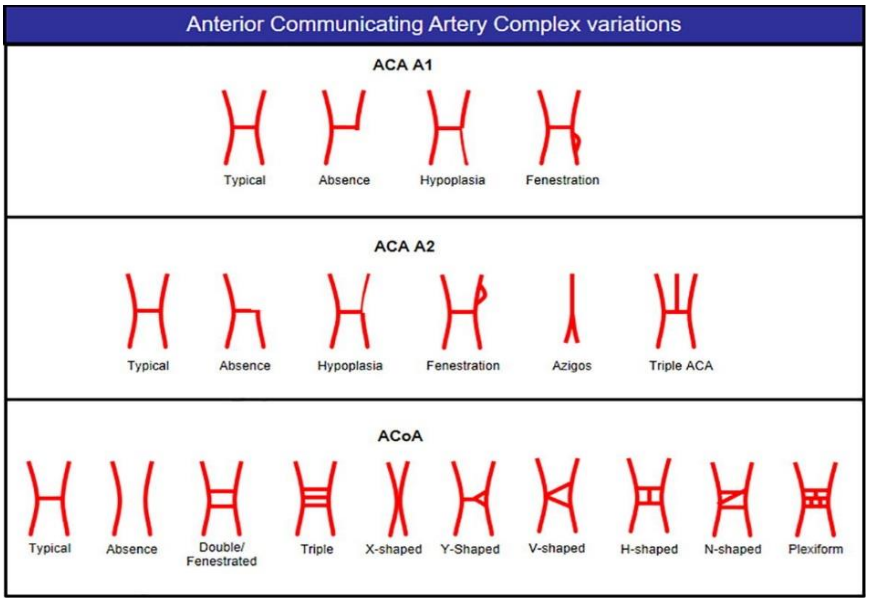

Figure 2.7: Anterior Communicating Artery Complex variations (López-Sala et al., 2020). ACA- anterior cerebral artery, A1- pre-communicating segment, A2- post-communicating segment, ACoA- anterior communicating artery

There are distinct differences between these variations. Together with fenestrated arteries, duplicated arteries are reported to be among the most frequent arterial variations (Iqbal, 2013; Abuelnor, 2017). Fenestrations occur when the arterial lumen of a vessel splits resulting in two separate channels that will eventually re-join (Kayembe *et al.,* 1984; Kovač *et al.*, 2014). This variation is reported to have a prevalence range of 0.3% to 28% depending on study methods used during investigations or research (Kayembe *et al.,* 1984; Kovač *et al.*, 2014; Abuelnor, 2017). Duplications differ from fenestrations as they are described as two arteries that have separate origins that later fuse downstream at a distal arterial segment (Menshawi et al., 2015).

The A1 segment is amongst the most frequent sites of anatomic variation which normally involves ACoA variations (Kayembe et al., 1984; Iqbal, 2013). Duplication, azygous ACA, or accessory ACA are some examples that usually occur at this segment. Tahir *et al*. (2019) reported that fused A2 segments or azygous ACA is found in up to 2% of the population. This variation is one midline artery that occurs due to the convergence of both A1 segments and the absence of the ACoA (Tahir *et al.*, 2019). In contrast, a bihemispheric ACA occurs when both A2 segments are present but one is dominant, and the other is hypoplastic or terminates early (Tahir *et al.*, 2019). A small medial ACA or third A2 segment arising from the ACoA is very rare in humans but is normally present in many vertebrates (López-Sala *et al.*, 2020).

There are various variants of the ACoA. Duplication and fenestrations are significantly common in the ACoA, recorded at 18% and 21% respectively (López-Sala *et al.*, 2020). The absence of this vessel has also been reported in 5% of surgical dissections although difficult to see in angiography because of its size (López-Sala *et al.*, 2020).

Tables 2.1, 2.2 and 2.3, show various anatomical variations of the A1 segment, A2 segment and ACoA. The incidence of variations is recorded and noted as percentages.

Table 2.1: **Summary of variations found in the A1 segment of the anterior cerebral artery.**

AUTHOR (YEAR)	REGION	MORPHOLOGICAL VARIANTS OF THE A1 SEGMENT OF THE ANTERIOR CEREBRAL ARTERY (%)					
		Agenesis	Hypoplasia	Duplication	Fenestration	Aplasia	Bihemispheric
Lopez-sala et al. (2020)	Spain	10.6	31.2	-	0.5	-	-
Sahin et al. (2018)	Turkey	-	14.6	-	1.06	-	4.53
Shatri et al. (2018)	Kosovo	5.65	-	-	-	2.55	-
Hossain et al. (2017)	India	-	13.3	-	-	5.3	-
Jiménez-sosa et al. (2017)	Mexico	5.65	5.30		2.12		
Cilliers et al. (2016)	South Africa	-	-	-	-	-	20
Rooprashee et al. (2016)	India	2	2	-	-	-	-
Zampakis et al. (2015)	Greece	0.4	27	-	-	9	-
Krzyzewski et al. (2014)	Poland	-	24	-	-	12	-
Gunnal et al. (2013)	India	1.8	8	1.1	-	-	-
Ansari et al. (2011)	USA	-	1	-	-	-	-
Zhao et al. (2009)	China	-	-	-	0.8	-	-
Uchino et al. (2006)	Japan	-	-	-	1.2	5.6	-

– refers to the absence of observations for a particular variation in that study.

Table 2.2 shows an example of the various studies showing the variations in the A2 segment of the anterior cerebral artery.

Table 2.2: Summary of variations found in the A2 segment of the anterior cerebral artery.

AUTHOR (YEAR)	REGION	MORPHOLOGICAL VARIANTS OF THE A2 SEGMENT OF THE ANTERIOR CEREBRAL ARTERY (%)							
		Agenesis	Hypoplasia	Fenestration	Azygous ACA	Triple ACA	Bihemi-spheric	Terminal Branches	Aplasia
Lopez-sala et al. (2020)	Spain	0.2	8.5	-	1.4	5.2	-	-	-
Hossain et al. (2017)	India	5.3	48	48	-	-	-	-	-
Jiménez-sosa et al. (2017)	Mexico	0.35	4.25	-	1.76	3.88	-	-	-
Cilliers et al. (2016)	South Africa	-	-	-	-	14.3	-	-	-
Rooprashee et al. (2016)	India	-	-	-	-	-	6.6	-	-
Krzyzewski et al. (2014)	Poland	-	4	-	-	-	-	-	2
Gunnal et al. (2013)	India	-	3.6	-	4.4	-	-	5.4	-
Zhao et al. (2009)	China	-	-	-	0.5	-	-	-	-
Uchino et al. (2006)	Japan	-	-	0.18	-	1.2	-	-	-

- refers to the absence of readings for a particular variation in that study.

Table 2.3 shows an example of the various studies showing the variations in the anterior communicating artery.

Table 2.3: **Summary of variations found in the anterior communicating artery.**

AUTHOR (YEAR)	REGION	MORPHOLOGICAL VARIANTS OF THE ANTERIOR COMMUNICATING ARTERY (%)									
		Agenesis	Dupli-cation	Fenes-tration	Triple	X-shaped	Y-shaped	Plexi-form	Hypo-plasia	Aplasia	Short
Lopez-sala et al. (2020)	Spain	4.7	-	0.9	0.2	1.2	0.2	0.2	-	-	-
Sahin et al. (2018)	Turkey	3.86	10.6	10.6	-	-	-	-	-	-	-
Shatri et al. (2018)	Kosovo	15.66	0.6	3.89	-	-	-	-	15.66	-	-
Cilliers et al. (2017)	South Africa	48.7	17.9	-	-	-	5.1	-	33.3	-	-
Hossain et al. (2017)	India	-	-	12	-	-	-	-	10.7	-	-
Jiménez-sosa et al. (2017)	Mexico	-	0.35	-	0.35	3.18	-	-	14.13	-	
Rooprashee et al. (2016)	India	-	-	21	-	-	-	-	-	-	-
Krzyzewski et al. (2014)	Poland	-	-	-	-	-	-	-	36	-	-
Gunnal et al. (2013)	India	-	9.8	4.5	-	-	-	-	5.4	-	11.6
Ansari et al. (2011)	USA	-	-	-	-	-	-	-	11	1	-

- refers to the absence of readings for a particular variation in that study.

2.5 Cerebral aneurysms and their link to anterior cerebral circulation

Swartbooi *et al*. (2016), identified that there is a gap in the literature pertaining to aneurysm characteristics within the South African population. Cerebral aneurysms are classically divided into status, shape, and size and depending on the size of these aneurysms, symptoms vary in severity (Kayembe *et al.,* 1984; Brisman, Song and Newell, 2006). There are three types of cerebral aneurysm, namely saccular, fusiform, and mycotic aneurysms (Brisman, Song and Newell, 2006). Figures 2.8 and 2.9 show these different types of cerebral aneurysms.

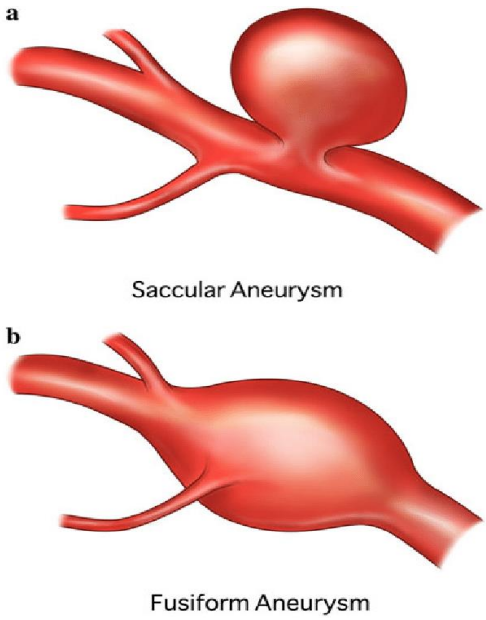

Figure 2.8: An illustration of saccular and fusiform cerebral aneurysms (Withers and Carolan-Rees, 2013).

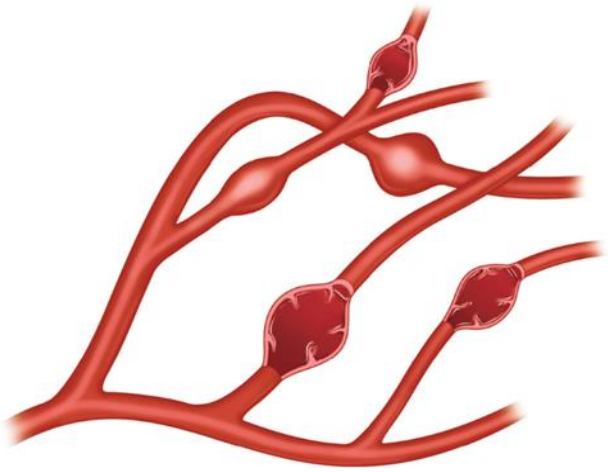

Figure 2.9: An illustration of mycotic aneurysms (Ren, 2022).

Saccular aneurysms are sometimes also referred to as berry aneurysms (Kayembe *et al.*, 1984. These are often described as rounded sacs that contain blood and are also adhered to the main artery or a branch of the main artery (Brisman, Song and Newell, 2006). Saccular aneurysms are said to account for as much as 95 % of all unruptured aneurysms (Burlakoti *et al.*, 2020; Jersey, 2022). These aneurysms are said to be the most common anterior circulation aneurysms (Feng *et al.*, 2014). A fusiform aneurysm is said to bulge out on all sides of an artery and these aneurysms account for 3-13% of all intracranial aneurysms. Mycotic aneurysms which account for 1.4% of all aneurysms, are said to occur when a bulging aneurysm occurs because of infection to the arteries of the brain (Burlakoti *et al.*, 2020).

As seen in Table 2.4, the sizes of cerebral aneurysms vary. They can be considered very small, medium, large, and very large (Backes *et al.*, 2014).

Table 2.4: Aneurysm categories and associated sizes.

ANEURYSM CATEGORY	SIZE
Very small	<3mm
Small	3mm – 6mm
Medium	7mm – 12mm
Large	13mm – 25mm
Very large	>25mm

There are many risk factors that are associated with cerebral aneurysms (Andreasen *et al.*, 2013; Orakdogen *et al.*, 2017). Sometimes the risk factors are inherited, or they develop over time. Some inherited risk factors include genetic connective tissue disorders that weaken artery walls and also polycystic kidney disease (Andreasen *et al.*, 2013). Other risk factors include untreated high blood pressure, cigarette smoking and drug abuse (cocaine or amphetamines) (Kayembe *et al*., 1984. Head injury, intracranial infection and brain tumours are said to be less common risk factors (Ogeng'o *et al.*, 2009).

Individuals with cerebral artery variation in the region of the anterior circulation are considered to be at risk of developing ACoA cerebral aneurysms or other cerebrovascular pathologies because of the imbalance in cerebral blood flow that occurs as a result of the variations (Ogeng'o *et al.*, 2009; Andreasen et al., 2013; Orakdogen *et al.*, 2017). The complex nature of the anterior cerebral circulation and the inherent variant morphologies resulting from such complexity, have been widely discussed in the literature (Van Den Bergh and Van Der Eecken, 1968; Krzyżewski *et al.*, 2014; Tahir *et al*., 2019; Shatri *et al.,* 2021) . The ACoA is said to be the most frequent site of cerebral aneurysms and many studies have highlighted that ACA (A1) variations are the most frequent anomalies that accompany ACoA aneurysms (Gunnal and Wabale, 2013; Tahir *et al.*, 2019). Furthermore, a high frequency of variation in the anterior cerebral circulation, namely the A1 segment, A2 segment and ACoA has been reported in various studies.

Cerebral artery variations are said to cause a hemodynamic force shift where optimum blood circulation is negatively affected (Castro *et al.*, 2009). Furthermore, it is believed that there is a correlation between the initiation and development of an aneurysm and hemodynamic force and vascular wall sheer stress (Wang *et al.*, 2013).

Increase in hemodynamic wall shear stress due to the impact of blood flow has been shown in various experimental glass model studies, computational fluid dynamic studies and in vivo studies to be one of the main risk factors that initiate intracranial aneurysm formation (Abuelnor, 2017). These aneurysms are reported to arise where the vessels are exposed to the maximum impact of hemodynamic stress. It is this hemodynamic stress that is said to be responsible for damage to the arterial wall (Wang *et al.*, 2013). This damage is mainly distinguished by a disrupted internal elastic lamina, fibronectin loss, smooth muscle cell loss and reduced smooth muscle cell proliferation (Abuelnor, 2017; Orakdogen *et al.*, 2017).

It has been shown that asymmetry of the A1 segments of the ACAC have a significant correlation with cerebral aneurysm formation at the junction of the dominant A1 segment and the ACoA or directly in the ACoA (Burlakoti *et al.*, 2020). It is hypothesized that it is the increased blood flow in the vessel with a larger diameter, which in turn increases the hemodynamic stress, that is responsible for this aneurysm formation (Burlakoti *et al.*, 2020; Sharma *et al.*, 2023).

Using glass models of the ACAC, a direct relationship between increased asymmetry of the A1 segments of both ACAs or increased flow in one of the two A1 segments and increased hemodynamic wall shear stress on

the ACoA was shown (Ujiie *et al.*, 1996). These results are also reflected in observations of vascular anomalies in humans and computational studies (Abuelnor, 2017).

Burlakoti *et al.* (2020) also recently reported that the likelihood of ACoA aneurysm development is predicted to be greater than 80% when the asymmetric ratio (larger vascular diameter/ smaller vascular diameter) between the left and right A1 segments is 1.42 or more (Burlakoti *et al.*, 2020). This further suggests that the size (diameter and length) of individual vessels of the CAC vary between a person with an aneurysm and people without aneurysms (Burlakoti *et al.*, 2020). Furthermore, the presence of aneurysms is shown to not be dependent on the average size of the blood vessels but rather on the overall morphological and morphometric variations of the individual segments of the cerebral basal arterial network (Abuelnor, 2017; Burlakoti *et al.*, 2020; Sharma *et al.*, 2023). Burlakoti et al. (2020) also highlighted that minimally variant segments of the CAC serve to efficiently equalize blood pressure spikes and thus prevent cerebral aneurysm development.

The hypoplastic or absent A1 segment variations were reported to also increase the incidence of aneurysm development, not only in the ACoA but also in the MCA and ICA as a result of the hemodynamic stress (Feng *et al.*, 2014; Burlakoti *et al.*, 2020; Sharma *et al.*, 2023). A direct link between intracranial aneurysm occurrence and anterior circulation variations is thus supported by literature stress (Feng *et al.*, 2014; Burlakoti *et al.*, 2020; Sharma *et al.*, 2023). Anterior cerebral morphological and morphometric variation may therefore, pose as a potential risk factor for intracranial aneurysm formation (Burlakoti *et al.*, 2020).

2.6 A brief history of angiography and neuroradiological imaging

Neuroradiology is a subset of radiology that focuses on the treatment and diagnosis of neurological diseases and disorders (Hoeffner *et al.*, 2012). Neuroradiology is vital in the ability to identify and treat issues with the brain, nerves, and spinal cord without having to use invasive procedures (Bull, 1970; Hoeffner *et al.*, 2012). The history of neuroradiology is extensive and involves a variety of interventional procedures.

Angiography use began in the early 19th century (Wilms and Baert, 1995). When Wilhelm Konrad Roentgen discovered X-rays in 1895, pursuing different experimental methods that explore the possibilities of x-ray began (Kamal *et al.*, 2020). Following exploring the development of ventriculography and pneumoencephalography (PEG), Egaz Moniz, a Portuguese physician and neurologist in 1927, pursued an interest in imaging centred on cerebral vasculature using radiopaque media contrast to investigate brain tumours (Bull, 1970; Wilms and Baert, 1995). Vascular radiographic technology to obtain better visualized imaging had continued to advance, refine, and improve such as when Seldinger developed the cerebral angiography technique in 1953 (Hoeffner *et al.*, 2012; Kamal *et al.*, 2020). Thereafter, computed tomography (CT) was used to observe vasculature and other organs in the 1960s. Alongside CT, modalities such as magnetic resonance images (MRIs), Positron emission tomography (PETs) and other ultrasound modalities are used today as diagnostic tools in neuroradiology (Hoeffner *et al.*, 2012).

2.7 Magnetic Resonance Angiography

The modality used in this study for neuroimaging is magnetic resonance. Magnetic resonance imaging (MRI) is a non-invasive technique that does not use radiation. It is used for obtaining structural and functional information for the human body and cerebral vasculature (Berger, 2002). This modality also has the capability of differentiating between vascular flow and nearby tissue and giving further insight into cerebrovascular diseases which is more accurately referred to as magnetic resonance angiography (MRA) (Berger, 2002).

The human body, which includes cerebral tissue, is largely made up of protons (hydrogen atoms) (Berger, 2002; Du Toit, 2015). The hydrogen atoms have a nucleus, electrons and two poles, namely North and South, that are continuously spinning on an angulated axis. This behaviour can be likened to a small 'bar magnet'(Berger, 2002). In the human body, under normal conditions, these protons spin with randomly aligned axes. However,

when the human body is placed in an MRI machine, which has a very strong magnetic field, the axes of these protons are uniformly organized (Berger, 2002). When a patient undergoes an MRI examination, they become the magnet, with all the protons in the body aligning along the strong magnetic field created by the MRI machine and spinning at an angle with a particular frequency (Berger, 2002). A magnetic vector is then created that is adjusted to the axes of the MRI scanner. The field strengths of MRI scanners vary between 0.5 to 1.5 tesla (Kapsalaki, Rountas and Fountas, 2012). When supplementary energy in the form of a radio wave is added to the magnetic field, there is a deflection of the magnetic vector (Tang *et al.*, 2019). A radio wave is an electromagnetic wave. When a radiofrequency pulse (RF) occurs, it is when radio wave is transmitted as rapid blast into the magnet that contains the patient (Berger, 2002). The 'resonance' in magnetic resonance imaging is then only produced when protons absorb the energy from the radio wave which can only occur when strength of frequency of the RF aligns with the frequency strength of the spinning protons (Berger, 2002). This results in pulse cancelation of magnetic effects of particular protons and elevates the magnetic effects and energy levels of other protons (Berger, 2002; Tang *et al.*, 2019). Thereafter, when the radio wave source is switched off and the magnetic vector returns to a state of resting, this emits a signal (Tang *et al.*, 2019). The protons that had experienced pulse cancellation return to a state of relaxation (original state and strength of magnetisation) which is categorised as a time constant T1. Similarly, the protons that had experienced higher levels of magnetisation and energy begin to lose their energy which is categorized at a time constant T2 (Berger, 2002; Tang *et al.*, 2019). Receiver coils that are around a particular area interest of the body will act as antennas to detect the emitted signal (Berger, 2002). A computer will then characterise the emitted radio waves from all points from the section of interest of the body and an MRI image is produced. (Du Toit, 2015; Tang *et al.*, 2019).

2.7.1 Time-of-flight Magnetic Resonance Angiography

The most conventional MRA techniques used to visualised arteries and veins are classified as phase contrast MRI, contrasted enhanced MRI and time of flight (TOF) (Berger, 2002; Bashir, 2012; Tang *et al.*, 2019). For this study, the TOF MRA technique, which is based on tesla, was used in the angiographic portion of this study. Time of flight MRA is a non-invasive and non- contrast enhanced MRA technique that can distinguish between stagnant tissue and blood vessels by manipulating magnetisation (i.e., blood inflow effects) (Tang *et al.*, 2019). This technique allows for better opacification of arteries that contain fast or continuous blood flow, such as intracranial arteries and removes venous contamination. (Berger, 2002). Figure 2.10 shows the difference in imaging between Time of flight MRA and contrast enhanced MRA.

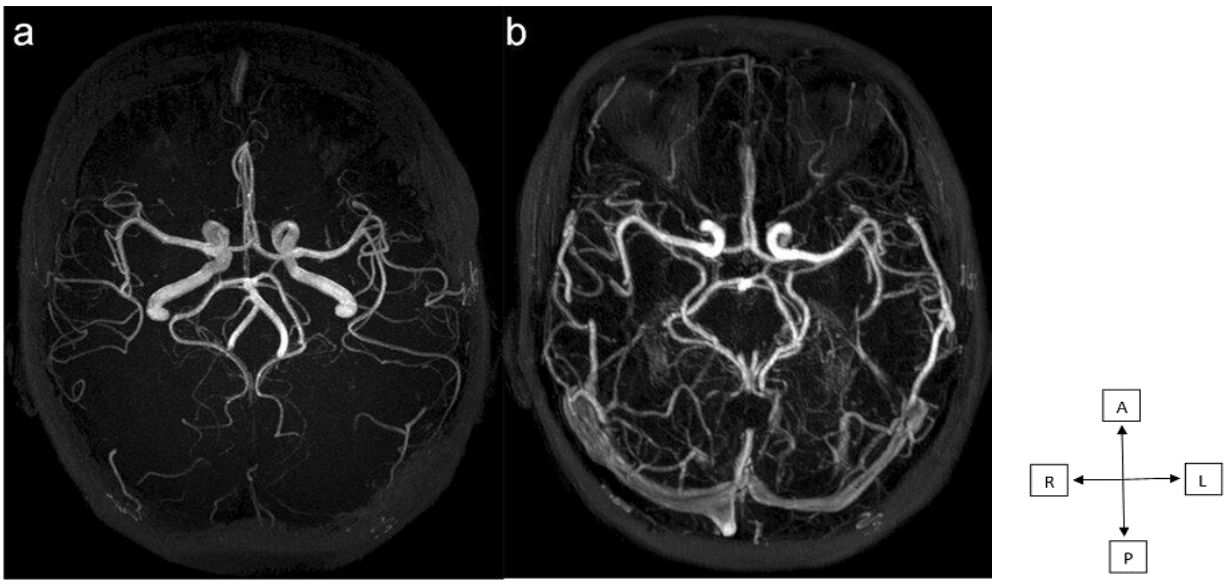

Figure 2.10: Brain MRA using (a) Time-of-flight MR angiography (TOF-MRA) and (b) contrast-enhanced MR angiography (Abousrafa and Mair, 2023). A- Anterior, P-Posterior, L-left, R-right.

2.8 Clinical significance of the present study

Amongst other modalities for treating intracranial aneurysms, endovascular coiling has become the primary intervention used by vascular neurosurgeons (Luckrajh *et al.*, 2022). Although this procedure has become popular because of its minimally invasive nature and reduction in risk during procedures in comparison to other modalities, unfavourable aneurysm formation and unexpected anatomical variations of vessels still pose significant challenges (Luckrajh *et al.*, 2022).

A high aneurysm rupture risk has been associated with anterior circulation aneurysms (Dhar *et al.*, 2008). ACAC aneurysms have been reported to be most likely to rupture compared to aneurysms that may be present elsewhere in the CAC (Jirjees *et al.*, 2020). Therefore, gaining and understanding the knowledge behind ACAC variations will be of great use to clinicians and neurosurgeons for the diagnosis and possible prevention of cerebral conditions such as aneurysms and strokes. Additionally, this knowledge will aid in the efficacy of neurosurgical and interventional procedures (Castro *et al.*, 2009; Jou *et al.*, 2010; Gunnal and Wabale, 2013; Iqbal, 2013).

Chapter 3: Materials and Methods

3.1 Study design

The study was descriptive, cross-sectional, and observational. The nature of this study encompasses both qualitative and quantitative aspects. Two methods employed in the study were the dissection of human bodies and the analysis of retrospective magnetic resonance angiographic data. The study comprised of a morphological component during the dissection phase and included both morphological and morphometric components in the angiographic phase.

3.2 Setting

The dissection component of this study was carried out in the Department of Human Biology at the University of Cape Town in Cape Town, South Africa. Data was made up by the observing ACAC morphological variations of human brains from 2022 - 2023. The angiographic component of this study was carried out in the Radiology Department at Groote Schuur Hospital in Cape Town, South Africa with data made up of observed morphological and morphometric ACAC variations from magnetic resonance angiograms (MRA) in 2023.

3.3 Sampling

This study used a non-probability purposive sample. For the dissection component, a sample population consisting of n= 89 formalin fixed human bodies (41 in 2022 and 48 in 2023) from the Department of Human Biology at the University of Cape Town were made available for dissection and observation. The sample population for the angiographic component of this study included n= 220 MRA images from individuals who underwent CAC MRA imaging at Groote Schuur Hospital between 1 January 2018 and 1 January 2023.

3.4 Sample size

As shown in figure 3.1, a total of 89 bodies (41 in 2022 and 48 in 2023) were available for dissection but after applying the exclusion criterion, only 68 bodies (35 female and 33 male) were included in this study. Post the application of the exclusion criteria on 220 MRA images, the sample size of the patient angiographic images used for this study only included 208 applicable MRA images, as shown in figure 3.2 and figure 3.3, (151 female and 57 male) from 1 January 2018 to 1 January 2023 from the Radiology department of Groote Schuur Hospital.

3.4.1 Inclusion and exclusion criteria for dissection sample

Brain samples were assessed by researcher for tissue damage and macroscopic evidence of pathology, and only those that showed no signs of damage and pathology were included in the study. Additionally, individual arteries that were damaged during dissection and/or undergraduate and post-graduate learning and research, where accurate observations could not be made, were excluded. Arteries that showed any macroscopic evidence of pathology were also excluded from this study.

3.4.2 Inclusion and exclusion criteria for angiograph sample

Magnetic resonance angiographs dating from 1 January 2018 to 1 January 2023 were included in this study. Only images that had a three-dimensional time of flight (3D-TOF) sequence were used. MRA images that had severe susceptibility artefact presence that obscured or hindered the visualisation of the arteries were excluded from the study. Individual arteries that were obscured or compromised by the presence of

endovascular coiling or other surgical intervention were excluded for morphometric and/or morphological analysis.

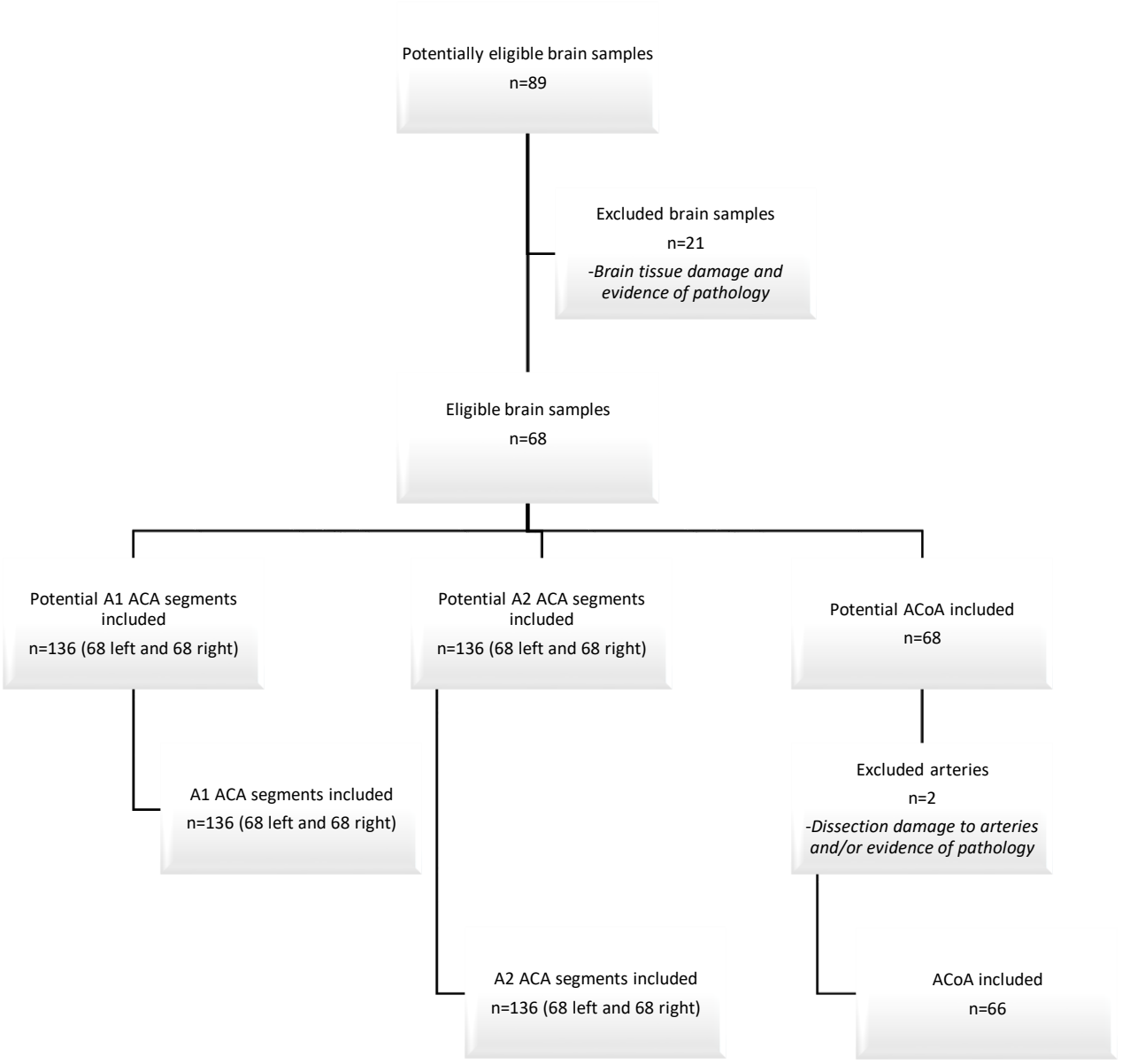

Figure 3.1: Procedure of sampling in the dissection component of the study.

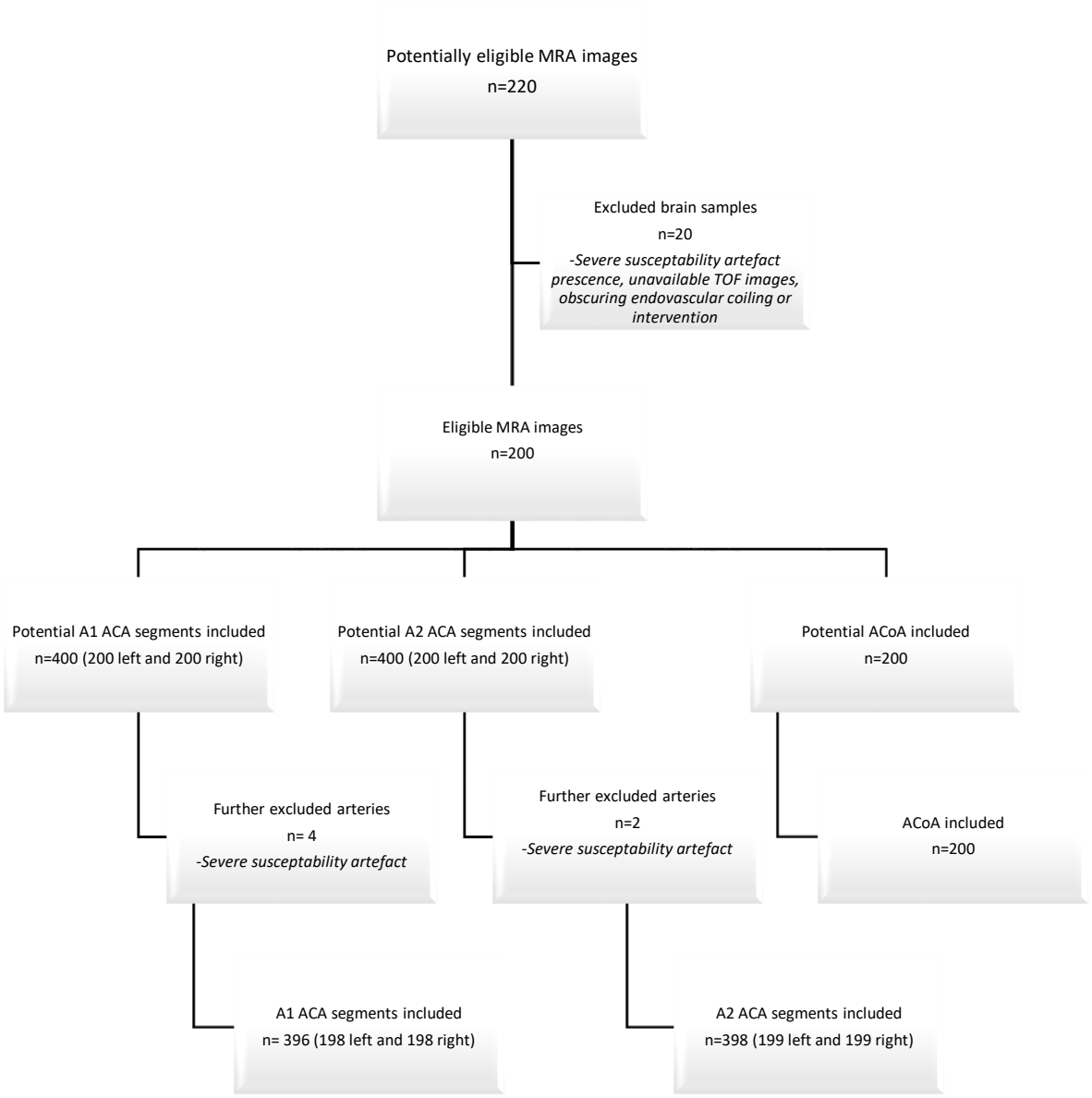

Figure 3.2: Procedure of sampling for morphological variations in the angiographic component of the study.

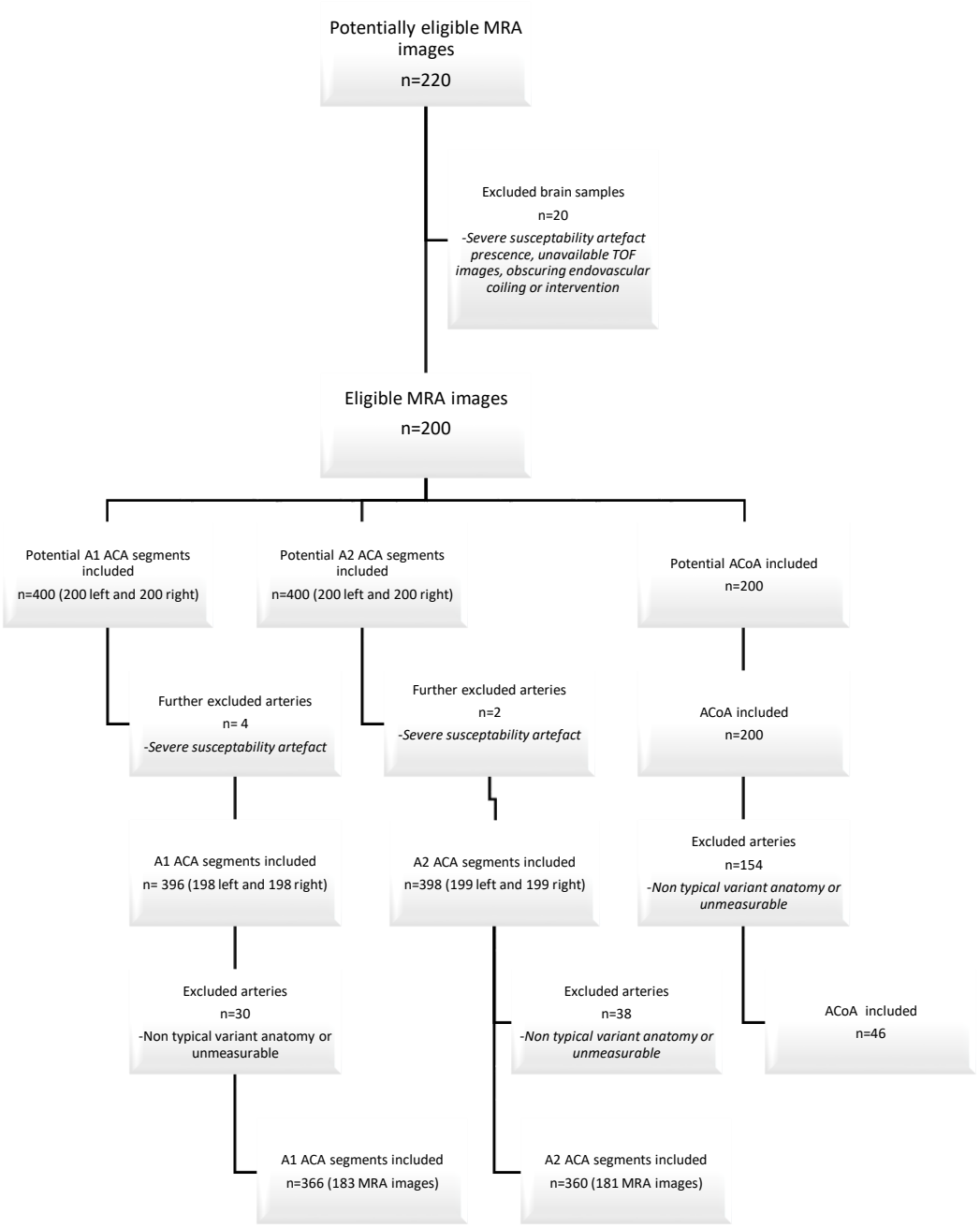

Figure 3.3: Procedure of sampling for morphometric analysis in the angiographic component of the study.

3.5 Research procedure

3.5.1 Dissection study

To study the anterior circulation of the brain samples included in the study, a set dissection approach was used to remove the brains from the bodies. The calvarium of all the skulls were opened with the assistance of anatomy technical staff using an oscillating saw. The vault of the skulls were then lifted and removed. A dissection kit was used by the researcher for the dissection procedure. The dissection kit included dissection scissors, forceps, a dissecting needle, scalpels, and scalpel blades.

The dura mater that lines the inside of the skull and surrounds the brain was removed to ensure complete isolation of the brain. In the anterior portion of the cranium, the falx cerebri adheres to the crista galli, using a scalpel, and forceps, the falx cerebri was then detached from the crista galli. The frontal lobes of the cerebral hemispheres were lifted upward to reveal the olfactory bulbs and tracts which were incised to free them from the brain. Thereafter, the optic nerves were cut at the optic chiasm.

Then at the margins of the sphenoid and petrous temporal bones, the cranial nerves III, IV, V and VI (the oculomotor, trochlear, trigeminal and abducent nerves, respectively) were severed. In the posterior cranial fossa, the tentorium cerebelli was detached across all attachments along the temporal and occipital bone. Once the tentorium had been detached, the brainstem, cerebellum and the origins of the remaining cranial nerves were exposed. The nerves were then cut through to free the brain completely. A final cut was made inferiorly to the medulla to separate the brain from the spinal cord and free the brain from the skull. At the base of the brain, the CAC was exposed with the focus on the anterior circulation for optimal exposure.

All variations of the anterior cerebral circulation were photographed at a 30cm ruler distance between the digital camera lens and the base of the brain, showing the best anatomical view of the arteries. The findings were then documented on a formulated excel datasheet, as seen in Appendix A, and was used for post data collection analysis. Each brain was assigned a numerical code for identification purposes. The variations of the ACA and ACoA anatomy were observed. Variations were divided into different categories for each artery and the prevalence of each of the variations observed were recorded. The categories of the variations were inferred from previous literature, as listed in figure 2.7. All variations were photographed and documented for post data collection analysis. Furthermore, sketch illustrations of all the variations observed were made and thereafter digitally re-drawn using a Wacom Intuos S drawing pad.

To account for body donor confidentiality, any personal information or person identifiers were removed from written material and only numerical codes were used. All data was stored on a secured one drive folder and SharePoint folder on the University of Cape Town network then transferred to the REDCap (Research Electronic Data Capture) software database, which was accessible only to authorised study staff with individual passwords and defined user rights.

3.5.1.1 Intra- and inter- observer error

To reduce any chance of subjectivity in this study, intra-observer and inter-observer error were accounted for.

Intra-observer error variation

To reduce the possibility of intra-observer error, using a sample set of 10 bodies a day, each artery was observed once on two consecutive days and their findings were recorded on a formulated data sheet (Appendix A). The brains showing the arterial supply were photographed in multiple angles, with a 30cm distance between the camera lens and the base of the brain, to be used for post-data collection analysis. Additionally, schematic illustrations of arterial variations were made.

Inter-observer error variation

A fellow applied anatomy Masters student was trained by the researcher to observe and record the findings of each artery once. The student observed approximately 20% of the overall sample (n=15). The observations and findings were compared to the observations and findings recorded by the intra-observer to assess reliability and reproducibility. The morphological observations and findings of both observers were required to be at least 85% identical to be considered in agreement. Once it was established that the findings of the intra-observer and inter-observer were in agreement, the data collection procedure did not need to be amended. Thus, the data collection process of the intra-observer was able to proceed as the findings were deemed reliable enough for data analysis.

3.5.2 Angiographic study

In the angiographic portion of the study, all MRA images used were taken between 1 January 2018 and 1 January 2023. These images were obtained from the picture archiving and communication digital imaging system (PACS) of the Department of Radiology, Groote Schuur Hospital with approval, and were analysed after extensive training.

Researcher training and consultations

The researcher obtained training to access and operate PACS from a technical staff member of the Department of Radiology. For the appropriate analysis of the MRA images and clinical notes, the researcher received training from two senior radiologists at Groote Schuur Hospital.

3.5.2.1 Morphometric observations

To study the anterior cerebral circulation of the brain MRA images, uncontrasted TOF 3D images were selected. Thereafter each image was analysed in multiplanar reformation (MPR) mode to see various dimensions and planes of the brain in the scan. To complete the A1 segment, A2 segment and ACoA diameter and length measurements, the axial plane and sagittal plane of MRA images presenting with typical anatomy were selected. Following that, the CAC was located by navigating through the various slices of the brain. The axial view was selected for optimum visualisation of the A1 segment and ACoA. However, the sagittal plane was selected for optimum visualisation of the A2 segment. Once the CAC was found, the ACAC was found by 'zooming in' to the anterior portion of the CAC.

As illustrated in figure 3.4, figure 3.5 and Appendix D, the straight distance and cross-path measuring functions on PACS were used for the measurements of the internal diameters and internal lengths of the A1 segment, A2 segment and ACoA, using hallmarks and anatomical landmarks. Various anatomical landmarks were used for the length measurements as follows:

- ACA (A1 segment): measurements were taken between the ICA terminal bifurcation point and the origin of ACoA.
- ACA (A2 segment): measurements were taken from where the ACoA joins the ACA on the left and right to the junction of the rostrum and genu of the corpus callosum and/or at the origin of the callosomarginal artery.
- ACoA: measurements were taken between the left and right ACA.

The diameter measurement hallmarks were conducted as follows:
The internal dimeter for each artery was taken at three points perpendicular to the long axis of the artery and thereafter averaged to allow for a more accurate measurement. The points were referred to as proximal diameter region (PD), middle diameter region (MD) and distal diameter region (DD).

- PD: measurements were taken at a region closest to the origin of the artery.
- MD: measurements were taken at a region approximately halfway between the origin and termination of each artery, i.e. halfway between PD and DD.
- DD: measurements were taken at a region closest to the termination of the artery.

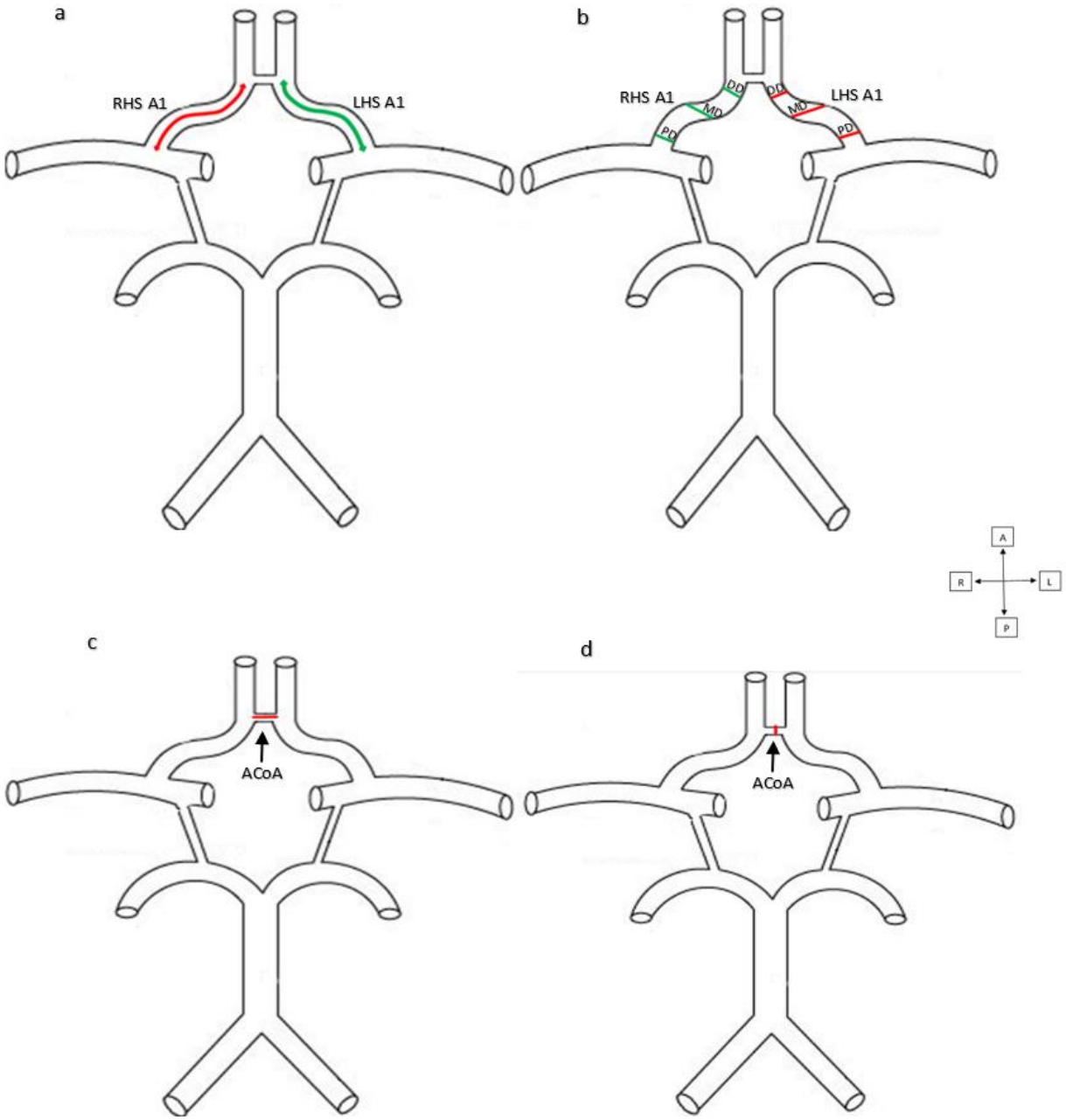

Figure 3.4: Diagram indicating where the measurements of the internal length and internal diameter of the right A1 segment, left A1 segment and the anterior communicating artery were taken on magnetic resonance angiograms (Adapted from Borgdorff and Tangelder, 2014).

(a) internal length of the right (red line) and left (green line) A1 segments, (b) internal diameters of the right and left A1 segments, (c) internal ACoA length and (d) internal ACoA diameter, RHS- right hand side, LHS- left hand side, A1- A1 segment of the anterior cerebral artery, ACoA- anterior communicating artery, DD- distal diameter region, MD- middle diameter region, PD- proximal diameter region, A-anterior, L-left, R-right, P-posterior.

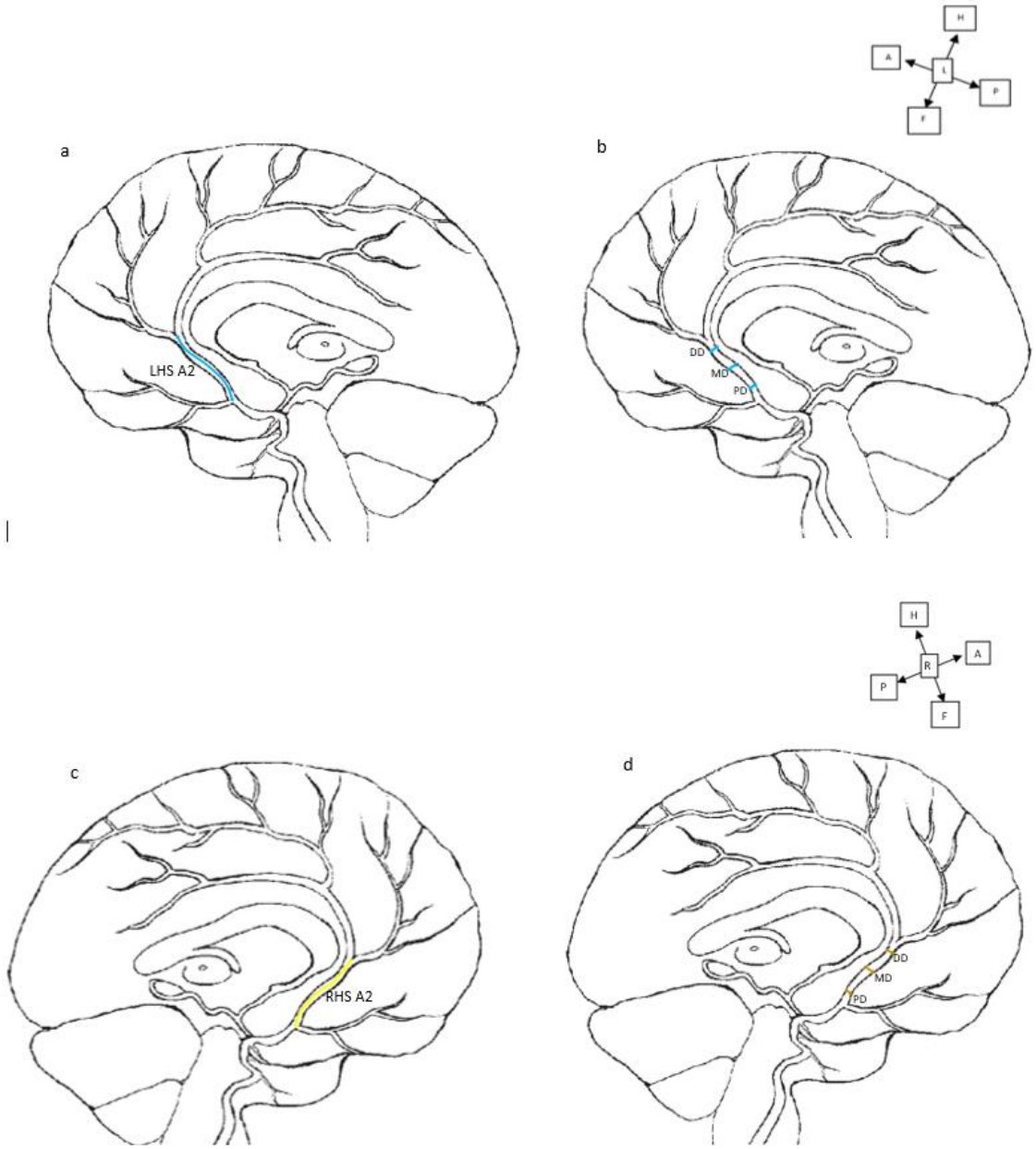

Figure 3.5: Diagram indicating where the measurements of the internal length and internal diameter of the right and left A2 segment were taken on magnetic resonance angiograms (Adapted from Scepkowski and Cronin-Golomb, 2004).

(a) internal length of the left A2 segment (blue line), (b) internal diameters of the left A2 segment, (c) internal length of the right A2 segment (yellow line) and (d) internal diameters of the right A2 segment, A2- A2 segment of the anterior cerebral artery, DD- distal diameter region, MD- middle diameter region, PD- proximal diameter region, A-anterior, L-left, R-right, P-posterior, H- head, F-foot

3.5.2.2 Morphological component

Similar to the dissection portion of the study, the morphological variations in anatomy of the A1 segment, A2 segment and ACoA were observed, and all variations were recorded. The volume rendering function of PACS was used on the 3D TOF MRA images for optimum three-dimensional visualisation of the arteries. Using the axial and sagittal plane alongside the volume rendering function, the anatomical variations of the ACAC were

observed and recorded. These observations were recorded on a formulated Microsoft Excel datasheet. Digital photographs of the variations were also taken using the Microsoft word screenshotting function.

The images and clinical notes of individuals were also used to determine any presence or history of aneurysms. If an aneurysm or aneurysmal intervention was observed in the region of the ACAC, the morphometric data of the affected vessel was not recorded as it would compromise the integrity of the measurements collected.

To account for patient confidentiality, any personal information or person identifiers were not recorded, and only numerical codes were used. All data was stored on a secured one drive folder and a SharePoint folder on the University of Cape Town network then transferred to the REDCap software database, accessible only to authorised study staff with individual passwords and defined user rights.

3.5.3 Intra- and inter- observer error

Intra-observer error variation

After training in the Department of Radiology at Groote Schuur Hospital, retrospective angiographic data was analysed using a sample set of n= 20 patient MRA images a day. For the internal lengths, each artery was measured twice and an average between the two measurements was obtained. However, the internal diameters were measured once at three different points across the artery and an average reading was obtained. Thereafter, morphological variations and cerebral aneurysm presence and/or history were observed with the aid of patient clinical notes. The findings were then documented on formulated Microsoft Excel datasheets (as seen in Appendix A). Multiple snapshots from the MRA scans of the arteries were be captured to be used for post data collection analysis.

Inter-observer error variation

A fellow applied anatomy Masters student who was also trained by a senior radiologist to use PACS, observed and measured each artery according to the research procedure. The inter-observer observed and measured 10% (n = 20) of the overall MRA images. The measurements were recorded and compared to the researcher's findings. There was less than 2,5mm and 1mm difference between the inter- and intra-observer length and diameter measurements, respectively. Therefore, the intra-observer data collection was not amended, and the findings were considered reliable enough to proceed to data analysis as the intraclass correlation coefficient generated would at least be between moderately reliable and excellent reliability.

3.6 Data management

For the dissection component of the study, all the data was recorded on a datasheet as seen in Appendix B and then transferred into REDCap software. For the angiographic component of the study, all the data was recorded on a datasheet as seen in Appendix A and then transferred into REDCap software. Quality assurance included 100% double data entry by the researcher. The inter-observer checked 20% of the data transferred from the datasheet to REDCap.

3.7 Statistical analysis

Sample data can be divided into qualitative and quantitative. Qualitative data also referred to as categorical data, is non-numerical thus cannot be counted nor measured. This type of data is referred to as descriptive

and can only be observed and recorded. It mainly serves to determine frequencies of characteristics or traits within the data set. However, quantitative data is numerical and can be counted or measured. Quantitative data is quantifiable information that can be used in mathematical and statistical calculations to extrapolate deductions or conclusions. When it comes to statistical analysis and analysing the results of a study, the distribution of the data is vital as it will provide a researcher guidance on which statistical analysis methodology is appropriate and it will further provide basis to the interpretation of the statistical tests performed. The distribution of data is dependent on the type of data. A normality test is used to determine whether the sample data is drawn from a population that is normally distributed. Normality tests are typically used to check if a continuous variable is normally distributed. Normal distribution also known as the Gaussian distribution, is the most common type of probability distribution. It is an important type of probability distribution in statistics because it accurately describes the distribution of values for many natural phenomena. This type of probability distribution is characterised by a bell-shaped curve when the data is plotted on a graph. Normally distributed data is unimodal, asymptotic and symmetrical about the mean with data closer to the mean occurring more frequently compared to the data further away from the mean. Additionally, the mode, mean and median are all equal.

Qualitative data distribution is simple and need not be tested for normality as the data is not continuous. Thus, the distribution is dependent on the number of categories being analysed. The probability distribution is displayed as listed categories with a count or percentage of individuals within each category and is commonly represented in the form of Tables and bar graphs. In contrast, quantitative data is continuous data and thus can be tested for normality. After the normality tests are run, the continuous data is categorized as either being normal or non-normal. Parametric statistical tests are used when the data is 'normal' and non-parametric statistical tests are used when the data is non-normal. Therefore, testing for normality is vital, as further statistical tests used and deductions made will be determined by the normality of the data.

Statistical analysis was performed on the recorded data transferred to REDCap software and was loaded onto the statistical package for the social sciences (SPSS). SPSS was used to determine the statistical significance of the data collected in this study.

The distribution of the data was tested with the data set considered as normal if the Shapiro-Wilk test reported a p-value > 0.05 and with kurtosis and skewness between -1 and +1. The observational and categorical data underwent frequency analysis and cross tabulations. Additionally, in order to accurately compare the categorical data found in this study to those found in previous studies, the weighted average of the data was calculated using SPSS by multiplying all values in the data set by their corresponding weights. Thereafter, the resulting products were added up and then divided by the sum of the weights.

The quantitative data in terms of measurements, went through further descriptive analysis allowing for more information to be obtained such as median, mean, interquartile range, standard deviations and variance. To analyse if the measurements differed between sex and age groups, correlation tests such as the Mann-Whitney U test or Kruskal-Wallis test analysis was completed. The 'Chart builder' and 'Chart editor' tools in SPSS were used to create graphs for the graphical representation of the data.

Inter- and Intra-observer error trials were also analysed using the SPSS programme, to determine the reliability of the data collected by both the inter-and intra-observer. This is referred to as inter-rater reliability (Jeyaraman *et al.*, 2020), which is the extent to which two or more observers or raters agree. The inter-rater reliability was assessed using SPSS, where an intraclass correlation coefficient (ICC) was obtained.

3.8 Ethical consideration

For this study, ethical clearance was applied for and obtained from the Human Research Ethics Committee (HREC): HREC 693/2022 and the Cadaver Research Governance Committee (CRGC) at the University of Cape Town, the Research Ethics Committee at Groote Schuur Hospital and from the Head of Radiology Department at Groote Schuur Hospital. The study was conducted according to the Declaration of Helsinki (World Medical

Association, 2013) and the South African Protection of Personal Information Act (POPIA)('Protection of Personal Information Act (POPI Act)', 2013). Additionally, any personal information or person identifiers were not recorded, and only numerical codes were used.

Chapter 4: Results

This results chapter is consistent with the aims and objectives that were described in Chapter 1. This chapter describes and reports the general findings of this study. Study demographics, statistical analysis, digital photographs, illustrations, and snapshots of MRA images are included in this section. Detailed statistical test outcomes can be found as supplementary information in the appendices.

4.1 Dissection sample

A total of 68 bodies were included in the study, 35 (51.5 %) female and 33 (48.5%) male. The sample was further categorized according to age cohorts as follows: <30 (1.47%); 31–40 (4.41%); 41–50 (4.41%); 51–60 (5,88%); 61–70 (10,29%); 71-80 (27,9%) and >81 (45,5%). The median age was recorded at 79 (18) years. Furthermore, the minimum age was found to be 30 years old, and the maximum age was 97 years old. To test for normality within the age distribution of the dissection sample, the Shapiro-Wilk test was completed as seen in Appendix C. The age in the dissection sample was found not to be normally distributed and was skewed to the left with a p-value of <0,001, kurtosis value of 1.36 and skewness recorded at -1.31. To numerically report the average age in this cohort, the median and interquartile range are used. Figures 4.1 and 4.2 show a summary of the study demographics from the dissection population.

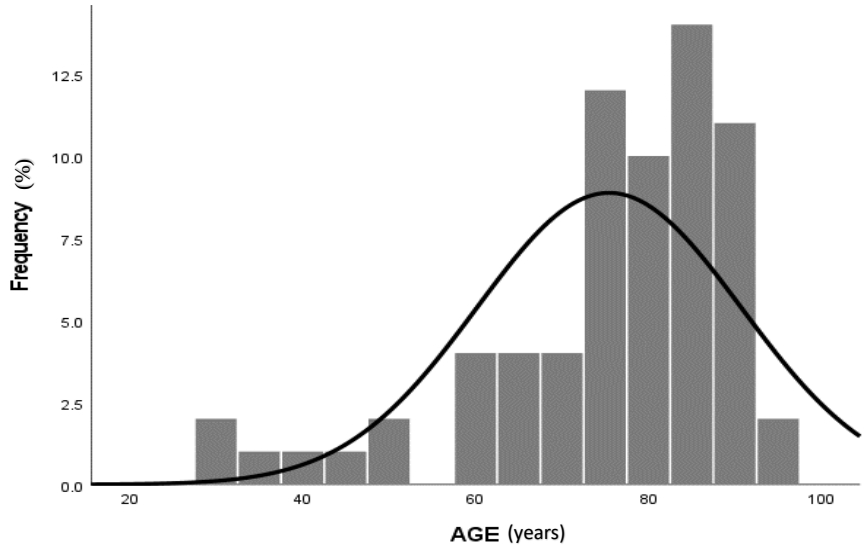

Figure 4.1: Histogram with distribution curve showing age distribution in the dissection sample in the study.

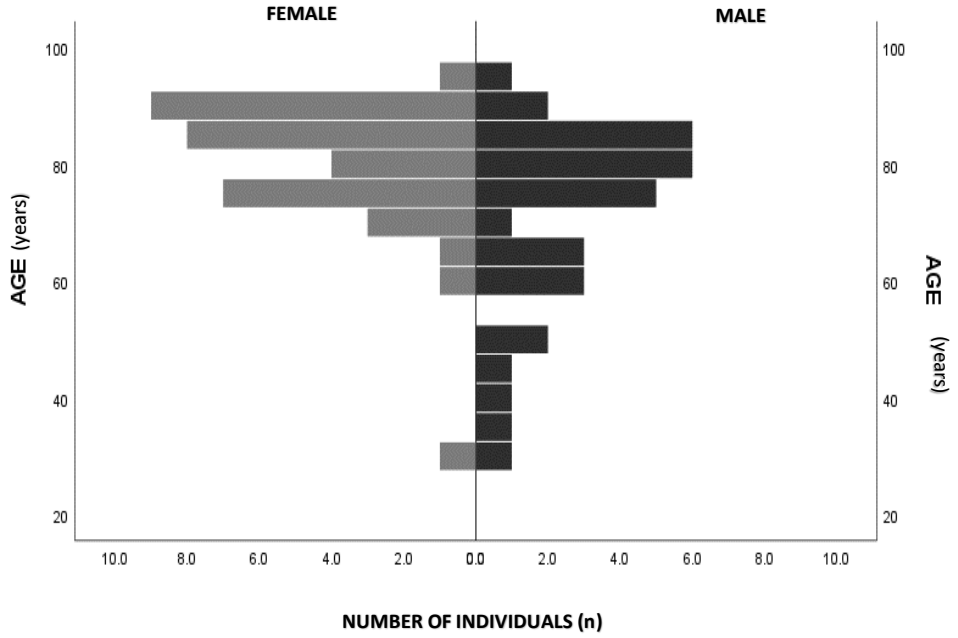

Figure 4.2: Histogram showing population pyramid frequency 'age by sex' in the dissection sample of this study.

4.2 Angiographic sample

A total of 208 patient MRA images were included in this study, 151 (72,6%) females and 57 (27,4%) males. The sample was further categorized according to age cohorts as follows: <30 (3,37%); 31–40 (12,98%); 41–50 (28,37%); 51–60 (26,44%); 61–70 (20,19%); 71-80 (5,29%) and >81 (3,37%). The mean age in the angiographic cohort was 52,84 (± 13,17) years old with the minimum age recorded at 17 years old and the maximum age at 84 years old. Similar to the dissection component, the Shapiro-Wilk test was used to test for normality. The age of the patients was normally distributed with a p-value of 0.359. Figures 4.3 and 4.4 show a summary of the study demographics from the angiographic component of this study.

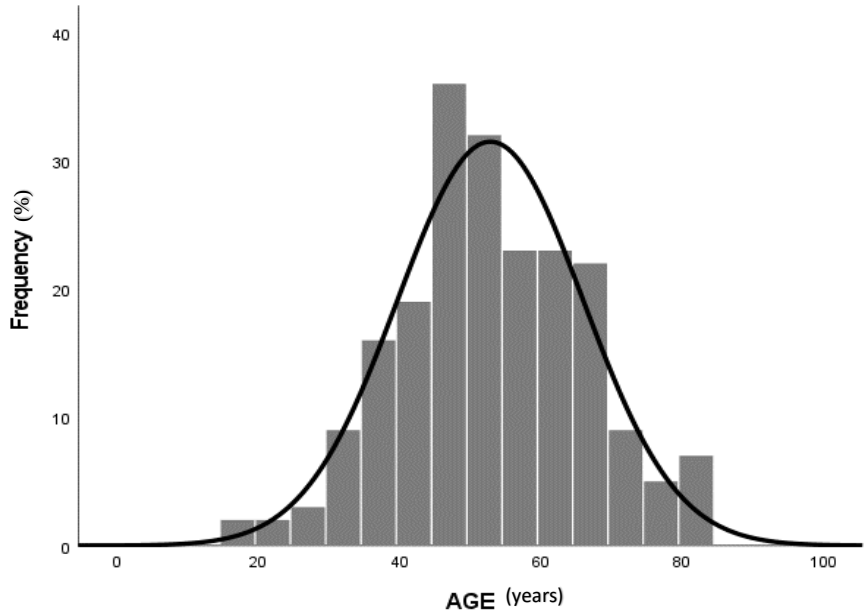

Figure 4.3: Histogram with distribution curve showing age distribution in the angiographic sample.

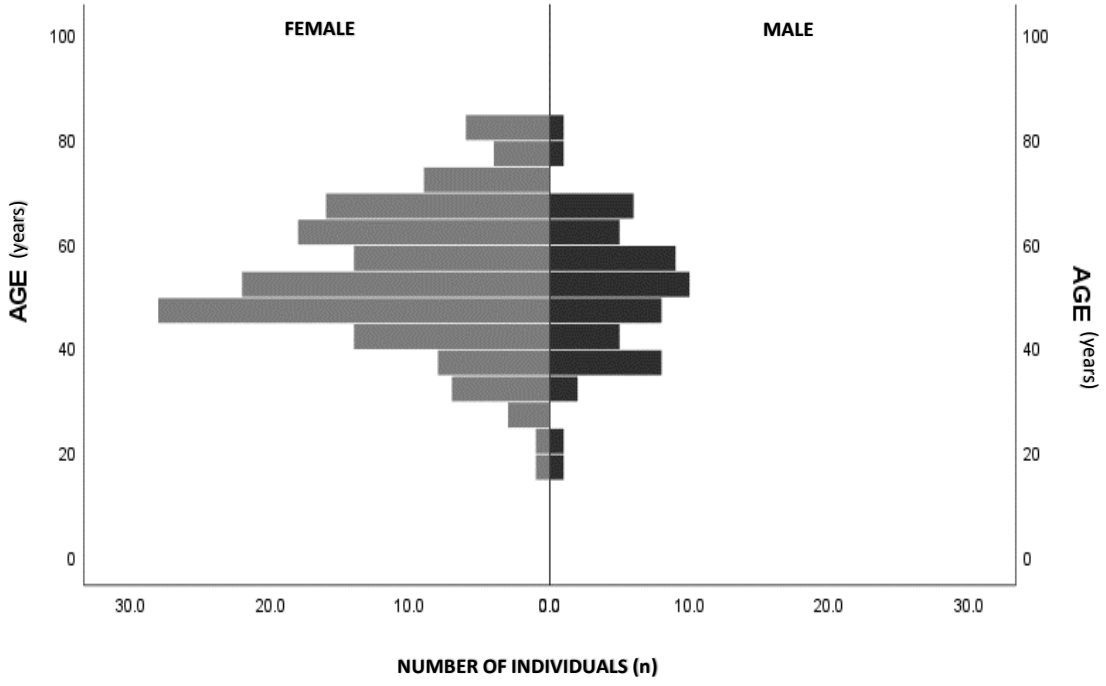

Figure 4.4: Histogram showing population pyramid frequency 'age by sex' in the angiographic sample.

4.3 Age distribution of study

In this study, the age distribution was tested for normality using the Shapiro-Wilk test on SPSS. The Shapiro Wilk test is a hypothesis test that will detect whether the sample is extracted from a normally distributed population i.e. whether the sample data fits a normal distribution. For this test, the null hypothesis is that the

sample is normally distributed, and the alternative hypothesis is that the sample is not normally distributed. With a degree of confidence chosen at 95%, if the resultant p-value is less than 5% (0,05), the null hypothesis is rejected. Typically, the Shapiro-wilk test for normality is used for smaller sizes (n<50) but it may also be used for larger data sets and is commonly used.

The distribution of age was tested for both the dissection and angiographic sample. The Shapiro-Wilk test result for age distribution for the dissection sample reported a p-value of < 0,001 thus the age distribution of the bodies was not normally distributed. As seen in figure 4.1, the age distribution in the dissection sample used in this study was not normally distributed but rather skewed to the left. This is portrayed by the skewed curve that follows the contour of the bars in the histogram. Additionally, the skewness, a measure of the lack of symmetry, of this curve was reported as -1.31 (Appendix C). Generally, if skewness is less than -1 or greater than 1, the distribution is considered to be highly skewed. Kurtosis is a statistical measure that informs on the heaviness of the tails of a distribution curve and provides information on the peakiness of the curve. Compared to normally distributed data, if the kurtosis value is greater than + 1.0, the distribution is leptokurtic. This means the curve has longer tails and thus greater outliers. If the value is less than -1.0, the distribution is platykurtic. Therefore, the curve has shorter tails and thus fewer outliers. The kurtosis value for age distribution in the dissection component of the present study was recorded at 1,36. Furthermore, median age was recorded at 79 years with an interquartile range of 18, a minimum age of 30 years old and a maximum age of 97 years old. Graphically and numerically, it is seen that the age distribution curve for the dissection sample was heavily skewed to the left with a long tail. This shows that the majority of the bodies were older individuals (>60 years old).
In contrast, investigating the normality of age distribution of the patients in the angiographic component revealed that normal distribution was seen. Similar to the dissection sample, the Shapiro-wilk test was used to test for the normality. The p-value was recorded at 0,359 and thus the null hypothesis was accepted, and it is concluded that the age distribution was normally distributed. The mean age in the MRA cohort was 52,84 years old with the minimum age recorded at 17 years old and the maximum age at 84 years old. Furthermore, the conclusion was also substantiated by the skewness and kurtosis values being significantly close to zero, 0,036 and -0.061 respectively (Appendix C).

4.4 Morphological variations present in the dissection sample

The ACAC across all bodies were observed and the variations were classified using variation classifications previously reported in literature. Figure 4.5 – 4.8 are examples of different types of variations that were found in the ACAC of the dissection sample. Figure 4.5 is an example of a brain from a 91-year-old female who exhibited typical ACAC anatomy.

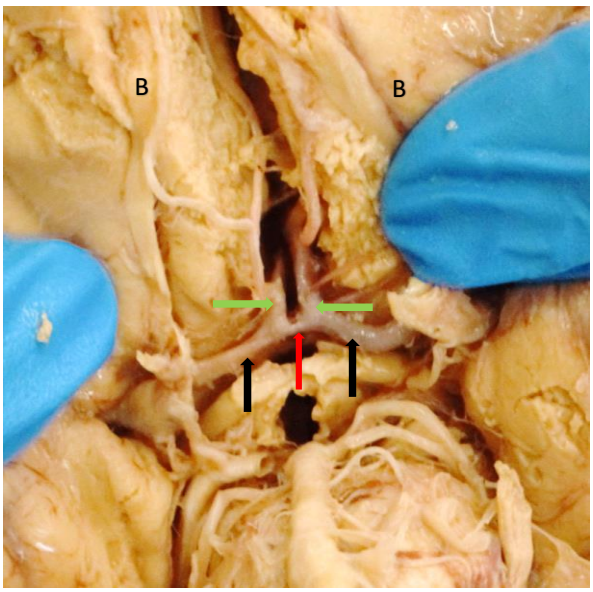

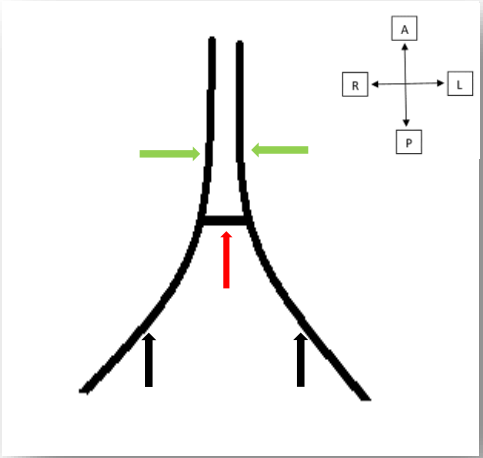

Figure 4.5: Inferior view of a brain and schematic illustration showing typical anatomy of the A1 segment, A2 segment and anterior communicating artery. Black arrows: A1 segment of ACA, Green arrows: A2 segment of ACA, Red arrow: ACoA. B: Inferior surface of frontal lobe of cerebrum. A-anterior, P-posterior, L-left, R-right.

The X-shaped anatomy of the ACoA is seen in figure 4.6, where the brain from a 63-year-old male exhibits standard A1 and A2 anatomy, in contrast to the ill-defined ACoA. Thus, this variation is classified as X-shaped anatomy of ACoA.

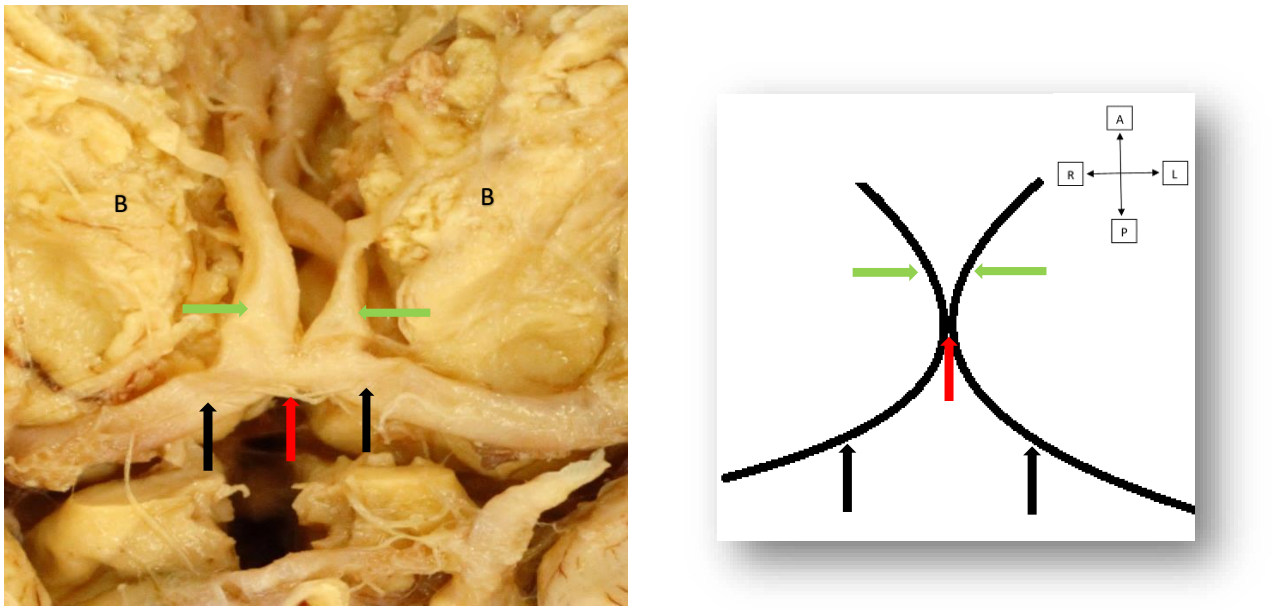

Figure 4.6: Inferior view of a brain and schematic illustration showing X-shaped anatomy of the ACoA. Black arrows: A1 segment of ACA, Green arrows: A2 segment of ACA, Red arrow: region of the ACoA. B: Inferior surface of frontal lobe of cerebrum. A-anterior, P-posterior, L-left, R-right.

The brain seen in figure 4.7, is a brain from a 87-year-old female that shows multiple types of ACAC variations. The variations include a fenestrated A1 segment and a wide ACoA. Additionally, a displaced branch of the left ACA, the orbitofrontal artery, can be seen originating at the junction of the left ACA and the wide ACoA.

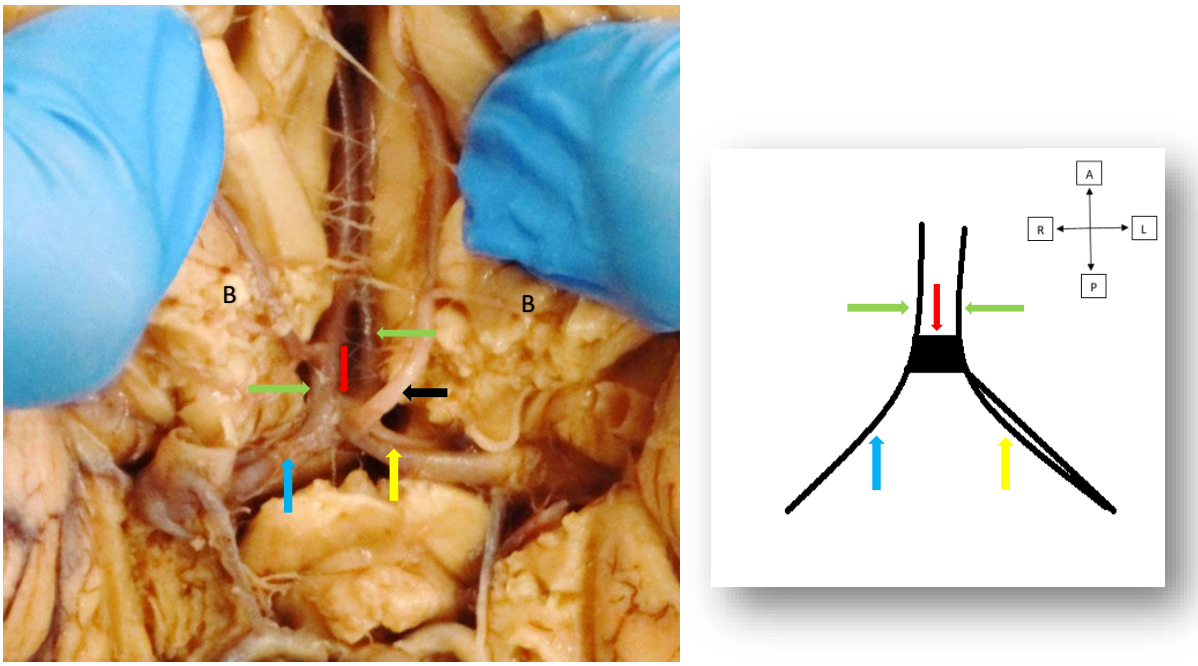

Figure 4.7: Inferior view of a brain showing fenestrated A1 (LHS) and a wideACoA. Yellow arrow: Fenestrated A1, Green arrows: A2 segment of ACA, Blue arrow: A1 segment of ACA, Red arrow: wide ACoA, Black arrow: displaced orbitofrontal artery, B: Inferior surface of frontal lobe of cerebrum

Figure 4.8 below is an example of a brain of an 89-year-old female who displayed a type of ACAC variation that is unique to this study and does not seem to be previously reported in literature. This variation was classified as a combination of fenestration and H-shaped ACoA and thus is reported as a 'Fenestrated H-shape' variation.

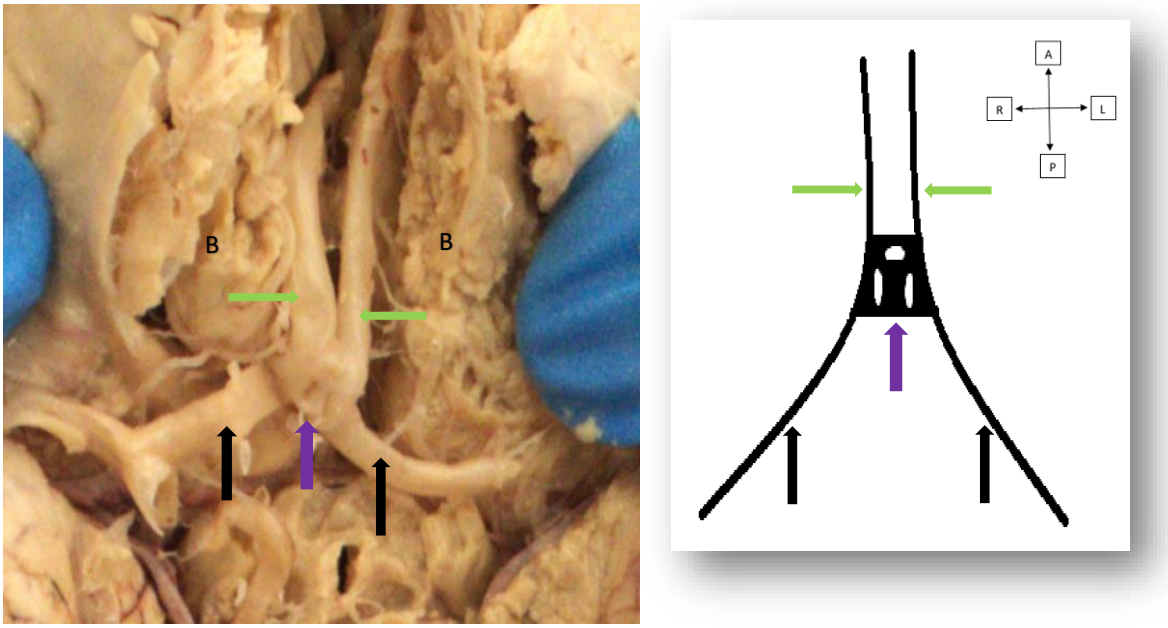

Figure 4.8: Inferior view of a brain and schematic illustration showing the fenestrated H-shaped variation of the ACoA. Black arrows: A1 segment of ACA, Green arrows: A2 segment of ACA, Purple arrow: fenestrated H-shape ACoA. B: Inferior surface of frontal lobe of cerebrum. B-anterior, P-posterior, L-left, R-right.

In Tables 4.1 – 4.3 below, the incidence, prevalence and classification results of the various variations found in the ACAC within the dissection sample have been tabulated as counts and percentages.

Table 4.1: Summary of incidence of anterior communicating artery complex variations

ANTERIOR COMMUNICATING ARTERY COMPLEX VARIATIONS	FEMALE	MALE	TOTAL
	n (%)	n (%)	n (%)
NO	9 (13,24)	11 (16,18)	20 (29,4)
YES	25 (36,8)	21 (30,88)	46 (67,6)
NOT APPLICABLE	1 (1,47)	1 (1,47)	2 (2,9)
TOTAL	35 (51,5)	33 (48,5)	68 (100)

Table 4.2: Prevalence of variations found in each artery of the anterior communicating artery complex

PREVALENCE OF VARIATIONS (n (%))	LEFT		RIGHT		
	A1	A2	A1	A2	ACOA
NO	57 (83,8)	62 (88,2)	62 (91,2)	61 (89,7)	27 (39,7)
YES	11 (16,2)	6 (11,2)	6 (8,8)	7 (10,3)	39 (57,4)

NOT APPLICABLE	-	-	-	-	2 (2,9)
TOTAL	68	68	68	68	68

- refers to the absence of observation.

Table 4.3: Types of variations found in each artery of the anterior communicating artery complex

	TYPE OF VARIATION	n	%
ACAC	TYPICAL	20	**29,4**
n=68			
ACoA	BULBOUS	4	**6,06**
n=66	CURVED	2	**3,03**
	DIAGONAL	2	**3,03**
	DOUBLE DEPRESSION	1	**1,52**
	DUPLICATED	1	**1,52**
	FEN x H	1	**1,52**
	FENESTRATED	6	**9,09**
	H	2	**3,03**
	HYPOPLASTIC	5	**7,58**
	SHORT	6	**9,09**
	TYPICAL	27	**40,91**
	WIDE	4	**6,06**
	X	5	**7,58**
ACA A1	ACCESSORY	2	**1,47**
n=136	DUPLICATED	1	**0,74**
	FENESTRATED	5	**3,68**
	HYPOPLASTIC	9	**6,62**
	TYPICAL	119	**87,50**
ACA A2	AZYGOUS	1	**0,74**
n=136	ANASTOMOSED	4	**2,94**
	DUPLICATED	2	**1,47**
	FENESTRATED	2	**1,47**
	HYPOPLASTIC	1	**0,74**
	TRIPLE ACA	1	**0,74**
	TYPICAL	125	**91,91**

4.5 Morphological variations present in angiographic sample

Similar to the dissection component, classification of variations found in the ACAC of the MRA images, was based on previously recorded ACAC variations found in previous studies (Chapter 2). Figure 4.9 and figure 4.10 are MRA images showing examples of some of the ACAC variations found in the images included in this study.

Figure 4.9 is an example of a brain from a 56-year-old female that displayed typical anatomy in the A1 segments and ACoA, and anastomosis in the A2 segments.

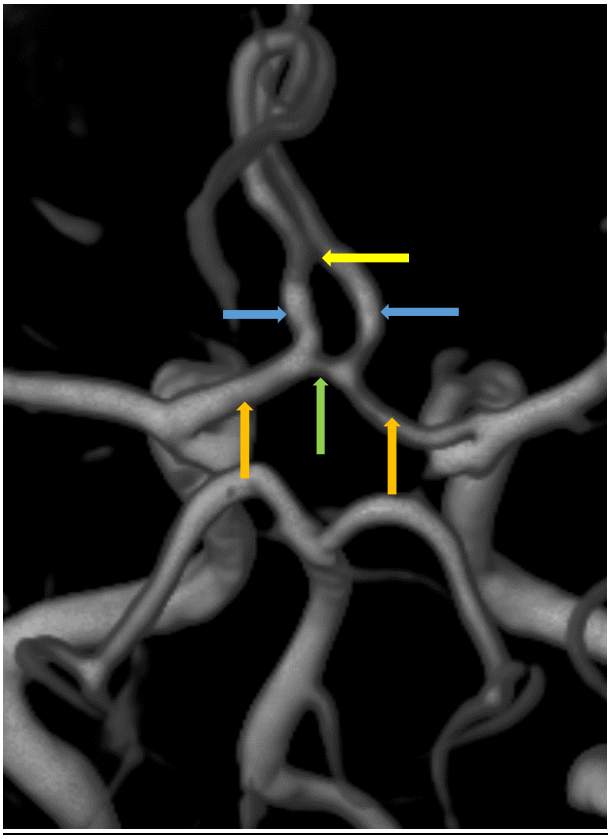

Figure 4.9: 3D volume rendered MRA image showing typical anatomy of the A1 segments and the anterior communicating artery. The A2 segments display anastomosis as a variation. Orange arrows: A1 segment of ACA, Blue arrows: A2 segment, Yellow arrow: point of anastomosis, Green arrow: ACoA. H-head, F-foot, A-anterior, P-posterior, L- left, R- right.

In figure 4.10, an example of a triple ACA variation is seen on a MRA scan from a 72-year-old female. This variation is characterised by the presence of three ACA A2 segments.

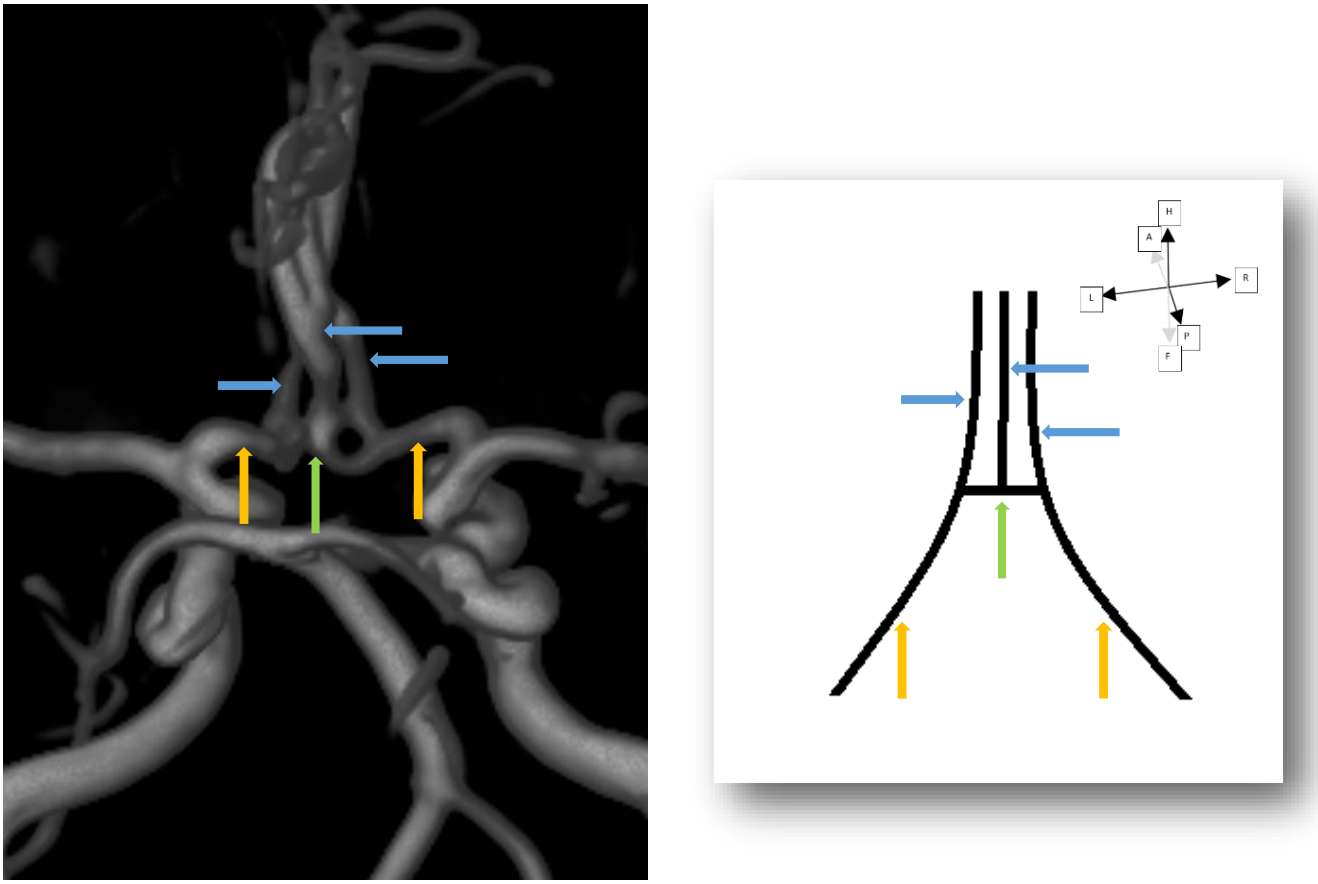

Figure 4.10: 3D volume rendered MRA image showing typical anatomy of the A1 segments and triple ACA variation of the A2 segments. Orange arrow: A1 segment of ACA, Blue arrow: A2 segment, Green arrow: region of ACoA, H-head, F-foot, A-anterior, P-posterior, L- left, R- right.

In Tables 4.4 – 4.6 below, the incidence, prevalence and classification results of the various variations found in the ACAC across the angiographic population of this study have been tabulated.

Table 4.4: Summary of incidence of anterior communicating artery complex variations found in the MRA images.

ANTERIOR COMMUNICATING ARTERY COMPLEX VARIATIONS	FEMALE	MALE	TOTAL
	n (%)	n (%)	n (%)
NO	35 (17,5)	6 (3)	41 (20,5)
YES	61 (30,5)	26 (13)	87 (43,5)
NOT APPLICABLE	49 (24,5)	23 (11,5)	72 (36)
TOTAL	145 (72,5)	55 (27,5)	200 (100)

Table 4.5: Prevalence of variations found in each artery of the anterior communicating artery complex across the MRA images.

PREVALENCE OF VARIATIONS	LEFT		RIGHT		
	A1	A2	A1	A2	ACOA
NO	188 (94,9)	180 (90,4)	179 (90,4)	181 (90,9)	45 (22,6)
YES	7 (3,5)	10 (5)	16 (8,1)	13 (6,5)	74 (36,7)

NOT APPLICABLE	3 (1,5)	9 (4,5)	3 (1,5)	5 (2,5)	81 (40,7)
TOTAL	198 (100)	199 (100)	198 (100)	199 (100)	200 (100)

Table 4.6: Types of variations found in each artery of the anterior communicating artery complex across the MRA images.

	TYPE OF VARIATION	n	%
ACAC	TYPICAL	41	**20,5**
n=200			
ACoA	ABSENT	5	**4,20**
n=119	AZYGOUS	1	**0,84**
	BULB x FEN	1	**0,84**
	CURVED	8	**6,72**
	DIAGONAL	3	**2,52**
	DUPLICATED	1	**0,84**
	FENESTRATED	1	**0,84**
	H	5	**4,20**
	HYPOPLASTIC	5	**4,20**
	LONG	1	**0,84**
	SHORT	3	**2,52**
	X	39	**32,77**
	TYPICAL	46	**38,66**
ACA A1	DUPLICATED	2	**0,51**
n=389	FENESTRATED	2	**0,51**
	HYPOPLASTIC	15	**3,86**
	TRIPLE	1	**0,26**
	ABSENT	3	**0,77**
	TYPICAL	366	**94,09**
ACA A2	ANASTOMOSED	5	**1,32**
n=378	DUPLICATED	4	**1,06**
	HYPOPLASTIC	1	**0,26**
	TRIPLE ACA	6	**1,59**
	FENESTRATED	1	**0,26**
	TYPICAL	361	**95,50**

In the present study, some variations were observed and recordered in both dissection and angiograpphic components that were described unique to this study or that seem not to be previously described in previous studies. These variations are included in Table 4.7.

Table 4.7: Unique variations found in the present study.

Variation type	Definition	Schematic illustration
Bulbous	When the entire ACoA artery seems more rotunded in comparison to the rest of the ACAC arteries. The entire ACoA needs to be rounded for this term to be applicable.	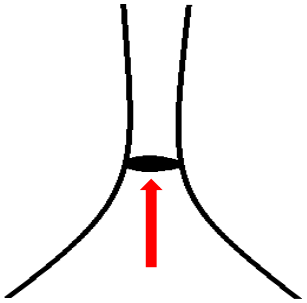
Curved	A curved ACoA is characterized by a slightly bent vessel, where the ACoA is curved in or out in comparison to its typical horizontal anatomy.	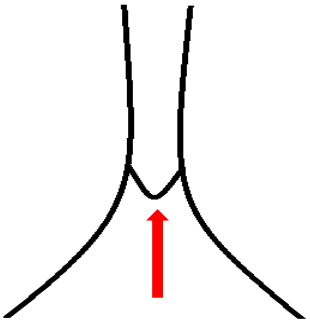
Double depression	Double depression is characterised by two divots in the ACoA. This variation is not classified as fenestrations as they only appear on one side of the artery and do not perforate the vessel.	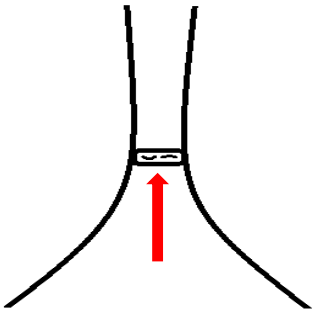
FEN x H	A combination of two variations (fenestrated and H-shaped). Fen x H ACoA is a vessel that has H-shaped anatomy with an addition fenestration either above or below the H-shape of the vessel (in total three fenestrations). This variation is not to be confused with the plexiform variation which has five perforations.	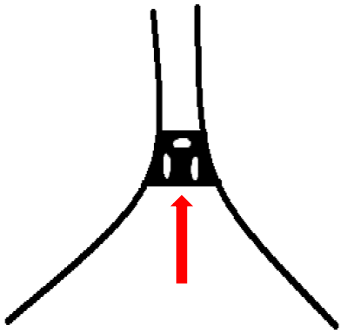

BULB x FEN	A combination of two variations (bulbous and fenestrated). A bulb x fen ACoA is rouned but also is fenestrated.	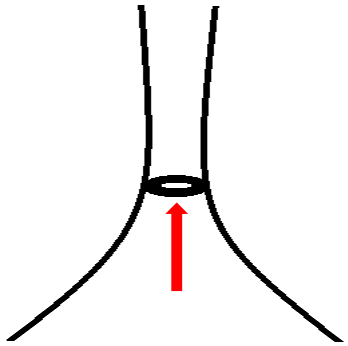
Short	A short ACoA is described as an ACoA that is shorter in length from the typical ACoA anatomy. Without physical measurements and using observations only, this variation can be seen as a small connection between the two adjacent ACAs. This variation is not to be confused with the X-shaped anatomy as there is a distinct connection at the region of the ACoA, albeit a short one.	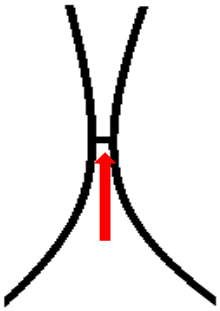
Wide	A wide ACoA is broader than the typical ACoA anatomy. This is obsereved when the ACoA width is either the same or wider than that of the rest of the ACAC vessels.	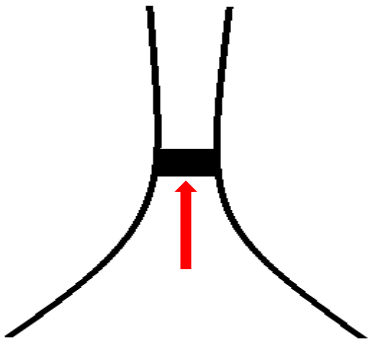
Anastomosed	This term is a deviation from the 'fused' variation. This variation is applicable when the adjacent A2 segments of the ACA are joined at one or more places along their lengths. This means that the vessel is not completely fused along their lengths but rather are joined at distinct areas, excluding the ACoA.	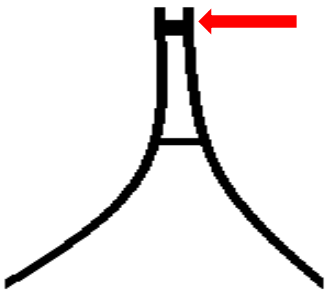

4.6 Morphometric parameters of the ACAC in MRA images

All the qualitative data was tested for normality using the Shapiro-Wilk test. All the measurements reported a p-value less than 0,05 except for the average lengths of the A2 segment on the right-hand side, which had a p-value of 0,091. Thus, most of the qualitative data was not normally distributed. The measurements are reported as the median value and interquartile range in parenthesis. The tests of normality for each segment may be found in Appendix C. Table 4.8 below shows the measurements for the internal length and diameter of all the ACAC arteries. Each measurement is reported as a median value with the interquartile range value in parenthesis. Additionally, the p-values reported in Table 4.8 below are an indication of the correlation of the measurements of each artery across the sex and age groups present in the study. The correlation tests used to obtain said values were the Mann-Whitney U test and the Kruskal-Wallis test, respectively.

Table 4.8: Morphometric parameters of the anterior communicating artery complex.

		RHS A1 LENGTH (mm)	LHS A1 LENGTH (mm)	RHS A1 DIAMETER (mm)	LHS A1 DIAMETER (mm)	RHS A2 LENGTH (mm)	LHS A2 LENGTH (mm)	RHS A2 DIAMETER (mm)	LHS A2 DIAMETER (mm)	ACOA LENGTH (mm)	ACOA DIAMETER (mm)
MEDIAN (IQR)		**13,5 (3,48)**	**12,85 (2,57)**	**2,26 (0,45)**	**2,25 (0,68)**	**23,4 (3,94)**	**23,7 (3,97)**	**2,3 (0,33)**	**2,37 (0,78)**	**1,5 (1,76)**	**0,85 (0,91)**
SEX	**MALE**	13,95 (3,3)	13,3 (2,65)	2,4 (0,2)	2,4 (0,2)	24 (3,53)	24,4 (3,69)	2,4 0,29)	2,5 (0,28)	0 (2)	0 (0,96)
	FEMALE	13,3 (3,5)	12,85 (2,5)	2,26 (0,44)	2,23 (0,76)	23,4 (4,07)	23,7 (4,05)	2,3 (0,35)	2,4 (0,89)	1,8 (1,7)	1,05 (0,88)
	P-VALUE[a]	0,105	0,223	**0,022**	0,342	0,259	0,095	0,11	0,219	0,284	0,134
AGE	**<30**	13,9 (6,69)	12,2 (4,04)	2,17 (0,16)	2,35 (2,9)	25,9 (3,03)	26,25 (5)	2,27 (0,97)	2,63 (0,67)	3,7 (1,66)	1,5 (1,17)
	31-40	13,25 (3,8)	13,25 (2,81)	2,4 (0,37)	2,3 (0,42)	26,45 (4,2)	24,55 (3,99)	2,3 (0,23)	2,57 (1,54)	1,75 (1,62)	0,4 (0,91)
	41-50	13,2 (4,12)	13,05 (2,64)	2,35 (0,33)	2,35 (0,33)	23,1 (3,5)	23,2 (3,92)	2,37 (0,27)	2,37 (0,28)	2,13 (1,8)	0,85 (0,84)
	51-60	13,35 (3,2)	13,1 (2,42)	2,28 (0,48)	2,2 (0,32)	22,95 (4,38)	24,3 (3,8)	2,3 (0,33	2,2 (0,99)	1,1 (1,77)	0,9 (0,96)
	61-70	12,9 (2,3)	12,1 (2,4)	2,38 (0,63)	2,35 (0,58)	24,15 (3,7)	25,1 (4,22)	2,38 (0,33)	2,27 (0,32)	1,3 (1,7)	1,12 (0,84)
	71-80	14,1 (2,63)	13,8 (2,18)	2,17 (0,21)	2,15 (0,13)	21,58 (3,9)	23,5 (4,4)	2,37 (0,11)	2,25 (0,17)	0 (1,2)	0 (1,07)
	81>	13,9 (2,5)	13,1 (2,7)	2,07 (0,13)	2,1 (0,32)	25,2 (4,1)	25,9 (4,2)	2,4 (0,11)	2,4 (0,3)	0 (1,2)	0 (0,96)
	P-VALUE[b]	0,757	0,783	0,229	0,299	0,233	0,825	0,779	**0,006**	0,107	0,764

a- These p-values were obtained by running a Mann-Whitney U test.

b- These p-values were obtained by running a Kruskal-Wallis test.

The p-value reported in Table 4.9 is an indication of the correlation of the measurements of each artery to each other (LHS vs RHS). The median correlation test used for this was the Wilcoxon Signed Rank test.

Table 4.9: Internal length and internal diameter measurements of the A1 and A2 segments from MRA images.

ACAC MEASUREMENTS (mm)	LEFT	RIGHT	P-VALUE
A1 LENGTH	12,85 (2,57)	13,5 (3,48)	0,41
A1 DIAMETER	2,25 (0,68)	2,26 (0,)	0,361
A2 LENGTH	23,7 (3.97)	23,4 (3.94)	0,059
A2 DIAMETER	2,37 (0,78)	2,3 (0,33)	0,347

Similarly, the average ACoA measurements were also tested for normality (Appendix C) and were also found not to be normally distributed. Table 4.10 shows the average length and width of the ACoA, represented as the median value and the interquartile range in parenthesis.

Table 4.10: Median length and diameter of the anterior communicating artery from the MRA images.

ACoA MEASUREMENTS (mm)	MED (IQR)
ACoA LENGTH	1,5 (1,76)
ACoA DIAMETER	0,85 (0.91)

4.7 Aneurysms in the angiographic component

A total of 48 MRA images displayed coiling of previous ACAC aneurysms. Forty-one of these images had coiled aneurysms at the location of the ACoA, with only five images showing coiled aneurysms at the A1 segment and 2 images showing coiled aneurysms at the A2 segment. Figure 4.11 is an example of a MRA scan from a 53-year-old female with a previously coiled ACoA aneurysm.

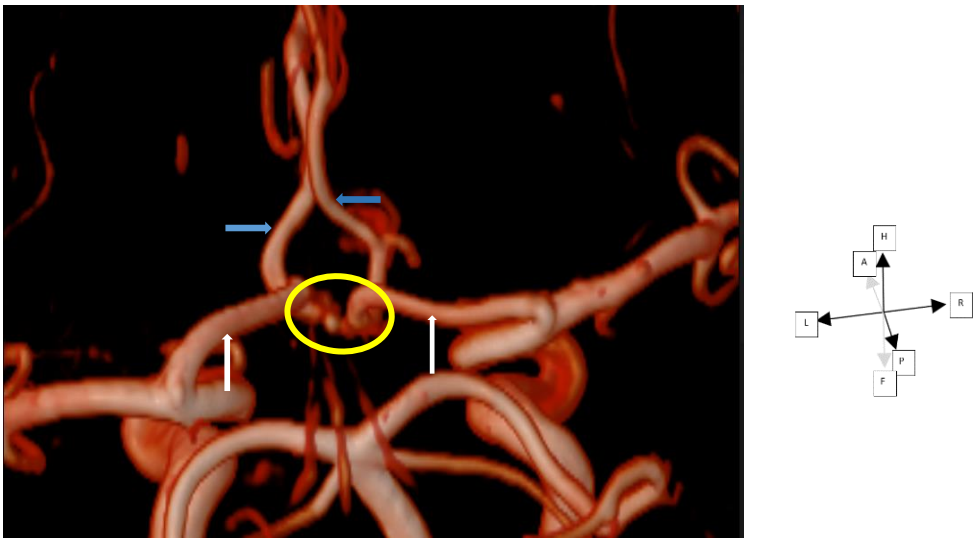

Figure 4.11: 3D volume rendered MRA image showing typical anatomy of the A1 segments and A2 segments and a pre-coiled anterior communicating artery aneurysm. White arrow: A1 segment of ACA, Blue arrow: A2 segment, Yellow circle: region of pre-coiled ACoA aneurysm, H-head, F-foot, A-anterior, P-posterior, L- left, R-right.

Table 4.11 and 4.12 below show the prevalence of the history of ACAC aneurysms and their locations within the anterior communicating artery complex with respect to sex.

Table 4.11: ACAC aneurysms found in the MRA images

ACAC ANEURYSMS	FEMALE	MALE	TOTAL
	n (%)	n (%)	n (%)
NO	115 (57,2)	38 (18,9)	153 (76,1)
YES	31 (15,4)	17 (8,5)	48 (23,9)
TOTAL	146 (72,6)	55 (27,4)	201 (100)

Table 4.12: Location of pre-coiled aneurysms found in the MRA images

LOCATION OF ANEURYSMS	FEMALE	MALE	TOTAL
	n (%)	n (%)	n (%)
ACA A1	4 (8,3)	1 (2,08)	5 (10,42)
ACA A2	0 (0)	2 (4,17)	2 (4,17)
ACOA	27 (56,2)	14 (29,17)	41 (85,42)
TOTAL	31 (64,5)	17 (35,4)	48 (100)

Additionally, using the Pearson Chi-Square test, no association was found between the ACAC variations and the prevalence of pre-coiled aneurysms nor was there an association found between ACAC variations and the location of the pre-coiled aneurysms (p-value <0,001)

4.7 Standard error analysis

Using SPSS, the ICC values across all the ACAC measurements taken were calculated. ICC values less than 0,5 are an indication of poor reliability, values between 0,5 and 0,75 are indicative of moderate reliability, those between 0.75 and 0.9 are an indication of good reliability, and then values greater than 0,90 imply excellent reliability that indicates an absolute agreement between the inter- and intra-observer data. Therefore, the closer the ICC is to the value of 1, the higher the ICC is and thus is an indication that there is high similarity between the values recorded in a specific group. For this study, the ICC ranged from 0,574 - 0,996. Excluding the RHS A1 diameter (0,631), RHS A2 diameter (0,574) and the LHS A2 diameter (0,768), all the ICC values were greater than 0,950. This is an indication that for this study, using this sample space, the measurements and observations can be considered reliable.

Chapter 5: Discussion

5.1 Demographics of the sample according to sex

As stated in chapter 4, the dissection sample of this study included 68 bodies and 208 MRA images in the angiographic component. For both components in this study, there were more females than males. In the dissection sample 51,5% of the bodies were female. Although it cannot be said that this figure is an exact representation of the South African population, it still however adheres to the general idea or inherent trend that the South African population has more females than males. The most recent STATS SA report of 2021 reported that in a 60,14 million population, 51,1% of the population was said to be female (STATS SA, 2021) .

A retrospective study performed by Jiang *et al.* (2020), investigated demographic factors that affect the whole-body donor programme within their institution (Nanjing Medical University, Nanjing, China) from 1 July 2009 to 30 June 2019 and found that males accounted for 66,9% of the sample, whereas females accounted for only 33,1%. Additionally, a similar study performed by Kramer *et al.* (2018), assessed the cadaver demographics within their institution (University of Witwatersrand, Johannesburg, South Africa) using cadaver records between 1921 and 2013. The study revealed similar findings to Jiang *et al.* (2020), where 69,7% of the total cadaver cohort was reported to be male and 30,3% of the cohort was reported to be female. In a South African context, Kramer and Hutchinson (2014) highlighted that a possible reason for the disparity between males and females with regards to whole body donation in earlier years, was the predominance of unclaimed bodies in their cadaver cohort, which in turn would most likely be male due to factors of migration as more males tend to be migrant workers than females. The sex distribution of the bodies in this study, deviates from what was presented in the literature, as the sample population had more females than males. In recent years, the majority of bodies used in whole body donor programmes across South African academic tertiary institutions are derived from bequeathed and donated sources and not from unclaimed bodies (Kramer *et al.*, 2019). Thus, this change could be a potential reason for the sex distribution of the dissection sample of the present study.

In the angiographic sample, 72,6% of the population was female. Albeit there were also more females than males in this sample, there is a marked difference when comparing this value to that of sex distribution statistics of the South African population. A review study performed by Hunt *et al.* (2011) revealed that females consult health care services more than males. Male reluctance to health care consults may be attributed to various factors such as the patriarchal view of gender roles, denial of weakness and perception of masculinity (Courtenay, 2000). Thus, these constructions of masculinity may be the reason behind having significantly more females than males in the angiographic sample.

5.2 Anterior Communicating Artery Complex morphological variations

5.2.1 Dissection component

A compilation of variations found in the anterior communicating artery complex across previous studies is seen in Table 5.1. The studies were all strictly cadaveric with the exception of one study that was classified as ‘cadaveric/autopsy’ (Dumitrescu, Cobzaru and Ripa, 2021). Furthermore, the studies also had varying sample sizes and varying population demographics.

Table 5.1: Morphological variations found in previous cadaveric studies

		Kayembe et al, 1984	De silva et al., 2013	Monroy-sosa et al., 2013	Iqbal et al., 2013	Kardile et al., 2013	Stojanovic et al., 2015	Kannabathula et al., 2017	Singh et al., 2017	Tripathi et al., 2021	Dumitrescu et al., 2021*		Present study
METHOD		CADAVERIC											
REGION		JAPAN	SRI LANKA	MEXICO	INDIA	INDIA	SERBIA	INDIA	INDIA	INDIA	ROMANIA	Weighted average	SOUTH AFRICA
SAMPLE (N)		148	225	30	50	100	56	75	75	100	28		68
ACAC (%)	TYPICAL	46,3	14,3	-	48,0	62,0	73,2	-	-	-	-	27,5	29,4
ACOA (%)	ABSENT	-	0,0	3,3	0,0	8,0	-	-	-	3,0	21,4	4,0	-
	TRIPLE	-	0,4	3,3	4,0	1,0	-	1,3	1,3	-	-	1,3	-
	BULBOUS	-	-	-	-	-	-	-	-	-	-	-	5,9
	CURVED	-	-	-	-	-	-	-	-	-	-	-	2,9
	DIAGONAL	-	-	-	-	-	-	-	-	56,0	-	6,3	2,9
	DOUBLE DEPRESSION	-	-	-	-	-	-	-	-		-	-	1,5
	DUPLICATED	-	-	13,3	12,0	-	-	-	-	-	7,1	3,7	1,5
	FEN x H	-	-	-	-	-	-	-	-	-	-	-	1,5
	FENESTRATED	-	-	-	-	-	-	-	-	-	-	-	8,8
	H	29,9	-	-	-	3,0	-	5,3	-	-	-	4,3	2,9
	HYPOPLASTIC	-	-	-	-	-	-	-	2,6	6,0	3,6	1,4	7,4
	SHORT	-	-	-	-	-	-	-	-	-	-	-	8,8
	WIDE	-	-	-	-	-	-	-	-	2,0	-	0,2	5,9
	X	21,1	23,0	-	-	3,0	-	2,7	-	-	-	5,6	7,4
	PLEXIFORM	-		-	-	-	-	1,3	-	-	-	0,2	-
ACA A1 (%)	ACCESSORY	-	-	-	-	-	-	1,3	1,3	-	-	0,3	2,9
	DUPLICATED	-	-	-	-	-	-	6,7	5,3	-	3,6	1,8	1,5
	FENESTRATED	-	-	3,3	-	-	-	6,7	-	-	3,6	1,5	7,4
	HYPOPLASTIC	11,0	4,1	3,3	8,0	10,0	16,0	-	8,0	-	32,1	10,4	13,2
ACA A2 (%)	AZYGOUS	-	-	3,3	-	2,0	-	-	-	-	-	0,6	1,5
	ANASTOMOSED	-	-	-	-	-	-	-	-	-	-	-	5,9
	DUPLICATED	-	-	-	-	-	-	-	-	-	-	-	2,9
	FENESTRATED	-	-	-	-	-	-	-	-	-	-	-	2,9
	HYPOPLASTIC	-	-	-	-	-	-	-	-	-	-	-	1,5
	TRIPLE ACA	14,6	2,0	-	8,0	1,0	7,1	-	-	-	-	3,7	2,9

* Study classified as 'cadaveric/autopsy'

- Indicates the absence of observation.

When looking at Table 5.1, it is evident that the various studies have incongruent results in the type and frequency of ACAC variations reported. Some studies have variations in common (Kayembe *et al*., 1984; De Silva *et al.*, 2013; Iqbal *et al*., 2013; Monroy-Sosa *et al.*, 2013), whilst others have variations unique to those particular studies (Kannabathula *et al.*, 2017; Tripathi *et al.*, 2021), much like some variations found in the present study.

For the A1 segment of the ACA, hypoplasia is the most common variation, reporting a weighted average of 10,4% across all the studies. This is also reflected in the present study, where hypoplasia is the most common A1 variation with a prevalence of 13,2%. Second and third to hypoplasia, duplication and fenestration are also common A1 variations, with only a marginal difference in prevalence (0,2%) between the two variations. A study performed by Dumitrescu *et al*. (2021) also displayed similar findings, wih hypoplasia reported to be the most common A1 ACA variation (32,1%). In the present study, although duplication and fenestration are also amongst the most common variations in the A1 segment, there is a significant difference in the prevalence of these variations. Fenestration reported a prevalence of 7,4% and duplication reported a prevalence of 1,5%. Whereas Dumitrescu *et al*. (2021) showed that fenestration and duplication were equally prevalent at 3,6 %. Across the previously reported studies, an accessory A1 segment was the least common variation reported

showing only a prevalence of 0,3%. However, in the current study, this variation showed a much higher prevalence (2,9%).

Triple ACA is a variation of the A2 segment, where there are three A2 segments present. This variation was reported to be the most frequent variation mentioned in Table 5.1. Triple ACA showed a weighted prevalence of 3,7%. Whereas, the present study only reported this variation having a prevalence of 2,9%. Thus, although it was not the most frequent variation, it came second to the variation 'anastomosed' alongside two other variations, namely duplication and fenestration. The variation 'anastomosed' is reported unique to this study and is characterised by the fusion of the left and right A2 segments at one or more distinct locations. This variation was the most frequent A2 variation and reported a prevalence of 5,9%. A hypoplastic A2 and a azygous A2 were the least frequent A2 variations at 1,9%. Contrarily, Kardile *et al*. (2013) reported that an azygous A2 ACA (2,0%) was the most common A2 ACA variation followed by triple ACA (1,0%).

Compared to the A1 and A2 segments, the studies in Table 5.1 show that in regards to the anatomy of ACoA, more varied pools of variations have been reported. X-shaped, H-shaped and absent were the top three most frequent types of variations, with prevalence of 5,7%, 4,3% and 4,0% respectively. The X-shaped anatomy is characterised by the 'regression' of the ACoA, where there is a fusion of the adjacent ACA at the region of the ACoA. H-shaped ACoA anatomy can be described as an ACoA that is relatively wide and has two fenetrations resulting in a rotated 'H' shape. Not to be confused for the X-shaped anatomy, absent anatomy is when the ACoA is not present and thus there is a distinct lack in connection between the adjacent ACA. Duplication was also reported as a significantly frequent variation with a weighted average of 3,7%. Contrary to the findings in the previous studies, the most frequent ACoA variations found in the present study were fenestration (8,8%), short (8,8%), hypoplasia (7,4%), X-shaped (7,4%), wide (5,9%) and bulbous (5,9%). Additionally, a study by Tripathi *et al.* (2021), proved to be an extreme outlier, with the diagonal ACoA variation reported as the most common ACoA variation (56,0%).

5.2.2 Angiographic component

Table 5.2 is a summary of the prevalence of different ACAC variations found across angiographic studies. Additionally, Table 5.2 includes studies that incorportated various angiographic modalities, such as CTA, MRA and digital subtraction angiography (DSA).

Hypoplasia is reported to be the most common variation of the A1 segment, with a weighted average of 3,1%. Similarly, the present study also shows that hypoplasia is the most common A1 variation with a prevalence of 7,6%. Hypoplasia was also shown to be the most common A1 ACA variation in a study performed by Lopez-Sala et al. (2020) with a prevalence reported at 31,2%. Fenestration and duplication were second to hypoplasia in the current study with a prevalence of 1,0% for both variation types.

When looking at Table 5.2, triple ACA (0,5%) and hypoplasia (0,4%) are the two most common A2 variations found in the literature. There is only a slight difference in prevalence of 0,1% across these two A2 variations. Triple ACA is also the most common A2 variation in the present study, with a prevalence of 3%. Unlike the previous studies, the variation 'anastomosed' is the second most common variation of the A2 segment (2,5%). Furthermore, hypoplasia was seen to be the least common A2 variation in the present study, with a prevalence of 0,5%. However, in contrast, evidence from Lopez-Sala et al. (2020) showed that hypoplasia was the most common A2 ACA variation (8,5%).

An absent ACoA seems to be the most common type of ACoA variation, seen as a weighted average of 1,9% in Table 5.2. The second and third most common variations are duplication (0,8%) and X-shaped (0,7%). For the present study, the X-shaped anatomy is the most prevalent ACoA variation with a prodigious prevalence of 19,6%. This finding is also supported by evidence from a study by Rajan (2021), where an X-shaped ACoA is reported to be the most prevalent ACoA variation (9,3%). A curved ACoA (4%) is the second most prevalent ACoA variation in this study. There are three types of variations, namely, absent, hypoplasia and H-shaped, that were the third most common amongst the ACoA variations.

Table 5.2: Morphological variations found in angiographic studies from previous literature and present study.

		Boleaga-durán et al., 2004	Dimmick et al., 2008	Li et al., 2011	Klimek-piotrowska et al., 2013	Kovac et al., 2014	Krzyzewski et al., 2015	Jimenez-sosa et al., 2016	Sahin et al., 2018	Uyanik et al., 2020	Lopez-sala et al., 2020	Yokus et al., 2021	Rajan, 2021		Present study
METHOD		MRA	CTA	CTA	CTA	CTA	CTA	CTA	CTA	DSA	CTA	CTA	MRA		MRA
REGION		MEXICO	AUSTRALIA	CHINA	POLAND	SERBIA	POLAND	MEXICO	TURKEY	TURKEY	SPAIN	TURKEY	INDIA	Weighted average	SOUTH AFRICA
SAMPLE		412	300	160	250	455	411	283	751	640	426	581	215		200
ACAC (%)	TYPICAL	9,2	-	76,3	47,2	-	52,6	66,1	-	-	45,5	40,6	-	7,6	20,5
ACOA (%)	ABSENT	4,0	5,0	9,4	22,8	-	19,7	14,1	3,9	-	4,7	-	0,5	1,9	2,5
	TRIPLE	-	-	-	-	-	-	0,4	-	-	0,2	-	-	0,0	-
	BULB x FEN	-	-	-	-	-	-	-	-	-	-	-	-	-	0,5
	CURVED	-	-	-	-	-	-	-	-	-	-	-	-	-	4,0
	DIAGONAL	-	-	-	-	-	-	-	-	-	-	-	-	-	1,5
	AZYGOUS	-	-	-	-	-	-	-	-	-	-	-	-	-	0,5
	DUPLICATED	-	18,0	2,5	-	0,2	0,5	0,4	10,1	-	0,9	0,9	0,5	0,8	0,5
	LONG	-	-	-	-	-	-	-	-	-	-	-	-	-	0,5
	FENESTRATED	-	-	-	-	-	-	0,0	10,1	-	-	-	3,7	0,3	0,5
	H	-	-	-	-	0,4	-	-	-	-	0,9	-	-	0,0	2,5
	HYPOPLASTIC	-	-	-	-	-	-	-	-	-	-	17,9	-	0,4	2,5
	SHORT	-	-	-	-	-	-	-	-	-	-	-	-	-	1,5
	X	-	-	-	9,6	-	6,3	3,2	-	-	1,2	1,0	9,3	0,7	19,6
ACA A1 (%)	ACCESSORY	-	-	-	-	-	-	-	-	0,3	-	-	-	0,0	-
	DUPLICATED	-	-	-	-	-	-	2,1	-	-	-	-	1,2	0,1	1,0
	FENESTRATED	-	0,1		-	0,6	0,2	5,3	1,1	0,2	0,5	-	-	0,2	1,0
	HYPOPLASTIC	9,6	10,0	10,0	4,0	17,6	7,3	-	14,6	13,5	31,2	7,1	11,2	3,1	7,6
ACA A2 (%)	AZYGOUS	0,2	2,1	-	0,4	1,5	-	1,8	-	1,2	1,4	1,2	-	0,2	-
	ANASTOMOSED	-	-	-	-	-	-	-	-	-	-	-	-	-	2,5
	DUPLICATED	-	-	-	-	-	-	-	-	-	-	-	-	-	0,5
	FENESTRATED	-	-	-	-	-	0,2	0,0	-	-	-	-	-	0,0	2,0
	HYPOPLASTIC	-	4,5	-	-	-	-	4,2	-	-	8,5	-	-	0,4	0,5
	TRIPLE ACA	-	1,7	-	2,8	1,9	1,0	3,9	-	-	5,2	4,3	-	0,5	3,0

- Indicates the absence of observation.

For both samples of the current study, 20-30% of the sample population exhibited typical anatomy of the entire ACAC, with a prevalence of 20,5% and 29,4% for the dissection and angiographic samples, respectively. The prevalence of typical ACAC anatomy in the studies mentioned in Table 5.1 is significantly similar to that of the present study, with a weighted average of 27,5%. However, Table 5.2 shows that the prevalence of typical ACAC anatomy shown in literature is less than half of that of the present study, with the weighted average reported to be only 7,6%. Differences in sensitivity, resolution and patient motion artifacts play a role in the accuracy of the various angiographic modalities (Feng and Shu, 2020). These factors used may be a potential reason for this significant difference in the angiographic findings.

The majority of the studies mentioned in Table 5.1 and Table 5.2 encompass populations in the continental region of Eurasia (Europe and Asia). With respect to the dissection sample, ACAC typical anatomy prevalence can be considered to reflect that of literature thus it may be potentially deduced that there is some degree of uniformity, between South Africa and Eurasia. However, further angiographic studies, using the same imaging

modality and a similar sample size, that investigate this relationship could potentially substantiate the validity of the proposed association.

When comparing both components of this study to each other, there are major morphological similarities for A1 and A2 variations found. A1 variations across both components reveal that hypoplasia is the most common type of variation in the present study sample. Furthermore, hypoplasia was the most common A1 variations across the literature and in the present study, therefore this variation may potentially be the most common A1 segment variation in the continental area of Afro-Eurasia (Africa, Europe and Asia). Similarily, triple ACA was the most common A2 variation across these regions. Additionally, X-shaped, H-shaped, hypoplasia and duplication are the only ACoA variations found in the majority of the studies. Thus, these variations may also be potentially considered the most common ACAC varitions in regions of Afro-Eurasia.

However, there is a noteable dissimilarity between the literature and the findings of this study. The present study has a more robust pool of variations in comparison to literature, with a few ACAC variations that appear unique to this study (Table 4.7) and thus potentially unique to the South African population. This may be due to the factors such as genetic variation, embryological development and epigenetic factors such as geographic location and diet.

5.3 Anterior Communicating Artery Complex morphometric variations

Table 5.3 is a compilation of various studies, inclusive of the present study, that investigated the morphometric parameters of either all the ACAC arteries or only individual arteries of the complex.

Table 5.3: A summary of studies showing morphometric parameters of the ACA A1 and ACA A2.

AUTHOR	REGION	SAMPLE (n)	RIGHT A1 LENGTH	LEFT A1 LENGTH	RIGHT A1 DIAMETER	LEFT A1 DIAMETER	*RIGHT A2 LENGTH	*LEFT A2 LENGTH	*RIGHT A2 DIAMETER	*LEFT A2 DIAMETER
Krishnamurthy et al., 2010	SPAIN	93	14,49 ± 0,28	14,22 ± 0,22	2,12 ± 0,07	2,32 ± 0,06	-	-	-	-
Zurada et al., 2010	POLAND	115	-	-	-	-	12,09 ± 5,06	11,63 ± 4,73	1,83 ± 0,37	1,88 ± 0,34
Aggarwal et al., 2012	INDIA	120	15,78 ± 3,71	17,37 ± 4,84	-	-	-	-	-	-
Kedia et al., 2013	INDIA	15	12,09 (10-15)	12 (10-15)	2,32 (2-3)	2,36 (1,5-3)	-	-	-	-
Karatas et al., 2016	TURKEY	100	14,44 ± 2,32	13,72 ± 2,12	1,87 ± 0,48	1,96 ± 0,49	-	-	-	-
Smita et al., 2016	INDIA	50	13 ± 0,86	12,04 ± 0,88	2,05 ± 0,43	2,8 ± 0,28	-	-	-	-
Cilliers et al., 2017	SOUTH AFRICA	61	14,11 ± 2,40	13,45 ± 2,09	-	-	-	-	-	-
Canaz et al., 2018	TURKEY	30	13,56 ± 2,25	13,76 ± 1,87	1,54 ± 0,37	1,84 ± 0,36	18,83 ± 3,18	18,73 ± 3,02	1,86 ± 0,13	1,84 ± 0,015
Shatri et al., 2019	GREECE	513	14,1 ± 1,51	13,87 ± 1,3	2,04 ± 0,28	2,06 ±0,26	-	-	-	-
Dhanalakshmi et al., 2019	INDIA	50	14,3 (11-18)	13, 7 (9-18)	1,76 (0,068-2,23)	1,8 (0,53-2,57)	-	-	-	-
Hassan et al., 2020	EGYPT	50	16,11 ± 3,4	15,83 ± 2,31	2,24 ± 0,33	2,18 ± 0,37	37,72 ± 3,33	37,93 ± 3,44	2,34 ± 0,62	2,27 ± 0,63
Luckrajh et al., 2022	SOUTH AFRICA	100	13,36 ± 2,70	12,43 ± 2,90	1,66 ± 0,47	1,77 ± 0,53	24,72 ± 6,12	25,07 ± 5,88	1,59 ± 0,42	1,6 ± 0,41

Present study	SOUTH AFRICA	183	13,5 (3,48)	12,85 (2,57)	2,26 (0,45)	2,25 (0,68)	23,4 (3,94)	23,7 (3,97)	2,3 (0,33)	2,37 (0,78)

*Total A2 sample (n) is 181

- Indicates the absence of measurement.

The internal lengths and diameters of the ACAC arteries were either recorded using mean ± standard deviation (SD), mean (min-max) or median (IQR) in millimetres (mm) depending on the distributions of the data. Similarly, in the present study, all the morphometric parameters are represented by the median (IQR) as this is more appropriate and accurate for a non-normal distribution of data.

The literature shows that the average length for the right A1 segment ranges from 12,09mm – 16,11 mm excluding their various standard deviations and/or ranges. The length of the right A1 segment in the present study falls within this range as it was recorded at 13,50 (3,80) mm. Canaz *et al.* (2018) reported a 13,56 ± 2,25 mm length for the right A1 segment, which is exceedingly similar to that of the present study. Another study completed in South Africa by Cilliers *et al.* (2017) reported a value slightly higher than the current one. The length of the right A1 segment was reported to be 14,11 ± 2,40 mm. Moreover, although it had close to half the sample size of the present study, a study also done in South Africa by Luckrajh *et al.* (2022), where all patients had ACoA aneurysms, had a similar right A1 length result, reported at 13,36 ± 2,70 mm.

Compared to the right A1 length, the left A1 segment length had a slightly larger range of 12,07-17,37 mm. However, from the present study, the average left A1 segment length measurement of 12,85 (2,57) mm is within the range reported in literature. Although marginally similar, Cilliers *et al.* (2017) reported the length of the left A1 segment to be 13,45 ± 2,09 mm. Whereas, Luckrajh *et al.* (2022) has a stronger agreement with the findings of the present study, with a reading of 12,43 ± 2,90 mm. In the present study, the diameter of the right A1 segment (2,26 (0,45) mm), narrowly falls within the range (1,66mm - 2,32 mm). The range for the left A1 segment, 1,77mm - 2,36 mm, also encompasses the result of the current study (2,25 (0,68) mm). For both the right and left A1 segment diameters, Hassan *et al.* (2020) reported very similar findings, 2,24 ± 0.33 mm and 2,18 ± 0,37 mm respectively.

When looking at Table 5.3, for both the right and left A2 segment lengths, a significantly large range of measurements is tabulated. For the right A2 length, an approximate range of 12,09mm - 37,93 mm is seen. Similar to the A1 findings, the average length of the right A2 segment for this study, 23,4 (3,94) mm, is within the previously reported range. For the left A2 length, an estimated range of 11,63 - 37,93 mm is reported and the present study reported a value of 23,7 (3,97) mm. Therefore, the left A2 length is also in agreement with literature. The large range of the A2 segment lengths may be explained by discrepancies in identifying and determining a uniform origin and termination of the A2 segment across the studies and differences in methodology. The left A2 diameter of this study is the only morphometric parameter that does not fall within the range shown in Table 5.3, reporting a value of 2,37 (0,78) mm in comparison to a range of ± 1,6 - 2,27 mm.

Table 5.4 shows that the ACoA length recorded in the present study is within the range provided by the previous studies in the Table. However, when strictly comparing the means and median, the ACoA diameter for this study does not fall within the range provided by previous studies.

Table 5.4: A summary of morphometric parameters of the anterior communicating artery.

AUTHOR	REGION	SAMPLE (n)	ACOA LENGTH	ACOA DIAMETER
Murray et al., 1963	AUSTRALIA	35	0,5	1
Cilliers et al., 2017	SOUTH AFRICA	61	3 ± 1,33	-
Shatri et al., 2019	GREECE	513	2,99 ± 0,62	1,16 ± 0,17
Tripathi et al., 2021	INDIA	100	2,80 (1,5-5,9)	1,11 (0,59-2,1)
Present study	SOUTH AFRICA	46	1,5 (1,76)	0,85 (0,91)

- Indicates the absence of measurement.

Using the Wilcoxon Signed Rank test, the parameters of the right A1 segment and A2 segment and the adjacent left A1 and A2 segment were compared to assess wether there was a significant difference between the measurement on each side (RHS vs LHS). As seen in Table 4.9, all the p-values were greater than 0,05 thus we can reject the hypothesis that there is a significant difference in morphometric parameters between the right A1 and A2 segment and the left A1 and A2 segment in the MRA images used for this study.

5.3.1 Morphormetric parameters of the ACAC across sex

To test whether there is a difference in the measurements of the ACAC parameters with regards to sex (female vs male), the Mann-Whitney U test was used. As seen in Table 4.8, all the p-values were greater than 0,05 except for the RHS A1 diameter which reported a p-value of 0,022. Therefore, the null hypothesis that there is no significant difference in A1 ACA length, A2 ACA length and ACoA length between females and males is accepted. Contrarily, Sharma *et al.* (2020) observed that ACA length is longer in females than in males. Additionally, the null hypothesis that there is no significant difference in RHS A1 segment diameter between females and males is rejected (p= 0,022). In Table 4.8 we can further see that females have a smaller RHS A1 diameter (2,26 (0,44)mm) compared to males (2,4 (0,2)mm). Similarily, previous studies from Krabbe-Hartkamp *et al*. (1998), Aggarwal et al. (2016) and Shatri *et al*. (2017) all concluded that the general ACA diameter is larger in males than in females. In contrast, Sharma *et al.* (2020) concludes that the general ACA diamter is smaller in males.

5.3.2 Morphometric parametres of the ACAC across age

The Kruskal-Willis test showed that when looking at the difference of the morphometric parameters in the ACAC with respect to age groups, no significance was found except for the LHS A2 diameter (p=0,006). The age group that had the largest A2 diameter was the '<30 years old' age group. Whereas, the '51-60 years old' age group had the smallest diameter. Thus, between the ages of 30 years old and 80 years old, a decrease in LHS A2 diameter can be seen. Similarily, evidence from a study by Sharma *et al*. (2020) showed that ACA diameter is greater in younger age groups (<40 years old). No significance was found between A1 ACA length, A2 ACA length and ACoA length in the present study, however, Sharma et al. (2020) concluded that ACA length is larger in younger age groups (<40 years old).

5.4 Prevalence of ACAC aneurysms

The 48 MRA images that presented with a history of aneurysms showed that the patients had already received treatement for the aneurysms via endovascular coiling. Furthermore, as seen in Table 4.12, the majority of the pre-coiled aneurysms were reported to be located at the ACoA (85,42%). Evidence from a study by Tetinou et.al (2021) showed that cerebral aneurysms are usually predominant in females, where prevalence in females

was recorded at 54% across the study cohorts. This observations is also propagated in the present study. As seen in Table 4.12, when compared to males, more pre-coiled aneurysms were found in females (64,5%). Additionally, the age groups 51-60 and 61-70 presented with the most cases of pre-coiled aneurysms.

5.5 Limitations of the present study

5.5.1 Dissection component

The equal and/or adequate representation of different age groups in the dissection sample was a challenge in this study. The minimum age in the dissection sample was only 30 years old and there were relatively few cadavers within the age range of 30-65 years old. Furthermore, since routine dissections were not completed solely for the purpose of this study but rather also for other educational purposes, some brain specimens and/or blood vessels were compromised due to dissection damage and/or extraction damage and thus did not meet the inclusion criteria. For this study to be more accurate and more reliable, a larger sample space and better range in demographics concerning age representation would be required to make more conclusive deductions. It is further recommended that the brain specimens involved in future studies should be primarily handled and extracted by the researcher to try and minimize any external dissection damage.

Moreover, the dissection sample only had morphological observations. Morphometric analyis of the ACAC in the cadavers would have been beneficial to the study as the findings could have been compared to the results found in the angiographic component of this study. Additionally, these potential morphometric parameters would have been able to assist in the definitive classification of hypoplastic ACA A1 and ACA A2 segments as previous literature have described hypoplasia of ACAC vessels to be characterised by a diameter less than 1mm.

5.5.2 Angiographic component

Although the South African population reportedly has more females than males, the number of MRA scans used in this study from female patients outnumbered those from male patients by a very large margin. Thus, comparisons of observations and measurements with relation to sex were subject to sampling bias. For future studies, a sample that closely reflects the true representation of the South African public would be advisable. Compared to the dissection portion of this study, the age distribution in the angiographic component was not skewed, However, better representation of the patients that are under of 30 years old and those above the age of 71 years old would be beneficial for more dependable deductions and conclusions.

Three dimensional TOF MRA scans are usually negatively affected by by signal loss due to spin dephasing when the blood flow is too slow or improperly orientated (not parrallel to the slice plane). In this study, the visual intergrity of several MRA scans was compromised. These MRA scans did not meet the inclusion criterion of this study and had to be excluded because of MRA susceptability artifacts. Additionally, the visualisation of the ACoA proved to be challenging. Therefore, it is recommended that future studies explore other imaging modalities in conjuction with 3D TOF MRA, such as catheter angiography for the visualisation of very small vessels like the ACoA. It would be beneficial for future studies to include other tertiary and/or quaternary hospitals from other provinces in South Africa so as to have have a true South African perspective.

Initially, one of the aims of this study was to investigate the type of aneurysms found in the ACAC and to investigate the relationship between the prevalence of ACAC variations and the presence of cerebral aneurysm. However, identifying cerebral aneurysms in the ACAC that had not received treatment via endovascular coiling was not possible. Thus, identifying whether an aneurysm was ´present' or not and the type of aneurysm at the time of observation by the researcher was not realisable.

Chapter 6: Conclusion

Literature about the morphology and morphometry of the anterior communicating artery complex is limited in Africa. This can also be extended to studies centred around investigating the characteristics of cerebral aneurysms and any potential link to cerebrovascular variations that these characteristics may have. Furthermore, the majority of these studies have been completed by countries in Europe and Asia. Similarities may be drawn between said countries and the present study. However, in a South African context, where cerebrovascular disease has a significant impact as a cause of morbidity, additional literature pertaining to the relationship between cerebrovascular variations and cerebrovascular diseases would be crucial in assisting clinicians. A limited number of studies in South Africa have concurrently investigated both the morphology and morphometry of all the arteries of the ACAC.

The primary aims of the present study were twofold. Firstly, this study aimed to explore morphological variations in anatomy, with a specific emphasis on investigating the morphometric parameters of the ACAC. Additionally, the study sought to examine the correlation between variant anatomy and demographic data such as age and sex, while also investigating the relationship between morphometric parameters and demographic information. Secondly, another key aim was to assess the association between anterior circulation cerebral aneurysms and the prevalence of ACAC variations. If established, this relationship could potentially provide insights into the likelihood of the presence or formation of ACAC aneurysms in the presence of vascular variations..

Typical ACAC anatomy accounted for close to a third of the combined sample space across both the dissection and angiographic components of this study. When looking at the different types of variations found across the individual arteries of the ACAC, although there is significant congruency, there is some slight dissonance between the findings from the dissection cohort and the MRA images. When considering the A1 segment, the most common variations found were hypoplasia, duplication and fenestration in both the dissection and angiographic components. Triple ACA is among the top two most common A2 variations for both components of this study. However, 'anastomosed', which is newly described in this study, was amongst the most common A2 segment variations in the dissection sample. Whereas in the angiographic component, hypoplasia was among the most common A2 variations. Overall, ACoA reported the most variations in the ACAC. There were various variations recorded for this artery, with some variations reported to be equally prevalent in each component. X-shaped ACoA and hypoplasia were the only variations that were reported to be amongst the most prevalent ACoA variations within both components of this study. Furthermore, newly described ACoA variations were found among the most common variations. In the cadaver cohort, short, wide and bulbous were part of the top five variations found. In the angiographic component, a curved ACoA was found to be the second most prevalent variation.

The morphometric parameters of the ACAC arteries in this study aim to populate the limited research for this complex within a South African sample. The measurements recorded in this study are within similar ranges with most published international studies and very similar to some studies previously conducted in a South African population. It is therefore imperative that these factors be investigated as they may be helpful in clinical settings such as in surgeries like revascularisation. Moreover, no significance difference was found in ACAC morphometry between the cerebral hemispheres.

When looking at the MRA, the prevalence of ACAC variations was significantly higher than that of the history of ACAC aneurysms. There was also no association found between the ACAC variations and the prevalence of pre-coiled aneurysms nor was there an association found between ACAC variations and the location of the pre-coiled aneurysms. These are not in agreement with literature, where a direct relationship has been proposed between ACAC variations and ACAC aneurysms (Gunnal and Wabale, 2013; Tahir *et al.*, 2019). This supports the implication that for a South African sample, there could be an additional causative factor that could play a role in the relationship between ACAC variations and anterior circulation cerebral aneurysms. Conversely, a study with a larger sample size and demographic might yield the results mentioned in previous literature.

Further research is needed to investigate these factors and their influence on the relationship between ACAC variations and anterior circulation cerebral aneurysms. When looking at sex, only the RHS A1 diameter recorded a significant difference between males and females. Additionally, concerning age, only the LHS A2 diameter showed a significant difference across all age groups. Other than those two parameters, no significant association was found between ACAC morphometry, sex and age. It can be argued that the sample space of this study may lend itself to inherent sample bias as there were significantly more females than males. However, similar to previous studies, more females presented with ACAC variations.

Anatomical variations are reported to have a crucial impact on surgery and surgical techniques. Furthermore, unanticipated anatomical variations often need surgical technique mitigation or modification. These variations, if not foreseen, may often cause intraoperative complexities and may lead to injuries due to surgical errors. As seen from this study, ACoA aneurysms are reported to be the most common anterior circulation aneurysms. Additionally, endovascular coiling was seen to be the primary intervention used by the vascular neurosurgeons for the treatment of the aneurysms. Therefore, to reduce any surgical complications and aid clinicians in their intervention techniques, it is imperative to understand both the morphological and morphometric characteristics of the anterior communicating artery complex.

Chapter 7: References

Abousrafa, S. and Mair, G. (2023) 'MRI for collateral assessment pre-thrombectomy and association with outcome: a systematic review and meta-analysis', *Neuroradiology*, 65, pp. 1–14. Available at: https://doi.org/10.1007/s00234-023-03127-8.

Abuelnor, M. (2017) 'Morphometric Variations of the Anterior Cerebral Artery', *World Journal of Pharmaceutical Research* [Preprint].

Andreasen, T.H., Bartek, J Jr., Andresen, M., Springborg, JB., Romner, B. (2013) 'Modifiable Risk Factors for Aneurysmal Subarachnoid Hemorrhage', *Stroke*, 44(12), pp. 3607–3612. Available at: https://doi.org/10.1161/STROKEAHA.113.001575.

Avci, E., Fossett, D., Aslan, M., Attar, A., Egemen, N. (2003) 'Branches of the anterior cerebral artery near the anterior communicating artery complex: an anatomic study and surgical perspective', *Neurologia Medico-Chirurgica*, 43(7), pp. 329–333; discussion 333. Available at: https://doi.org/10.2176/nmc.43.329.

Backes, D., Vergouwen, MD., Velthuis, BK., Van der Schaaf, IC., Bor, AS., Algra, A., Rinkel, GJ. (2014) 'Difference in Aneurysm Characteristics Between Ruptured and Unruptured Aneurysms in Patients With Multiple Intracranial Aneurysms', *Stroke*, 45(5), pp. 1299–1303. Available at: https://doi.org/10.1161/STROKEAHA.113.004421.

Bashir, U. (2012) *Time of flight angiography | Radiology Reference Article | Radiopaedia.org*, *Radiopaedia*. Available at: https://doi.org/10.53347/rID-18193.

Berger, A. (2002) 'Magnetic resonance imaging', *British Medical Journal*, 324(7328), p. 35.

Bertulli, L. and Robert, T. (2021) 'Embryological development of the human cranio-facial arterial system: a pictorial review', *Surgical and Radiologic Anatomy*, 43(6), pp. 961–973. Available at: https://doi.org/10.1007/s00276-021-02684-y.

Blignaut, G., Loggenberg, E. and Vries, C. de (2014) 'The radiological appearance of intracranial aneurysms in adults infected with the human immunodeficiency virus (HIV)', *South African Journal of Radiology*, 18(1), p. 4.

Bonasia, S. and Robert, T. (2021) 'Retractorless combined pterional and interhemispheric approach to achieve proximal control in pericallosal artery aneurysm: how I do it', *Acta Neurochirurgica*, 163. Available at: https://doi.org/10.1007/s00701-021-04782-7.

Borgdorff, P. and Tangelder, G. (2014) 'Incomplete Circle of Willis and Migraine: Role for Shear-Induced Platelet Aggregation?', *Headache*, 54, pp. 1054–6. Available at: https://doi.org/10.1111/head.12348.

Brisman, J.L., Song, J.K. and Newell, D.W. (2006) 'Cerebral Aneurysms', *New England Journal of Medicine*, 355(9), pp. 928–939. Available at: https://doi.org/10.1056/NEJMra052760.

Bull, J.W. (1970) 'The history of neuroradiology.', *Proceedings of the Royal Society of Medicine*, 63(6), pp. 637–643.

Burlakoti, A., Kumaratilake, J., Taylor, D., Henneberg, M. (2020) 'Quantifying asymmetry of anterior cerebral arteries as a predictor of anterior communicating artery complex aneurysm', *BMJ Surgery, Interventions, & Health Technologies*, 2(1), p. e000059. Available at: https://doi.org/10.1136/bmjsit-2020-000059.

Casale, J. and Giwa, A.O. (2022) 'Embryology, Branchial Arches', in *StatPearls*. Treasure Island (FL): StatPearls Publishing. Available at: http://www.ncbi.nlm.nih.gov/books/NBK538487/ (Accessed: 17 June 2022).

Castro, M.A., Putman, C.M., Sheridan, M.J., Cebral, J.R. (2009) 'Hemodynamic Patterns of Anterior Communicating Artery Aneurysms: A Possible Association with Rupture', *American Journal of Neuroradiology*, 30(2), pp. 297–302. Available at: https://doi.org/10.3174/ajnr.A1323.

Chandra, A., Li, William, A., Stone, Christopher, R., Geng, Xiaokun, Ding, Yuchuan. (2017) 'The cerebral circulation and cerebrovascular disease I: Anatomy', *Brain Circulation*, 3(2), pp. 45–56. Available at: https://doi.org/10.4103/bc.bc_10_17.

Courtenay, W.H. (2000) 'Constructions of masculinity and their influence on men's well-being: a theory of gender and health', *Social Science & Medicine*, 50(10), pp. 1385–1401. Available at: https://doi.org/10.1016/S0277-9536(99)00390-1.

Dhar, S., Tremmel, M., Mocco, J., Kim, M., Yamamoto, J., Siddiqui, AH., Hopkins, LN., Meng, H. (2008) 'Morphology Parameters for Intracranial Aneurysm Rupture Risk Assessment', *Neurosurgery*, 63(2), pp. 185–197. Available at: https://doi.org/10.1227/01.NEU.0000316847.64140.81.

D'Souza, S. (2015) 'Aneurysmal Subarachnoid Hemorrhage', *Journal of Neurosurgical Anesthesiology*, 27(3), pp. 222–240. Available at: https://doi.org/10.1097/ANA.0000000000000130.

Du Toit (2015) *Circulus Arteriosus Cerebri: Anatomical variations and their correlation to Cerebral Aneurysms*. University of Cape Town. Available at: https://open.uct.ac.za/bitstream/handle/11427/16481/thesis_hsf_2015_du_toit_francesca%20%281%29.pdf?sequence=1&isAllowed=y.

Dumitrescu, A., Cobzaru, R. and Ripa, C. (2021) 'Anatomical Variations of the Anterior Part of the Circle of Willis - An Autopsic Study', *Journal of Universal Surgery* [Preprint].

Feindel, W. (1962) 'Thomas Willis (1621-1675)-The Founder of Neurology', *Canadian Medical Association journal*, 87, pp. 289–96.

Feng, W., Zhang, L., Li, W., Zhang, G., He, X., Wang, G., Li, M., Qi, S. (2014) 'Relationship between the morphology of A-1 segment of anterior cerebral artery and anterior communicating artery aneurysms', *African Health Sciences*, 14(1), pp. 83–88. Available at: https://doi.org/10.4314/ahs.v14i1.13.

Feng, Y. and Shu, S.J. (2020) 'Diagnostic Value of Low-Dose 256-Slice Spiral CT Angiography, MR Angiography, and 3D-DSA in Cerebral Aneurysms', *Disease Markers*, 2020, p. e8536471. Available at: https://doi.org/10.1155/2020/8536471.

Fréneau, M., Baron-Menguy, C., Vion, AC., Loirand, G. (2022) 'Why Are Women Predisposed to Intracranial Aneurysm?', *Frontiers in Cardiovascular Medicine*, 9, p. 815668. Available at: https://doi.org/10.3389/fcvm.2022.815668.

Gaillard, F. (2008a) *Anterior cerebral artery | Radiology Reference Article | Radiopaedia.org*, *Radiopaedia*. Available at: https://doi.org/10.53347/rID-4803.

Gaillard, F. (2008b) 'Anterior communicating artery', *Radiopaedia.org* [Preprint]. Available at: https://doi.org/10.53347/rID-4804.

Gerecht-Nir, S., Osenberg, S., Nevo, O., Ziskind, A., Coleman, R., Itskovitz-Eldor, J. (2004) 'Vascular Development in Early Human Embryos and in Teratomas Derived from Human Embryonic Stem Cells1', *Biology of Reproduction*, 71(6), pp. 2029–2036. Available at: https://doi.org/10.1095/biolreprod.104.031930.

Ghods, A.J., Lopes, D. and Chen, M. (2012) 'Gender Differences in Cerebral Aneurysm Location', *Frontiers in Neurology*, 3, p. 78. Available at: https://doi.org/10.3389/fneur.2012.00078.

Good, D.C. (1990) 'Cerebrovascular Disease', in H.K. Walker, W.D. Hall, and J.W. Hurst (eds) *Clinical Methods: The History, Physical, and Laboratory Examinations*. 3rd edn. Boston: Butterworths. Available at: http://www.ncbi.nlm.nih.gov/books/NBK378/ (Accessed: 17 June 2022).

Gunnal, S.A. and Wabale, R.N. (2013) 'Variations of anterior cerebral artery in human cadavers', *Neurology Asia*, pp. 249–259.

Gupta, G. (2022) 'Circle of Willis Anatomy: Overview, Gross Anatomy, Natural Variants', 15 March. Available at: https://emedicine.medscape.com/article/1877617-overview (Accessed: 13 May 2022).

Gupta, S.K., Gulati, G.S. and Anderson, R.H. (2016) 'Clarifying the anatomy of the fifth arch artery', *Annals of Pediatric Cardiology*, 9(1), pp. 62–67. Available at: https://doi.org/10.4103/0974-2069.171392.

Hacking, C. and Safitiri, D. (2019) 'Anterior circulation', *Radiopaedia.org* [Preprint]. Available at: https://doi.org/10.53347/rID-71653.

Hoeffner, E.G., Mukherji, SK., Srinivasan, A., Quint, DJ. (2012) 'Neuroradiology Back to the Future: Brain Imaging', *American Journal of Neuroradiology*, 33(1), pp. 5–11. Available at: https://doi.org/10.3174/ajnr.A2936.

Hughes, J.D. *et al.* (2018) 'Estimating the Global Incidence of Aneurysmal Subarachnoid Hemorrhage: A Systematic Review for Central Nervous System Vascular Lesions and Meta-Analysis of Ruptured Aneurysms', *World Neurosurgery*, 115, pp. 430-447.e7. Available at: https://doi.org/10.1016/j.wneu.2018.03.220.

Iqbal, S. (2013) 'A Comprehensive Study of the Anatomical Variations of the Circle of Willis in Adult Human Brains', *Journal of Clinical and Diagnostic Research,* 7(11), pp. 2423–2427. Available at: https://doi.org/10.7860/JCDR/2013/6580.3563.

Javed, K. and M Das, J. (2022) 'Neuroanatomy, Anterior Choroidal Arteries', in *StatPearls*. Treasure Island (FL): StatPearls Publishing. Available at: http://www.ncbi.nlm.nih.gov/books/NBK538189/ (Accessed: 13 May 2022).

Javed, K., Reddy, V. and Lui, F. (2022) 'Neuroanatomy, Cerebral Cortex', in *StatPearls*. Treasure Island (FL): StatPearls Publishing. Available at: http://www.ncbi.nlm.nih.gov/books/NBK537247/ (Accessed: 17 June 2022).

Javed, K., Reddy, V. and M Das, J. (2022) 'Neuroanatomy, Posterior Cerebral Arteries', in *StatPearls*. Treasure Island (FL): StatPearls Publishing. Available at: http://www.ncbi.nlm.nih.gov/books/NBK538474/ (Accessed: 13 May 2022).

Jersey, A.M. (2022) 'Cerebral Aneurysm', in *StatPearls*. Treasure Island (FL): StatPearls Publishing. Available at: http://www.ncbi.nlm.nih.gov/books/NBK507902/ (Accessed: 17 June 2022).

Jeyaraman, M.M., Al-Yousif, N., Robson, RC., Copstein, L., Balijepalli, C., Hofer, K., Fazeli, MS., Ansari, MT., Tricco, AC., Rabbani, R., Abou-Setta, AM. (2020) 'Inter-rater reliability and validity of risk of bias instrument

for non-randomized studies of exposures: a study protocol', *Systematic Reviews*, 9(1), p. 32. Available at: https://doi.org/10.1186/s13643-020-01291-z.

Jirjees, S., Htun, ZM., Aldawudi, I., Katwal, PC., Khan S. (2020) 'Role of Morphological and Hemodynamic Factors in Predicting Intracranial Aneurysm Rupture: A Review', *Cureus*, 12(7), p. e9178. Available at: https://doi.org/10.7759/cureus.9178.

Jones, J. (2009) 'Posterior cerebral circulation', *Radiopaedia* [Preprint]. Available at: https://doi.org/10.53347/rID-5874.

Jou, L.-D., Lee, D.H. and Mawad, M. (2010) 'Cross-flow at the anterior communicating artery and its implication in cerebral aneurysm formation', *Journal of biomechanics*, 43, pp. 2189–95. Available at: https://doi.org/10.1016/j.jbiomech.2010.03.039.

Jung, K.-H. (2018) 'New Pathophysiological Considerations on Cerebral Aneurysms', *Neurointervention*, 13(2), pp. 73–83. Available at: https://doi.org/10.5469/neuroint.2018.01011.

Kamal, H., Fine, EJ., Shakibajahromi, B., Mowla, A. (2020) 'A history of the path towards imaging of the brain: From skull radiography through cerebral angiography', *Current Journal of Neurology*, 19(3), pp. 131–137. Available at: https://doi.org/10.18502/cjn.v19i3.5426.

Kannabathula, A.B., Rai, G. and Sunam, H. (2017) 'ANATOMICAL VARIATIONS OF ANTERIOR CEREBRAL ARTERY AND ANTERIOR COMMUNICATING ARTERY: A CADAVERIC STUDY', *International Journal of Anatomy and Research*, 5(2.3), pp. 3882–3890. Available at: https://doi.org/10.16965/ijar.2017.179.

Kapsalaki, E.Z., Rountas, C.D. and Fountas, K.N. (2012) 'The Role of 3 Tesla MRA in the Detection of Intracranial Aneurysms', *International Journal of Vascular Medicine*, 2012, p. 792834. Available at: https://doi.org/10.1155/2012/792834.

Karatas, A., Yilmaz, H., Coban, G., Koker, M., Uz, A. (2015) 'The anatomy of circulus arteriosus cerebri (circle of willis): a study in turkish population', *Turkish Neurosurgery* [Preprint]. Available at: https://doi.org/10.5137/1019-5149.JTN.13281-14.1.

Kayembe, K.N., Sasahara, M. and Hazama, F. (1984) 'Cerebral aneurysms and variations in the circle of Willis', *Stroke*, 15(5), pp. 846–850. Available at: https://doi.org/10.1161/01.str.15.5.846.

Klostranec, J.M. and Krings, T. (2022) 'Cerebral neurovascular embryology, anatomic variations, and congenital brain arteriovenous lesions', *Journal of NeuroInterventional Surgery* [Preprint]. Available at: https://doi.org/10.1136/neurintsurg-2021-018607.

Konan, L.M., Reddy, V. and Mesfin, F.B. (2023) 'Neuroanatomy, Cerebral Blood Supply', in *StatPearls*. Treasure Island (FL): StatPearls Publishing. Available at: http://www.ncbi.nlm.nih.gov/books/NBK532297/ (Accessed: 5 June 2023).

Kovač, J.D., Stanković, A., Stanković, D., Kovač, B., Šaranović, D. (2014) 'Intracranial arterial variations: A comprehensive evaluation using CT angiography', *Medical Science Monitor: International Medical Journal of Experimental and Clinical Research*, 20, pp. 420–427. Available at: https://doi.org/10.12659/MSM.890265.

Krabbe-Hartkamp, M.J., van der Grond, J., de Leeuw, FE., de Groot, JC., Algra, A., Hillen, B., Breteler, MM., Mali, WP., (1998) 'Circle of Willis: morphologic variation on three-dimensional time-of-flight MR angiograms.', *Radiology*, 207(1), pp. 103–111. Available at: https://doi.org/10.1148/radiology.207.1.9530305.

Kramer, B. *et al.* (2019) 'Making the Ethical Transition in South Africa: Acquiring Human Bodies for Training in Anatomy', *Anatomical Sciences Education*, 12(3), pp. 264–271. Available at: https://doi.org/10.1002/ase.1814.

Krzyżewski, R., Tomaszewska IM., Lorenc, N., Kochana, M., Goncerz, G., Klimek-Piotrowska, W., Walocha, K., Urbanik, A. (2014) 'Variations of the anterior communicating artery complex and occurrence of anterior communicating artery aneurysm: A2 segment consideration', *Folia medica Cracoviensia*, 54, pp. 13–20.

Krzyżewski, R.M., Tomaszewski, K.A. and Kochana, M. (2015) 'Anatomical variations of the anterior communicating artery complex: gender relationship', *Surgical and Radiologic Anatomy*, 37(1), pp. 81–86. Available at: https://doi.org/10.1007/s00276-014-1313-7.

Lehecka, M., Dashti, R., Lehto, H., Kivisaari, R. (2010) 'Distal Anterior Cerebral Artery Aneurysms', in *Surgical Management of Cerebrovascular Disease*. Vienna: Springer (Acta Neurochirurgica Supplementum), pp. 15–26. Available at: https://doi.org/10.1007/978-3-211-99373-6_3.

López-Sala, P., Alberdi, N., Mendigaña, M., Bacaicoa, MC., Cabada, T. (2020) 'Anatomical variants of anterior communicating artery complex. A study by Computerized Tomographic Angiography', *Journal of Clinical Neuroscience: Official Journal of the Neurosurgical Society of Australasia*, 80, pp. 182–187. Available at: https://doi.org/10.1016/j.jocn.2020.08.019.

Margeta, M. and Perry, Arie (2020) 'The Central Nervous System', in *Robbins & Cotran Pathologic Basis of Disease*. 10th edn. Elsevier, pp. 1241–1304. Available at: https://www-clinicalkey-com.ezproxy.uct.ac.za/#!/content/book/3-s2.0-B9780323531139000285 (Accessed: 6 July 2022).

Menshawi, K., Mohr, Jay P and Gutierrez, J. (2015) 'A Functional Perspective on the Embryology and Anatomy of the Cerebral Blood Supply', *Journal of Stroke*, 17(2), pp. 144–158. Available at: https://doi.org/10.5853/jos.2015.17.2.144.

Monroy-Sosa, A., Pérez-Cruz, JC. and Reyes-Soto, G. (2013) 'Importancia de la anatomía microquirúrgica del complejo A1-arteria comunicante anterior', *Cirugia y cirujanos*, 81, pp. 274–281.

National Institute of Neurological Disorders and Stroke (2023) *Cerebral Aneurysms*, *National Instituite of Nuerological Disorders and Stroke*. Available at: https://www.ninds.nih.gov/health-information/disorders/cerebral-aneurysms (Accessed: 25 January 2024).

Ogeng'o, J.A., Otieno, BO., Kilonzi, J., Sinkeet, SR., Muthoka, JM. (2009) 'Intracranial aneurysms in an African country', *Neurology India*, 57(5), pp. 613–616. Available at: https://doi.org/10.4103/0028-3886.57816.

Orakdogen, M., Tural Emon, S., Somay, H., Engin, T., IS, M., Hakan, T. (2017) 'Vascular Variations Associated with Intracranial Aneurysms', *Turkish Neurosurgery*, 27(6), pp. 853–862. Available at: https://doi.org/10.5137/1019-5149.JTN.17839-16.1.

'Protection of Personal Information Act (POPI Act)' (2013). Available at: https://popia.co.za/ (Accessed: 13 May 2022).

Purves, D. *et al.* (2001) *The Blood Supply of the Brain and Spinal Cord*. 2nd edn. Sinauer Associates. Available at: https://www.ncbi.nlm.nih.gov/books/NBK11042/ (Accessed: 13 May 2022).

Ren, Z. (2022) 'Infectious Aneurysms (Mycotic Aneurysms)', in Z. Ren (ed.) *Eight Aneurysms: Handbook of Cerebral Aneurysm Embolization*. Cham: Springer International Publishing, pp. 229–235. Available at: https://doi.org/10.1007/978-3-030-97216-5_14.

Rivera, P.A. and Dattilo, J.B. (2022) 'Pseudoaneurysm', in *StatPearls*. Treasure Island (FL): StatPearls Publishing. Available at: http://www.ncbi.nlm.nih.gov/books/NBK542244/ (Accessed: 12 September 2022).

Scepkowski, L. and Cronin-Golomb, A. (2004) 'The Alien Hand: Cases, Categorizations, and Anatomical Correlates', *Behavioral and cognitive neuroscience reviews*, 2, pp. 261–77. Available at: https://doi.org/10.1177/1534582303260119.

Sharma, S., Dixit, SG., Khera, PS., Nayyar, AK., Ghatak, S. (2020) 'Morphometric evaluation of Anterior Cerebral Artery (on Digital Subtraction Angiography)–Potential implications', *Morphologie*, 104(345), pp. 109–116. Available at: https://doi.org/10.1016/j.morpho.2019.07.001.

Sharma, S., Krishna, H., Dixit, SG., Nayyar, AK., Khera, P., Ghatak, S. (2023) 'Systematic Review of Morphometric Analysis of Anterior Cerebral Artery (ACA) Emphasizing on Its Clinical Implications', *Cureus*, 15(4), p. e37744. Available at: https://doi.org/10.7759/cureus.37744.

Shatri, J., Bexheti, D., Bexheti, S., Kabashi, S., Krasniqi, S., Ahmetgjekaj, I., Valbona, Z.(2017) 'Influence of Gender and Age on Average Dimensions of Arteries Forming the Circle of Willis Study by Magnetic Resonance Angiography on Kosovo's Population', *Open Access Macedonian Journal of Medical Sciences*, 5(6), pp. 714–719. Available at: https://doi.org/10.3889/oamjms.2017.160.

Shatri, J., Bexheti, S., Shatri, M., Kabashi, A., Mucaj, S. (2021) 'Anatomical Variations in the Circulus Arteriosus Cerebri with Clinical Importance – Results of an Magnetic Resonance Angiography Study and Review of Literature', *Journal of Clinical Imaging Science*, 11, p. 8. Available at: https://doi.org/10.25259/JCIS_100_2020.

Standring, S. (2020) 'Head and neck: Overview and surface anatomy', in *Gray's Anatomy : The anatomical basis of clinical practice*. 42nd edn. Elsevier, pp. 546–557. Available at: https://www-clinicalkey-com.ezproxy.uct.ac.za/#!/content/book/3-s2.0-B9780702077050000331 (Accessed: 5 July 2022).

Stats SA (2018) 'Mortality and causes of death in South Africa: Findings from death notification'. Statistics South Africa. Available at: https://www.statssa.gov.za/publications/P03093/P030932018.pdf.

Tahir, R.A., Haider, S., Kole, M., Griffith, B., Marin, H. (2019) 'Anterior Cerebral Artery: Variant Anatomy and Pathology', *Journal of Vascular and Interventional Neurology*, 10(3), pp. 16–22.

Tang, H., Hu, N., Yuan, Y., Xia, C., Liu, X., Zuo, P., Stalder, AF., Schmidt, M., Zhou, X., Song, B., Sun, J. (2019) 'Accelerated Time-of-Flight Magnetic Resonance Angiography with Sparse Undersampling and Iterative Reconstruction for the Evaluation of Intracranial Arteries', *Korean Journal of Radiology*, 20(2), pp. 265–274. Available at: https://doi.org/10.3348/kjr.2017.0634.

Tarulli, E., Sneade, M., Clarke, A., Molyneux, AJ., Fox, AJ. (2014) 'Effects of circle of Willis anatomic variations on angiographic and clinical outcomes of coiled anterior communicating artery aneurysms', *AJNR. American journal of neuroradiology*, 35(8), pp. 1551–1555. Available at: https://doi.org/10.3174/ajnr.A3991.

Tetinou, F., Kanmounye, US., Sadler, S., Nitcheu, I., Oriaku, AJ., Ndajiwo, AB., Bankole, N. (2021) 'Cerebral aneurysms in Africa: A scoping review', *Interdisciplinary Neurosurgery*, 26, p. 101291. Available at: https://doi.org/10.1016/j.inat.2021.101291.

Tripathi, A., Kausar, H., Patel, AK., Raizaday, S., Jain, S., Khare, S. (2021) 'Retrospective Study of Variations in Anterior Communicating Artery in Human Cadaveric Brains in Western Uttar Pradesh Region', *Mædica*, 16(3), p. 400. Available at: https://doi.org/10.26574/maedica.2021.16.3.400.

Ujiie, H., Liepsch, DW., Goetz, M., Yamaguchi, R., Yonetani, H., Takakura, K. (1996) 'Hemodynamic Study of the Anterior Communicating Artery', *Stroke; a journal of cerebral circulation*, 27, pp. 2086–93; discussion 2094. Available at: https://doi.org/10.1161/01.STR.27.11.2086.

Van Den Bergh, R. and Van Der Eecken, H. (1968) 'Anatomy and Embryology of Cerebral Circulation', in W. Luyendijk (ed.) *Progress in Brain Research*. Elsevier (Cerebral Circulation), pp. 1–25. Available at: https://doi.org/10.1016/S0079-6123(08)61433-8.

Vilela, P. (2019) 'Cranial Vessel Embryology and Imaging Anatomy', in F. Barkhof et al. (eds) *Clinical Neuroradiology*. Cham: Springer International Publishing, pp. 95–135. Available at: https://doi.org/10.1007/978-3-319-68536-6_20.

Wang, F., Xu, B., Sun, Z., Wu, C., Zhang, X. (2013) 'Wall shear stress in intracranial aneurysms and adjacent arteries', *Neural Regeneration Research*, 8(11), pp. 1007–1015. Available at: https://doi.org/10.3969/j.issn.1673-5374.2013.11.006.

Wilms, G. and Baert, A.L. (1995) 'The history of angiography', *Journal Belge De Radiologie*, 78(5), pp. 299–302.

Withers, K. and Carolan-Rees, G. (2013) 'Embolization Device for the Treatment of Complex Intracranial Aneurysms: A NICE Medical Technology Guidance', *ResearchGate* [Preprint]. Available at: https://doi.org/10.1007/s40258-012-0005-x.

World Medical Association (2013) 'World Medical Association Declaration of Helsinki: Ethical Principles for Medical Research Involving Human Subjects', *Journal of the American Medical Association*, 310(20), pp. 2191–2194. Available at: https://doi.org/10.1001/jama.2013.281053.

Yokuş, A., Toprak, N., Gündüz, A.M., Akdeniz, H., Akdemir, Z., Dündar, İ., Arslan, H. (2021) 'Anterior Cerebral Artery and Anterior Communicating Artery Variations: Assessment with Magnetic Resonance Angiography.', *World Neurosurgery*, 155, e203–e209. https://doi.org/10.1016/j.wneu.2021.08.027

Żurada, A., Gielecki, J., Tubbs, R.S., Loukas, M., Cohen-Gadol, A.A., Chlebiej, M., Maksymowicz, W., Nowak, D., Zawiliński, J., Michalak, M., (2010) 'Three-dimensional morphometry of the A2 segment of the anterior cerebral artery with neurosurgical relevance.', *Clinical Anatomy*, 23, 759–769. https://doi.org/10.1002/ca.21036

Appendix A: Formulated data sheets

Formulated data sheets for dissection sample.

DATE					
CODE					
SEX					
AGE					
VARA1_LHS					
VARA1_RHS					
TYPEA1_LHS					
TYPEA1_RHS					
VARA2_LHS					
VARA2_RHS					
TYPEA2_LHS					
TYPEA2_RHS					
VAR_ACOA					
TYPE_ACOA					

Formulated datasheets for angiographic sample.

DATE								
UNIQUE CODE								
SEX								
AGE								
A1_LENGTH_LHS1								
A1_LENGTH_LHS2								
AVERAGE_A1_LENGTH_LHS								
A1_LENGTH_RHS1								
A1_LENGTH_RHS2								
AVERAGE_A1_LENGTH_RHS								
A1_WIDTH_LHS_P								
AVERAGE_A1_WIDTH_LHS								
A1_WIDTH_RHS_D								
A1_WIDTH_RHS_M								
A1_WIDTH_RHS_P								
AVERAGE_A1_WIDTH_RHS								
VARA1 _LHS								
VARA1_RHS								
TYPEA1_LHS								
TYPEA1_RHS								
ACOA LENGTH								
AVERAGE_ACOA_LENGTH								
ACOA WIDTH								
AVERAGE_ACOA_WIDTH								

VARACOA								
TYPE								
A2_LENGTH_LHS								
AVERAGE_A2_LENGTH_LHS								
A2_LENGTH_RHS								
AVERAGE_A2_LENGTH_RHS								
A2_WIDTH_LHS_D								
A2_WIDTH_LHS_M								
A2_WIDTH_LHS_P								
AVERAGE_A2_WIDTH_LHS								
A2_WIDTH_RHS_D								
A2_WIDTH_RHS_M								
A2_WIDTH_RHS_P								
AVERAGE_A2_WIDTH_RHS								
VARA2_LHS								
VARA2_RHS								
TYPEA2_LHS								
TYPEA2_RHS								
ANEURYSM_PRESENT								
ANEURYSM_HISTORY								
NOTES								

Appendix B: REDCap datasheets

CADAVER DATA COLLECTION

RECORD ID	_____
CODE	_____
SEX	○ Male ○ Female
AGE	_____
A1 VARIATION LHS	○ Yes ○ No ○ N/A
A1 VARIATION RHS	○ Yes ○ No ○ N/A
A1 VARIATION TYPE LHS	_____
A1 VARIATION TYPE RHS	_____
A2 VARIATION LHS	○ Yes ○ No ○ N/A
A2 VARIATION RHS	○ Yes ○ No ○ N/A
A2 VARIATION TYPE LHS	_____
A2 VARIATION TYPE RHS	_____
ACoA VARIATION	○ Yes ○ No ○ N/A
ACoA VARIATION TYPE	_____
NOTES	_____

GSH DATA COLLECTION

RECORD ID	_____
UNIQUE CODE	_____
CODE	_____
SEX	○ Male ○ Female
AGE	_____
A1 LHS LENGTH1	_____
A1 LHS LENGTH2	_____
A1 LHS LENGTH AVERAGE	_____
A1 RHS LENGTH1	_____
A1 RHS LENGTH2	_____
A1 RHS LENGTH AVERAGE	_____
A1 LHS WIDTH P	_____
A1 LHS WIDTH M	_____
A1 LHS WIDTH D	_____
A1 LHS WIDTH AVERAGE	_____
A1 RHS WIDTH P	_____
A1 RHS WIDTH M	

A1 RHS WIDTH D	_____
A1 RHS WIDTH AVERAGE	_____
A1 VARIATION LHS	○ Yes ○ No ○ N/A
A1 VARIATION RHS	○ Yes ○ No ○ N/A
A1 VARIATION TYPE LHS	_____
A1 VARIATION TYPE RHS	_____
A2 LHS LENGTH1	_____
A2 LHS LENGTH2	_____
A2 LHS LENGTH AVERAGE	_____
A2 RHS LENGTH1	_____
A2 RHS LENGTH2	_____
A2 RHS LENGTH AVERAGE	_____
A2 LHS WIDTH P	_____
A2 LHS WIDTH M	_____
A2 LHS WIDTH D	_____
A2 LHS WIDTH AVERAGE	_____
A2 RHS WIDTH P	_____
A2 RHS WIDTH M	_____

A2 RHS WIDTH D	_____
A2 RHS WIDTH AVERAGE	_____
A2 VARIATION LHS	○ Yes ○ No ○ N/A
A2 VARIATION RHS	○ Yes ○ No ○ N/A
A2 VARIATION TYPE LHS	_____
A2 VARIATION TYPE RHS	_____
ACOA LENGTH1	_____
ACOA LENGTH12	_____
ACOA LENGTH AVERAGE	_____
ACOA WIDTH1	_____
ACOA WIDTH2	_____
ACOA WIDTH AVERAGE	_____
ACOA VARIATION	○ Yes ○ No ○ N/A
ACOA VARIATION TYPE	_____
ANEURYSM PRESENT	○ Yes ○ No ○ N/A
ANEURYSM HISTORY	○ Yes ○ No ○ N/A
ANEURYSM LOCATION	○ A1 ○ A2 ○ ACOA

Appendix C: Normality Tests

Descriptives and normality test for the age distribution in the dissection samples.

Case Processing Summary

	Cases					
	Valid		Missing		Total	
	N	Percent	N	Percent	N	Percent
AGE	68	100.0%	0	0.0%	68	100.0%

Descriptives

			Statistic	Std. Error
AGE	Mean		75.44	1.853
	95% Confidence Interval for Mean	Lower Bound	71.74	
		Upper Bound	79.14	
	5% Trimmed Mean		76.74	
	Median		79.00	
	Variance		233.474	
	Std. Deviation		15.280	
	Minimum		30	
	Maximum		97	
	Range		67	
	Interquartile Range		18	
	Skewness		-1.310	.291
	Kurtosis		1.357	.574

Tests of Normality

	Kolmogorov-Smirnov[a]			Shapiro-Wilk		
	Statistic	df	Sig.	Statistic	df	Sig.
AGE	.168	68	<,001	.878	68	<,001

a. Lilliefors Significance Correction

Descriptives and normality test for the age distribution in the angiographic samples.

Case Processing Summary

	Cases					
	Valid		Missing		Total	
	N	Percent	N	Percent	N	Percent
AGE	208	100.0%	0	0.0%	208	100.0%

Descriptives

			Statistic	Std. Error
AGE	Mean		52.84	.913
	95% Confidence Interval for Mean	Lower Bound	51.04	
		Upper Bound	54.64	
	5% Trimmed Mean		52.81	
	Median		52.00	
	Variance		173.538	
	Std. Deviation		13.173	
	Minimum		17	
	Maximum		84	
	Range		67	
	Interquartile Range		17	
	Skewness		.036	.169
	Kurtosis		-.061	.336

Tests of Normality

	Kolmogorov-Smirnov[a]			Shapiro-Wilk		
	Statistic	df	Sig.	Statistic	df	Sig.
AGE	.061	208	.061	.992	208	.359

a. Lilliefors Significance Correction

Tests of Normality

	Kolmogorov-Smirnov[a]			Shapiro-Wilk		
	Statistic	df	Sig.	Statistic	df	Sig.
AVERAGE_A1_LENGTH_LHS	.098	100	.018	.970	100	.022
AVERAGE_A1_WIDTH_LHS	.137	100	<,001	.933	100	<,001
AVERAGE_A2_LENGTH_LHS	.095	100	.026	.963	100	.007
AVERAGE_A2_WIDTH_LHS	.147	100	<,001	.960	100	.004
AVERAGE_A1_LENGTH_RHS	.110	100	.005	.970	100	.023
AVERAGE_A1_WIDTH_RHS	.133	100	<,001	.945	100	<,001

AVERAGE_A2_LENGTH_RHS	.094	100	.028	.978	100	.091
AVERAGE_A2_WIDTH_RHS	.120	100	.001	.971	100	.028
AVERAGE_ACOA_LENGTH	.234	100	<,001	.866	100	<,001
AVERAGE_ACOA_WIDTH	.260	100	<,001	.845	100	<,001

a. Lilliefors Significance Correction

Appendix D: MRA images showing measurement sites of ACAC arteries.

These figures show the measurement sites for the morphometric parameters of the ACAC arteries using an MRA scan from a 64-year-old female

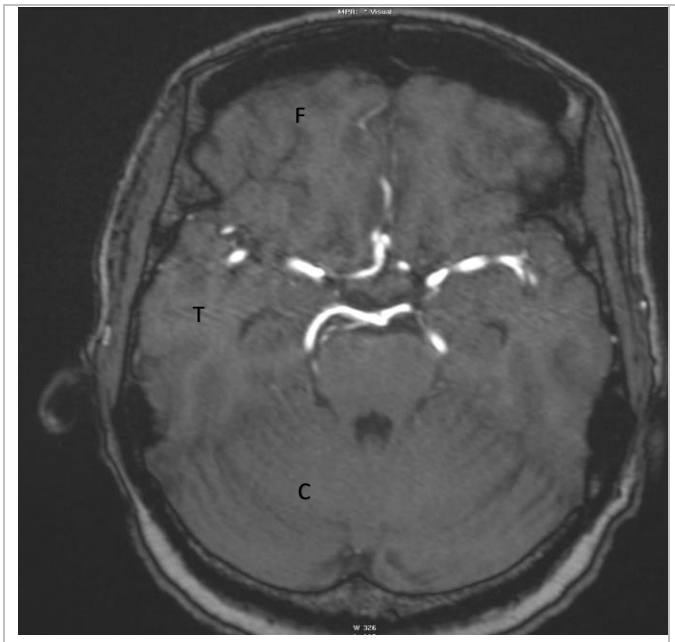

Uncontrasted brain MRA in an axial plane showing the full CAC.
*F- Frontal lobe
T-Temporal lobe
C-Cerebellum
A-anterior
L-left
R-right
P-posterior

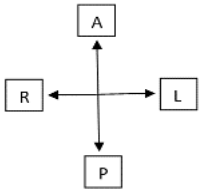

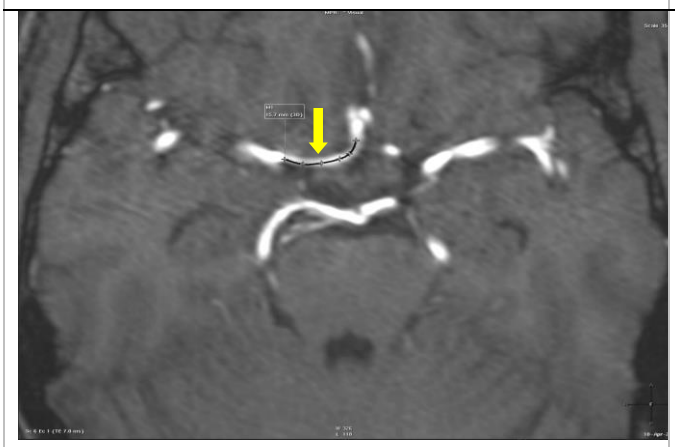

Uncontrasted brain MRA in axial plane showing length measurement (black line) across left A1 segment.
*Yellow arrow= A1 segment (LHS)

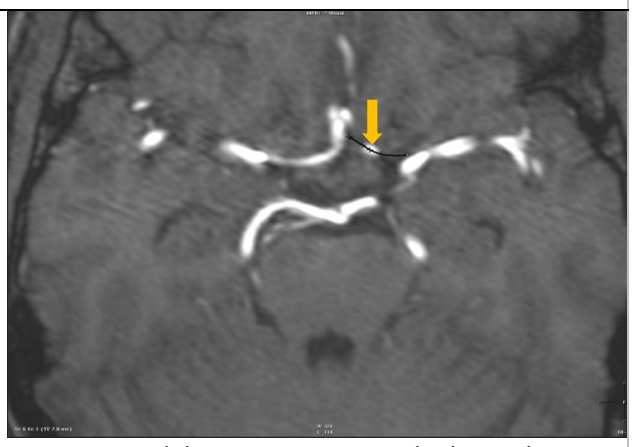

Uncontrasted brain MRA in axial plane showing length measurement (black line) across right A1 segment.
*Orange arrow= A1 segment (RHS)

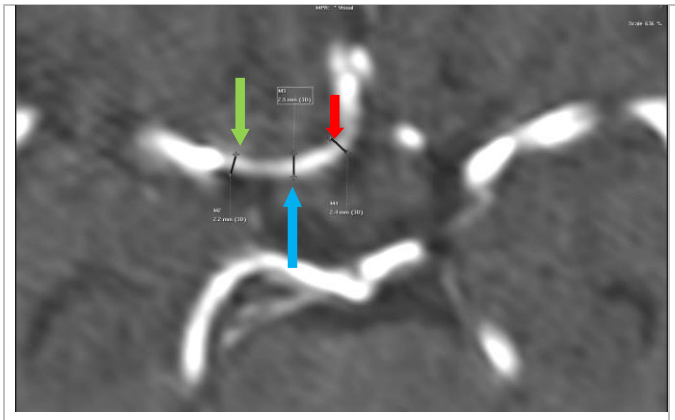

Uncontrasted brain MRA in axial plane showing diameter measurements (black lines) across left A1 segment. *Green arrow= PD, Blue arrow= MD Red arrow= DD

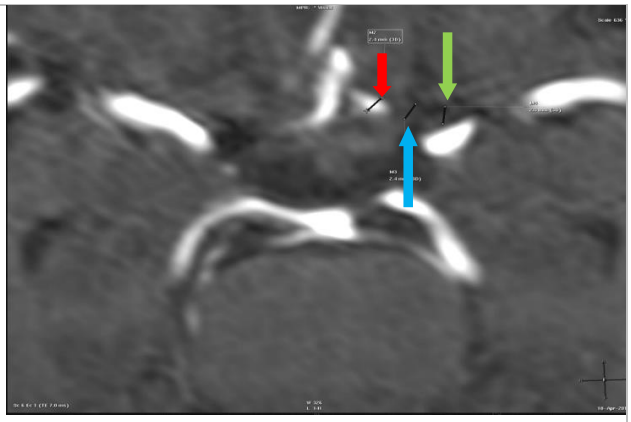

Uncontrasted brain MRA in axial plane showing diameter measurements (black line across right A1 segment. *Green arrow= PD, Blue arrow= MD, Red arrow = DD

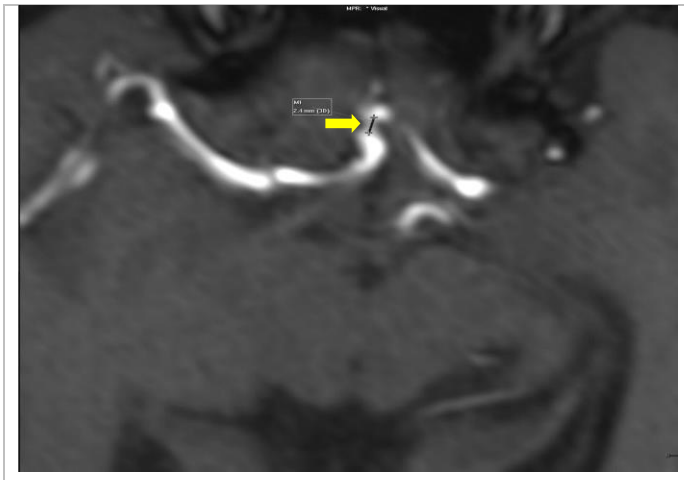

Uncontrasted brain MRA in an axial plane showing length measurement of ACoA.
*Yellow arrow= ACoA

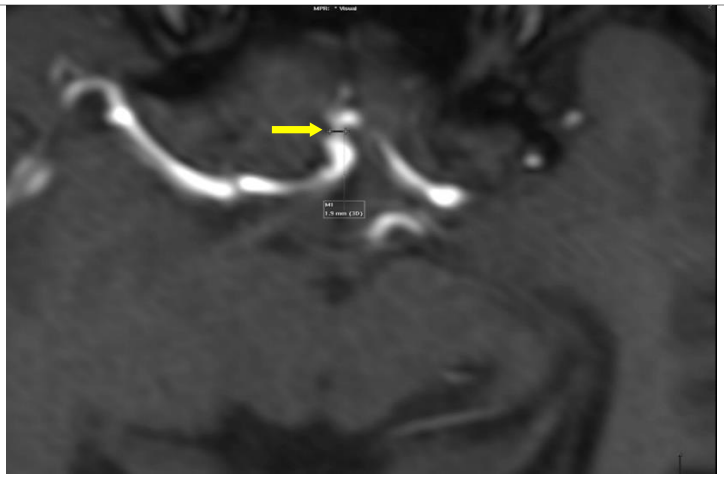

Uncontrasted brain MRA in an axial plane showing diameter measurement of ACoA.
*Yellow arrow= ACoA

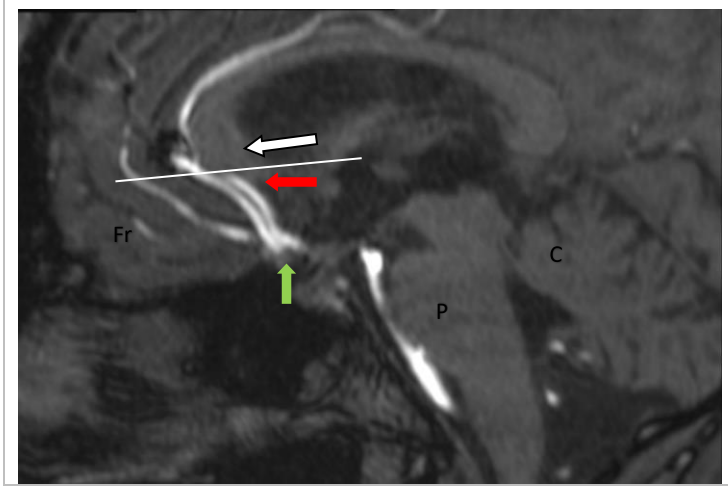

Uncontrasted brain MRA in a sagittal plane showing both left and right A2 segments of the ACA.
*Fr= Frontal lobe
P= Pons
C=Cerebellum
A= anterior
L=left
P=posterior
F=foot
H=head
White line= where rostrum and genu of Corpus Callosum meet
Red arrow= rostrum of Corpus Callosum
White arrow= Genu of Corpus Callosum
Green arrow= ACoA

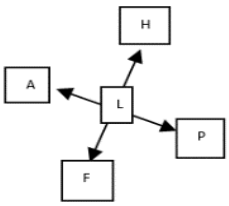

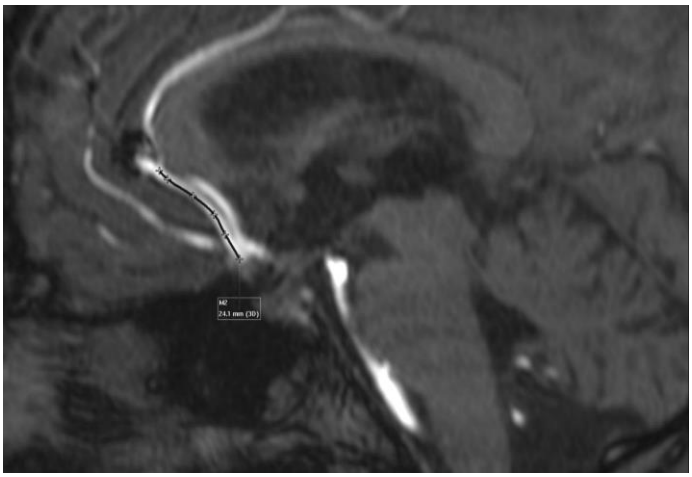

Uncontrasted brain MRA in sagittal view showing length measurement (black line) of the right A2 segment.

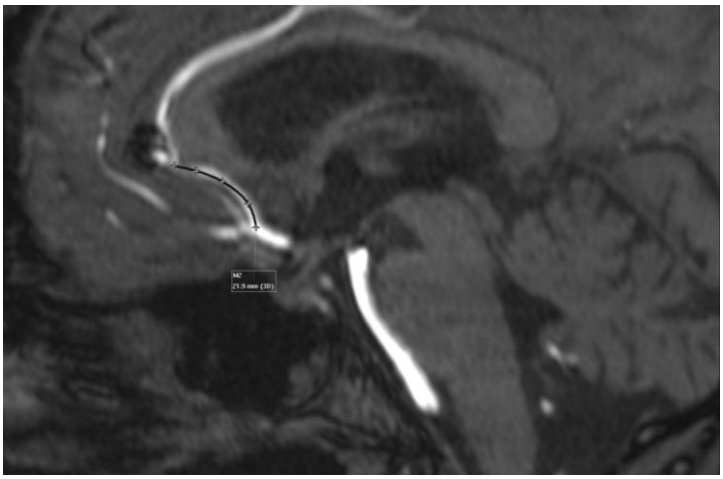

Uncontrasted brain MRA in sagittal view showing length measurement (black line) of the left A2 segment.

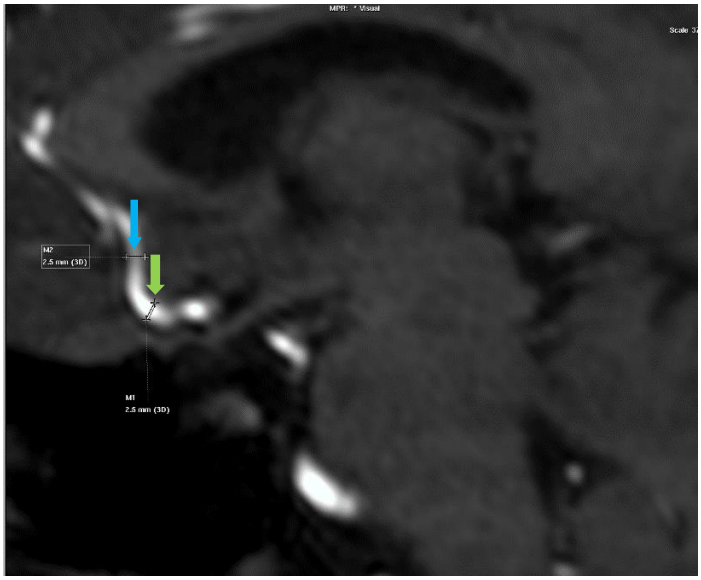

Uncontrasted brain MRA in a sagittal plane showing diameter measurements (white lines) across right A2 segment.

*Green arrow= PD

Blue arrow= MD

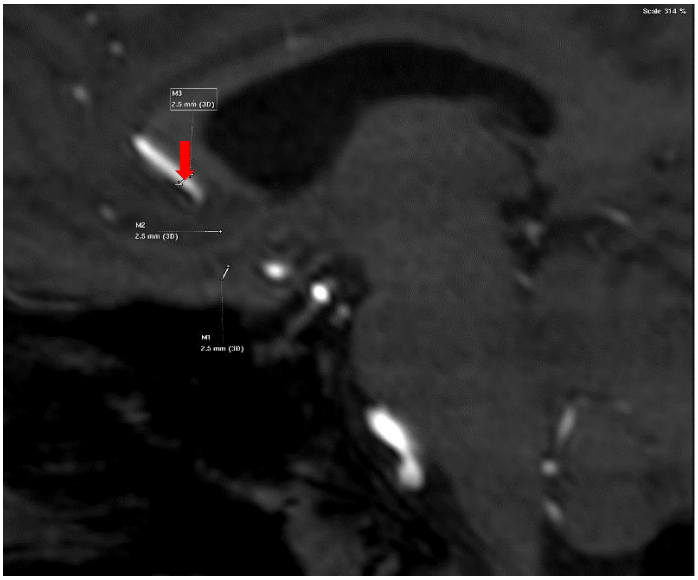

Uncontrasted brain MRA in a sagittal plane showing diameter measurements (white lines) across right A2 segment.

*Red arrow= DD

Appendix E: HREC approval

UNIVERSITY OF CAPE TOWN
Faculty of Health Sciences
Human Research Ethics Committee

Room 45 E-52-E-Floor- Old Main Building
Groote Schuur Hospital
Observatory 7925
Telephone [021] 406 6492
Email: hrec-submissions@uct.ac.za
Website: www.health.uct.ac.za/home/human-research-ethics

17 January 2023

HREC REF: 693/2022

Dr K Mpolokeng
Division of Clinical Anatomy
FHS
Email: kentse.mpolokeng@uct.ac.za
Student: mdlmba005@myuct.ac.za

Dear Dr Mpolokeng

PROJECT TITLE: A DISSECTION AND ANGIOGRAPHIC STUDY OF ANATOMICAL VARIATIONS IN THE ANTERIOR COMMUNICATING ARTERY COMPLEX IN A SOUTH AFRICAN SAMPLE. (MASTER'S DEGREE - MISS MBALENTLE MADOLO)

Thank you for your response letter, addressing the issues raised by the Faculty of Health Sciences Human Research Ethics Committee (HREC).

It is a pleasure to inform you that the HREC has **formally approved** the above-mentioned study.

Approval is granted for one year until the 30 January 2024.

Please submit a progress form, using the standardised Annual Report Form (FHS016) if the study continues beyond the approval period. Please submit a Standard Closure form if the study is completed within the approval period.
(Forms can be found on our website: www.health.uct.ac.za/fhs/research/humanethics/forms)

The HREC acknowledge that the student: Miss Mbalentle Madolo will also be involved in this study.

Please quote the HREC REF 693/2022 in all your correspondence.

Please note that the ongoing ethical conduct of the study remains the responsibility of the principal investigator.

Please note that for all studies approved by the HREC, the principal investigator **must** obtain appropriate institutional approval, where necessary, before the research may occur.

Yours sincerely

PROFESSOR M BLOCKMAN
CHAIRPERSON, FACULTY OF HEALTH SCIENCES HUMAN RESEARCH ETHICS COMMITTEE

HREC/ref 693.2022

UNIVERSITY OF CAPE TOWN

FACULTY OF HEALTH SCIENCES
Human Research Ethics Committee

FHS016: Annual Progress Report / Renewal

HREC office use only (FWA00001637; IRB00001938)			
This serves as notification of annual approval, including any documentation described below.			
☑ Approved	Annual progress report	Approved until/next renewal date	30.01.2025
☐ Not approved	See attached comments		
Signature Chairperson of the HREC/ Designee		Date Signed	17/1/2024

Note: Please email this form and supporting documents (if applicable) in a combined pdf-file to hrec-enquiries@uct.ac.za.
Please clarify your plan for research-related activities during COVID-19 lockdown.
Please use the latest form found on our website:
http://www.health.uct.ac.za/fhs/research/humanethics/forms

HUMAN RESEARCH ETHICS COMMITTEE
17 JAN 2024
HEALTH SCIENCES FACULTY
UNIVERSITY OF CAPE TOWN

Comments to PI from the HREC

Principal Investigator to complete the following:

1. Protocol information

Date (when submitting this form)	16/01/2024		
HREC REF Number	693/2022	Current Ethics Approval was granted until	30/01/2024
Protocol title	A dissection and angiographic study of anatomical variations in the anterior communicating artery complex in a South African sample.		
Protocol number (if applicable)	N/A		
Are there any sub-studies linked to this study?		☐ Yes	✓ No
If yes, could you please provide the HREC Reference number for all sub-studies? **Note:** A separate FHS016 must be submitted for each sub-study.	N/A		
Principal Investigator	Dr Kentse Mpolokeng		